

Comparison of some Entropy Conservative Numerical Fluxes for the Euler Equations

Hendrik Ranocha

January 10, 2017

Entropy stability is a well-known design principle for numerical methods in gas dynamics. Entropy conservative numerical fluxes can be used as ingredients in two kinds of schemes: Firstly, as building blocks in the subcell flux differencing form of Fisher and Carpenter (2013) and secondly (enhanced by dissipation) as numerical surface fluxes in finite volume like schemes. In this article, the flux differencing theory is extended, guaranteeing high-order for symmetric and consistent numerical fluxes. Additionally, an extension to simplices using a genuinely multi-dimensional framework of summation-by-parts operators is investigated for the first time in this framework. Moreover, several new entropy conservative numerical fluxes are developed and compared extensively with existing ones, both in theory and in numerical tests, using the flux differencing and the finite volume framework.

1 Introduction

Entropy stability has long been used as design principle for numerical schemes for gas dynamics. As an ingredient, entropy conservative numerical fluxes can be used in two kinds of application: They can be used as volume fluxes in the flux differencing framework of Fisher and Carpenter (2013a) and – enhanced with additional dissipation operators – as numerical fluxes in a finite volume framework.

In this article, the theory of the flux differencing form by Fisher and Carpenter (2013a) is extended. Thus, high order can be guaranteed not only for the entropy conservative flux of Tadmor (1987), but also for every consistent and symmetric numerical flux, as observed in all numerical experiments known to the author. Secondly, for the first time, a genuinely multi-dimensional formulation of generalised summation-by-parts operators is used to investigate the extension of the framework to simplices.

Afterwards, the construction of affordable entropy conservative fluxes is briefly reviewed and several new entropy conservative numerical fluxes are constructed – with and without the kinetic energy preserving property of Jameson (2008).

Finally, the numerical fluxes are enhanced with several dissipation operators and are compared both theoretically and in diverse test cases. Included in this comparison are the classical local Lax-Friedrichs flux and the Suliciu relaxation solver described by Bouchut (2004).

This article is organised as follows. At first, some well-known properties of the Euler equations are summed up in section 2 in order to fix the notation and for further reference. Afterwards, the extension of the flux differencing theory of Fisher and Carpenter (2013a) is presented in section 3.

Thereafter, several entropy conservative numerical fluxes are constructed in sections 4 and 5. To get numerical surface fluxes usable in finite volume methods, the addition of dissipation is discussed in section 6, especially with regard to positivity preservation. After that, the methods are tested and compared using several problems in section 7. Finally, the results are summed up in section 8, conclusions are drawn and remaining open problems are formulated.

2 Euler equations

In this section, some well known properties of the Euler equations in two space dimensions are given in order to fix the notation and refer to them later. The Euler equations are

$$\underbrace{\partial_t \begin{pmatrix} \varrho \\ \varrho v_x \\ \varrho v_y \\ \varrho e \end{pmatrix}}_{=u} + \underbrace{\partial_x \begin{pmatrix} \varrho v_x \\ \varrho v_x^2 + p \\ \varrho v_x v_y \\ (\varrho e + p)v_x \end{pmatrix}}_{=f_x(u)} + \underbrace{\partial_y \begin{pmatrix} \varrho v_y \\ \varrho v_x v_y \\ \varrho v_y^2 + p \\ (\varrho e + p)v_y \end{pmatrix}}_{=f_y(u)} = 0, \quad (1)$$

where ϱ is the density of the gas, $v = (v_x, v_y)$ its speed, ϱv the momentum, e the specific total energy, and p the pressure. The total energy ϱe can be decomposed into the internal energy $\varrho \varepsilon$ and the kinetic energy $\frac{1}{2}\varrho v^2$, i.e.

$$\varrho e = \varrho \varepsilon + \frac{1}{2}\varrho v^2. \quad (2)$$

For a perfect gas,

$$p = \varrho R T = (\gamma - 1)\varrho \varepsilon = (\gamma - 1) \left(\varrho e - \frac{1}{2}\varrho v^2 \right), \quad (3)$$

where R is the gas constant, T the (absolute) temperature, and γ the ratio of specific heats. For air, $\gamma = 1.4$ will be used, unless stated otherwise.

The (mathematical) entropy (scaled by a constant for convenience, as chosen inter alia by Ismail and Roe (2009) and Chandrashekar (2013)) used is

$$U = -\frac{\varrho s}{\gamma - 1}, \quad (4)$$

where the (physical) specific entropy is given by

$$s = \log \frac{p}{\varrho^\gamma} = \log p - \gamma \log \varrho. \quad (5)$$

With the associated entropy flux

$$F = U v = -\frac{\varrho s}{\gamma - 1} v, \quad (6)$$

smooth solutions fulfil $\partial_t U + \partial_x F_x + \partial_y F_y = 0$, and the entropy inequality

$$\partial_t U + \partial_x F_x + \partial_y F_y \leq 0 \quad (7)$$

will be used as an additional admissibility criterion for weak solutions.

For $\varrho, p > 0$, the entropy $U(u)$ is strictly convex, and the entropy variables

$$w = U'(u) = \left(\frac{\gamma}{\gamma - 1} - \frac{s}{\gamma - 1} - \frac{\varrho v^2}{2p}, \frac{\varrho v_x}{p}, \frac{\varrho v_y}{p}, -\frac{\varrho}{p} \right)^T \quad (8)$$

can be used interchangeably with the conservative variables u . The flux potentials

$$\psi_x = \varrho v_x, \quad \psi_y = \varrho v_y \quad (9)$$

fulfil $\psi'_{x/y}(w) = f_{x/y}(u(w))$ and $F_{x/y} = w \cdot f_{x/y} - \psi_{x/y}$.

3 Flux differencing form

Entropy conservative two-point numerical fluxes can be used to create a high-order method by the approach of Fisher and Carpenter (2013a,b). Using diagonal-norm nodal SBP bases including boundary nodes, they constructed high-order numerical fluxes from given symmetric and consistent two-point fluxes f^{vol} .

Using the derivative matrix $\underline{\underline{D}}$ with entries $D_{i,k}$, the corresponding discretisation of the divergence $\partial_x f$ at x_i in one dimension reads

$$\sum_{k=0}^p 2D_{i,k} f_{i,k}^{\text{vol}}, \quad (10)$$

where $f_{i,k}^{\text{vol}} = f^{\text{vol}}(u_i, u_k)$. If the two-point flux f^{vol} used is the entropy conservative one proposed by Tadmor (1987),

$$f^{\text{vol}}(u_i, u_k) = \int_0^1 f\left(u\left(w(u_i) + t(w(u_k) - w(u_i))\right)\right) dt, \quad (11)$$

Fisher and Carpenter (2013a, Theorem 3.1) showed that the resulting discretisation (10) of $\partial_x f(x_i)$ is of the same order as the SBP derivative operator $\underline{\underline{D}}$.

Additionally, Fisher and Carpenter (2013a, Theorem 3.2) showed that by using a consistent and symmetric two-point flux f^{vol} that is also entropy conservative in the sense of Tadmor (1987), i.e. $\llbracket w \rrbracket \cdot f^{\text{vol}} - \llbracket \psi \rrbracket = 0$, the discretisation (10) is also entropy conservative. Here and in the following, $\llbracket a \rrbracket = a_+ - a_-$ denotes the jump of a quantity.

In the following, extensions to generalised SBP operators in multiple dimensions as well as generalisations / variations of the Theorems 3.1 and 3.2 of Fisher and Carpenter (2013a) will be developed.

3.1 Multiple dimensions

In order to apply the methods to multi-dimensional problems, it is common to use rectangular grids and tensor product bases using the results of the one-dimensional case. However, genuinely multi-dimensional SBP operators can be constructed as well and the extension of the flux differencing form with its high-order as well as entropy conserving properties for one-dimensional nodal diagonal-norm SBP operators by Fisher and Carpenter (2013a, Theorems 3.1 and 3.2) can be described as follows.

Multi-dimensional SBP operators can be described in a numerical setting (more adopted to finite difference methods) or an analytical setting (more common in finite element / discontinuous Galerkin methods). Here, the numerical setting of Hicken, Fernández, and Zingg (2016) will be described using the notation of the analytical setting of Ranocha (2016a, Section 6).

An SBP operator on a d dimensional element Ω consists of the following components.

- Derivative operators $\underline{\underline{D}}_i$, $i \in \{1, \dots, d\}$, approximating the partial derivative in the i -th coordinate direction. These are required to be exact for polynomials of degree $\leq p$.
- A mass matrix $\underline{\underline{M}}$, approximating the L_2 scalar product on Ω via

$$\underline{u}^T \underline{\underline{M}} \underline{v} = \langle \underline{u}, \underline{v} \rangle_M \approx \langle u, v \rangle_{L_2(\Omega)} = \int_{\Omega} uv, \quad (12)$$

where u, v are functions on Ω and $\underline{u}, \underline{v}$ their approximations in the SBP basis.

- A restriction operator $\underline{\underline{R}}$ performing interpolation to the boundary $\partial\Omega$ of Ω .
- A boundary mass matrix $\underline{\underline{B}}$ approximating the L_2 scalar product of $\partial\Omega$ via

$$\underline{u_B}^T \underline{\underline{B}} \underline{v_B} = \langle \underline{u_B}, \underline{v_B} \rangle_B \approx \langle u_B, v_B \rangle_{L_2(\partial\Omega)} = \int_{\partial\Omega} u_B v_B, \quad (13)$$

where u_B, v_B are functions on $\partial\Omega$ and $\underline{u_B}, \underline{v_B}$ their approximations in the SBP basis.

- Multiplication operators $\underline{\underline{N}}_i$, $i \in \{1, \dots, d\}$, performing multiplication of functions on the boundary $\partial\Omega$ with the i -th component of the outer unit normal.
- Together, the restriction and boundary operators approximate

$$\underline{u}^T \underline{\underline{R}}^T \underline{\underline{B}} \underline{\underline{N}}_i \underline{\underline{R}} \underline{v} \approx \int_{\partial\Omega} uv n_i, \quad (14)$$

where n_i is the i -th component of the outer unit normal n , and this approximation has to be exact for polynomials of degree $\leq p$.

- Finally, the SBP property

$$\underline{\underline{M}} \underline{\underline{D}}_i + \underline{\underline{D}}_i^T \underline{\underline{M}} = \underline{\underline{R}}^T \underline{\underline{B}} \underline{\underline{N}}_i \underline{\underline{R}} \quad (15)$$

has to be fulfilled, mimicking integration by parts (i.e. the divergence theorem) on a discrete level

$$\int_{\Omega} u (\partial_i v) + \int_{\Omega} (\partial_i u) v \approx \underline{u}^T \underline{\underline{M}} \underline{\underline{D}}_i \underline{v} + \underline{u}^T \underline{\underline{D}}_i^T \underline{\underline{M}} \underline{v} = \underline{u}^T \underline{\underline{R}}^T \underline{\underline{B}} \underline{\underline{N}}_i \underline{\underline{R}} \underline{v} \approx \int_{\partial\Omega} uv n_i. \quad (16)$$

In the following, the SBP bases used to represent functions on the volume Ω and the boundary $\partial\Omega$ are nodal bases. Nonlinear operations will be performed pointwise and often the mass matrix $\underline{\underline{M}}$ will be assumed to be diagonal, corresponding to a quadrature rule on Ω , as described inter alia by Hicken and Zingg (2013) and Hicken, Fernández, and Zingg (2016, Theorem 3.2).

In one dimension, an entropy conservative numerical flux f^{vol} in the sense of Tadmor (1987, 2003) has to fulfil $(w_i - w_k) \cdot f^{\text{vol}}(u_i, u_k) - (\psi_i - \psi_k) = 0$, where w are the entropy variables $w = U'(u)$ and ψ is the flux potential obeying $\partial_w \psi(w) = f(u(w))$. A natural extension to multiple dimensions is to use fluxes f_j in the j -th coordinate direction such that $\text{div } f = \sum_j \partial_j f_j$ and corresponding flux potentials ψ_j obeying $\partial_w \psi_j(w) = f_j(u(w))$. Then, the j -th entropy flux $F_j = w \cdot f_j - \psi_j$ fulfils

$$\begin{aligned} F'_j(u) &= w'(u) \cdot f_j + w \cdot f'_j(u) - \psi'_j(u) \\ &= w'(u) \cdot f_j + w \cdot f'_j(u) - \partial_w \psi_j(u) \cdot w'(u) \\ &= U'(u) \cdot f'_j(u), \end{aligned} \quad (17)$$

since $w = U'(u)$ and $\partial_w \psi_j = f_j$. Thus, smooth solutions u of

$$\partial_t u + \sum_j \partial_j f_j(u) = 0 \quad (18)$$

fulfil

$$\begin{aligned} \partial_t U &= U'(u) \cdot \partial_t u = - \sum_j U'(u) \cdot \partial_j f_j(u) = - \sum_j U'(u) \cdot f'_j(u) \cdot \partial_j u \\ &= - \sum_j F'_j(u) \cdot \partial_j u = - \sum_j \partial_j F_j(u), \end{aligned} \quad (19)$$

and the entropy inequality

$$\partial_t U + \sum_j \partial_j F_j(u) \leq 0 \quad (20)$$

can be used as additional admissibility criterion.

The natural extension of the one-dimensional flux differencing form is then given as follows. Choose consistent and symmetric numerical volume fluxes f_j^{vol} , $j \in \{1, \dots, d\}$. Then, the approximation of $\partial_j f_j$ at x_i is given by

$$\sum_k 2 \left[\underline{\underline{D}}_j \right]_{i,k} f_j^{\text{vol}}(u_i, u_k). \quad (21)$$

That is, dropping the index j , it has the same form as in one space dimension, using appropriate derivative matrices $\underline{\underline{D}}_j$ and corresponding volume fluxes f_j^{vol} consistent with the flux f_j in the j -th coordinate direction.

3.2 Order of approximation

The basic argument of Fisher and Carpenter (2013a, Theorem 3.1) can be generalised as follows. Assume that for fixed w_i , the j -th component of the volume flux can be written as

$$f_j^{\text{vol}}(w_i, w_k) = f_j(w_i) + \frac{1}{2} f'_j(w_i) \cdot (w_k - w_i) + \sum_{|\alpha| \geq 2} c_\alpha (w_k - w_i)^\alpha, \quad (22)$$

where multi-index notation has been used and w denotes any variable, i.e. conservative variables, primitive variables, or entropy variables. Note that a general Taylor expansion of $f_j^{\text{vol}}(w_i, \cdot)$ around w_i would read

$$f_j^{\text{vol}}(w_i, w_k) = f_j^{\text{vol}}(w_i, w_i) + \partial_2 f_j^{\text{vol}}(w_i, w_i) \cdot (w_k - w_i) + \sum_{|\alpha| \geq 2} c_\alpha (w_k - w_i)^\alpha. \quad (23)$$

Using this, the volume discretisation at x_i (21) can be rewritten (dropping the indices of the derivative operator and the flux) as

$$\sum_{k=0}^p 2D_{i,k} f^{\text{vol}}(w_i, w_k) = \sum_{k=0}^p 2D_{i,k} f(w_i) + \sum_{k=0}^p D_{i,k} f'(w_i) \cdot (w_k - w_i) + \sum_{k=0}^p D_{i,k} \sum_{|\alpha| \geq 2} c_\alpha (w_k - w_i)^\alpha. \quad (24)$$

Since the derivative is exact for constants, i.e. $\underline{D} \underline{1} = 0$, the first sum on the right hand side of (24) vanishes. By the same reason, the second sum can be rewritten as

$$\sum_{k=0}^p D_{i,k} f'(w_i) \cdot (w_k - w_i) = f'(w_i) \cdot \sum_{k=0}^p D_{i,k} w_k \quad (25)$$

and is therefore of the desired order. Finally, the third sum in (24) is a higher order correction to the product rule. Writing

$$\sum_{|\alpha| \geq 2} c_\alpha (w_k - w_i)^\alpha = \sum_{|\alpha| \geq 2} c_\alpha \sum_{\beta \leq \alpha} \binom{\alpha}{\beta} w_k^\beta (-w_i)^{\alpha-\beta} \quad (26)$$

for multi-indices α, β , it becomes

$$\sum_{|\alpha| \geq 2} c_\alpha \sum_{\beta \leq \alpha} \binom{\alpha}{\beta} \sum_{k=0}^p (-w_i)^{\alpha-\beta} D_{i,k} w_k^\beta. \quad (27)$$

By the product rule, a smooth function w of x satisfies

$$\partial_x w^\beta = \partial_x (w_1^{\beta_1} \dots w_n^{\beta_n}) = \sum_{j=1}^d \beta_j w_1^{\beta_1} \dots w_{j-1}^{\beta_{j-1}} w_j^{\beta_j-1} w_{j+1}^{\beta_{j+1}} \dots w_n^{\beta_n} \partial_x w_j = \sum_{j=1}^d \beta_j w^{\beta-e_j} \partial_x w_j, \quad (28)$$

where e_j is the j -th unit vector, $(e_j)_l = \delta_{jl}$. Thus, the third sum in (24) is an approximation of the same order as the derivative matrix \underline{D} to

$$\begin{aligned} & \sum_{|\alpha| \geq 2} c_\alpha \sum_{\beta \leq \alpha} \binom{\alpha}{\beta} \sum_{k=0}^p (-w_i)^{\alpha-\beta} D_{i,k} w_k^\beta \\ & \approx \sum_{|\alpha| \geq 2} c_\alpha \sum_{\beta \leq \alpha} \binom{\alpha}{\beta} (-w_i)^{\alpha-\beta} \sum_{j=1}^d \beta_j w_i^{\beta-e_j} \sum_{k=0}^p D_{i,k} w_{k,j} \\ & = \sum_{|\alpha| \geq 2} c_\alpha \sum_{j=1}^d \underbrace{\sum_{\beta \leq \alpha} \binom{\alpha}{\beta} \beta_j (-\mathbb{1})^{\alpha-\beta} w_i^{\alpha-e_j}}_{\text{derivative matrix}} \sum_{k=0}^p D_{i,k} w_{k,j}, \end{aligned} \quad (29)$$

where $\mathbb{1}$ is the vector with components 1 of the same size as w_i and $w_{k,j}$ is the j -th component of the vector w_k approximating w at $x = x_k$. The sum depending on β vanishes, since

$$\begin{aligned}\partial_{w_j}(-\mathbb{1} + w)^\alpha &= \partial_{w_j} \sum_{\beta \leq \alpha} \binom{\alpha}{\beta} (-\mathbb{1})^{\alpha-\beta} w^\beta = \sum_{\beta \leq \alpha} \binom{\alpha}{\beta} (-\mathbb{1})^{\alpha-\beta} \beta_j w^{\beta-e_j} \\ &\xrightarrow{w=\mathbb{1}} 0 = \alpha_j (-\mathbb{1} + \mathbb{1})^{\alpha-e_j} = \sum_{\beta \leq \alpha} \binom{\alpha}{\beta} (-\mathbb{1})^{\alpha-\beta} \beta_j.\end{aligned}\tag{30}$$

Thus, (21) is an approximation of the same order as $\underline{\underline{D}}_j$ to $\partial_{x_j} f_j(w)$ at x_i , if (22) is fulfilled. Finally, the assumption (22) is true, if the numerical flux f^{vol} is consistent and symmetric, i.e.

$$\forall w: f^{\text{vol}}(w, w) = f(w) \quad \wedge \quad \forall w_1, w_2: f^{\text{vol}}(w_1, w_2) = f^{\text{vol}}(w_2, w_1).\tag{31}$$

Denoting the partial derivative with respect to the l -th component of the second argument of f_m^{vol} as $\partial_{2,l} f_m^{\text{vol}}(w, w)$,

$$\begin{aligned}\partial_{2,l} f_m^{\text{vol}}(w, w) &= \lim_{\delta \rightarrow 0} \frac{f_m^{\text{vol}}(w, w + \delta e_l) - f_m^{\text{vol}}(w, w)}{\delta} \\ &= \lim_{\delta \rightarrow 0} \frac{f_m^{\text{vol}}(w + \delta e_l, w) - f_m^{\text{vol}}(w, w)}{\delta} = \partial_{1,l} f_m^{\text{vol}}(w, w),\end{aligned}\tag{32}$$

and the gradient has the form $\nabla_{(\cdot,l)} f_m^{\text{vol}}(w, w) = (\partial_{2,l} f_m^{\text{vol}}(w, w), \partial_{2,l} f_m^{\text{vol}}(w, w))$. Thus, the directional derivative in direction $\frac{1}{\sqrt{2}}(1, 1)^T$ is given by

$$\begin{aligned}\frac{2}{\sqrt{2}} \partial_{2,l} f_m^{\text{vol}}(w, w) &= \frac{1}{\sqrt{2}}(1, 1) \cdot \nabla_{(\cdot,l)} f_m^{\text{vol}}(w, w) = \lim_{\delta \rightarrow 0} \frac{f_m^{\text{vol}}(w + \frac{\delta}{\sqrt{2}} e_l, w + \frac{\delta}{\sqrt{2}} e_l) - f_m^{\text{vol}}(w, w)}{\delta} \\ &= \lim_{\delta \rightarrow 0} \frac{f_m(w + \frac{\delta}{\sqrt{2}} e_l) - f_m(w)}{\delta} = \frac{1}{\sqrt{2}} \lim_{\delta \rightarrow 0} \frac{f_m(w + \delta e_l) - f_m(w)}{\delta} = \frac{1}{\sqrt{2}} \partial_l f_m(w).\end{aligned}\tag{33}$$

Therefore, $\partial_{2,l} f_m^{\text{vol}}(w, w) = \frac{1}{2} \partial_l f_m(w)$, as required. This proves the following generalisation of Theorem 3.1 of Fisher and Carpenter (2013a)

Theorem 1. *If the numerical flux f_j^{vol} is smooth, consistent with f_j , and symmetric, the flux differencing form (21) is an approximation to $\partial_{x_j} f_j(w)$ of the same order as the SBP derivative matrix $\underline{\underline{D}}_j$.*

3.3 Entropy conservation

The entropy conservation proved by Fisher and Carpenter (2013a, Theorem 3.2) can be extended similarly — at least in a setting based on 'small' elements and looking at entropy conservation across elements. An extension of the subcell entropy conservation property as proved by Fisher and Carpenter (2013a, Theorem 3.2) is not aspired here.

Dropping the index j in (21), the following assumptions will be used.

- The volume flux f^{vol} is symmetric, consistent with the flux f , and entropy conservative in the sense $(w_i - w_k) \cdot f_{i,k}^{\text{vol}} = \psi_i - \psi_k$, where $f_{i,k}^{\text{vol}} = f^{\text{vol}}(u_i, u_k)$, w are the entropy variables, and ψ is the flux potential.
- A nodal SBP basis with diagonal mass matrix $\underline{\underline{M}}$ is used.
- The boundary operator $\underline{\underline{R}}^T \underline{\underline{B}} \underline{\underline{N}} \underline{\underline{R}}$ is diagonal, i.e. there are enough nodes on the boundary to get the required exactness of integration.

These assumptions on the SBP bases are fulfilled for tensor product Lobatto-Legendre nodes.

Using these assumptions in a semidiscrete setting, the rate of change of the total entropy $\int_{\Omega} U$ is discretely approximated as

$$\frac{d}{dt} \int_{\Omega} U \approx \underline{w}^T \underline{\underline{M}} \partial_t \underline{u}, \quad (34)$$

and (dropping again the index j of the derivative operator) the flux difference form (21) yields due to the SBP property (15)

$$\sum_{i,k} 2w_i \cdot \left[\underline{\underline{M}} \underline{\underline{D}} \right]_{i,k} f_{i,k}^{\text{vol}} = \sum_{i,k} w_i \cdot \left[\underline{\underline{M}} \underline{\underline{D}} + \underline{\underline{R}}^T \underline{\underline{B}} \underline{\underline{N}} \underline{\underline{R}} - \underline{\underline{D}}^T \underline{\underline{M}} \right]_{i,k} f_{i,k}^{\text{vol}}. \quad (35)$$

Since the mass matrix $\underline{\underline{M}}$ is diagonal, the volume term can be written as

$$\begin{aligned} \sum_{i,k} w_i \cdot \left[\underline{\underline{M}} \underline{\underline{D}} - \underline{\underline{D}}^T \underline{\underline{M}} \right]_{i,k} f_{i,k}^{\text{vol}} &= \sum_{i,k} (M_{ii} D_{ik} - M_{kk} D_{ki}) w_i \cdot f_{i,k}^{\text{vol}} \\ &= \sum_{i,k} M_{ii} D_{ik} (w_i - w_k) \cdot f_{i,k}^{\text{vol}}, \end{aligned} \quad (36)$$

where the indices i, j have been exchanged in the second part of the sum, using the symmetry of f^{vol} . Then, by entropy conservation $(w_i - w_k) \cdot f_{i,k}^{\text{vol}} = \psi_i - \psi_k$,

$$\begin{aligned} \sum_{i,k} M_{ii} D_{ik} (w_i - w_k) \cdot f_{i,k}^{\text{vol}} &= \sum_{i,k} M_{ii} D_{ik} (\psi_i - \psi_k) = - \sum_{i,k} M_{ii} D_{ik} \psi_k \\ &= - \sum_{i,k} \left[\underline{\underline{M}} \underline{\underline{D}} \right]_{i,k} \psi_k = - \sum_{i,k} \left[\underline{\underline{R}}^T \underline{\underline{B}} \underline{\underline{N}} \underline{\underline{R}} - \underline{\underline{D}}^T \underline{\underline{M}} \right]_{i,k} \psi_k \\ &= - \sum_{i,k} \left[\underline{\underline{R}}^T \underline{\underline{B}} \underline{\underline{N}} \underline{\underline{R}} \right]_{i,k} \psi_k, \end{aligned} \quad (37)$$

since the derivative $\underline{\underline{D}}$ is exact for constants, i.e. $\underline{\underline{D}} \underline{1} = 0$.

The boundary term can be written, using that $\underline{\underline{R}}^T \underline{\underline{B}} \underline{\underline{N}} \underline{\underline{R}}$ is diagonal, as

$$\begin{aligned} \sum_{i,k} w_i \cdot \left[\underline{\underline{R}}^T \underline{\underline{B}} \underline{\underline{N}} \underline{\underline{R}} \right]_{i,k} f_{i,k}^{\text{vol}} &= \sum_k \left[\underline{\underline{R}}^T \underline{\underline{B}} \underline{\underline{N}} \underline{\underline{R}} \right]_{k,k} w_k \cdot f_{k,k}^{\text{vol}} \\ &= \sum_k \left[\underline{\underline{R}}^T \underline{\underline{B}} \underline{\underline{N}} \underline{\underline{R}} \right]_{k,k} w_k \cdot f_k, \end{aligned} \quad (38)$$

since the volume flux f^{vol} is consistent with the flux f . Therefore, the total expression becomes

$$\begin{aligned} \sum_{i,k} 2w_i \cdot \left[\underline{\underline{M}} \underline{\underline{D}} \right]_{i,k} f_{i,k}^{\text{vol}} &= \sum_k \left[\underline{\underline{R}}^T \underline{\underline{B}} \underline{\underline{N}} \underline{\underline{R}} \right]_{k,k} \underbrace{(w_k \cdot f_k - \psi_k)}_{=F_k} \\ &= \sum_{i,k} \left[\underline{\underline{R}}^T \underline{\underline{B}} \underline{\underline{N}} \underline{\underline{R}} \right]_{i,k} F_k \\ &= \underline{1}^T \underline{\underline{R}}^T \underline{\underline{B}} \underline{\underline{N}} \underline{\underline{R}} F, \end{aligned} \quad (39)$$

since the entropy flux F is given by $F = w \cdot f - \psi$. This results in a consistent discretisation of

$$\int_{\Omega} w \cdot \partial_j f_j = \int_{\partial\Omega} F_j n_j \quad (40)$$

for each j and entropy conservation follows. This proves the following generalisation / variation of Theorem 3.2 of Fisher and Carpenter (2013a)

Theorem 2. *If the numerical fluxes f_j^{vol} are consistent with f_j , symmetric, and entropy conservative, the nodal mass matrix $\underline{\underline{M}}$ is diagonal, and the boundary operators $\underline{\underline{R}}^T \underline{\underline{B}} \underline{\underline{N}} \underline{\underline{R}}$ are diagonal, too, the flux differencing form (21) is entropy conservative.*

Remark 3. To the author's knowledge, there are no known SBP operators on simplices in general with diagonal $\underline{\underline{R}}^T \underline{\underline{B}} \underline{\underline{N}} \underline{\underline{R}}$. In the framework of Hicken, Fernández, and Zingg (2016), this operator is called E_j and they mention (Remark 4 in section 4.2) that they have not been able to get diagonal operators that are sufficiently accurate. However, using tensor products of Lobatto-Legendre nodes in cubes, these operators are diagonal.

4 Entropy conservative fluxes

In the semidiscrete setting of Tadmor (1987, 2003), an entropy conservative numerical flux f^{num} has to obey

$$[[w]] \cdot f^{\text{num},j} - [[\psi_j]] = 0, \quad (41)$$

where w are the entropy variables (8), $f^{\text{num},j}$ is the numerical flux in direction j , ψ_j is the flux potential in direction j , and

$$[[a]] = a_+ - a_- \quad (42)$$

denotes the jump of a quantity. Since the flux f_j is the gradient of the potential ψ_j , i.e. $f_j = \partial_w \psi_j$, the condition (41) for an entropy conservative flux determines $f^{\text{num},j}$ as an appropriate mean value of f_j . Indeed, the entropy conservative flux proposed by Tadmor (1987, Equation (4.6a)) has the form of an integral mean

$$f^{\text{num},j}(w_-, w_+) = \int_{s=0}^1 f_j \left(u(w_- + s(w_+ - w_-)) \right) ds. \quad (43)$$

However, this integral mean value is difficult to compute in general. Tadmor (2003, Theorem 6.1) proposed another integral mean based on a piecewise linear path in phase space to compute an integral mean similar to (43). Nevertheless, another approach will be used here.

Following the well-known proverb “*Differentiation is mechanics, integration is art.*”, the integral mean can be exchanged by some kind of differential mean. Sadly, there is no differential mean value theorem giving some kind of numerical flux fulfilling (41) directly in general. However, the mean value theorem can be used for scalar variables. In this way, the affordable, entropy conservative numerical fluxes of Ismail and Roe (2009) and Chandrashekar (2013) can be constructed using the same general approach. This general procedure can be described as

- Express the flux potentials ψ (9) and the entropy variables w (8) using the chosen set of variables.
- Express the jumps of ψ, w as products of some mean values and jumps of the chosen variables using some kind of product / chain rule as in the mean value theorem.

There are several mean values that can be used for this task. The simplest one is the arithmetic mean

$$\{a\} = \frac{a_- + a_+}{2}, \quad (44)$$

with corresponding product and chain rule

$$[[ab]] = \{a\}[[b]] + \{b\}[[a]], \quad [[a^2]] = 2\{a\}[[a]]. \quad (45)$$

This is enough to get some entropy conservative fluxes for the shallow water equations, since the entropy variables w and the flux potential ψ can both be expressed as polynomials in both the primitive variables and the entropy variables as described by Ranocha (2016b).

However, this is not true for the Euler equations. Therefore, other means have to be used. Roe (2006) proposed the logarithmic mean

$$\{a\}_{\log} = \frac{a_+ - a_-}{\log a_+ - \log a_-}, \quad (46)$$

described by Ismail and Roe (2009), including a numerically stable implementation. The corresponding chain rule reads as

$$[[\log a]] = \frac{1}{\{a\}_{\log}} [[a]]. \quad (47)$$

Another criterion for a numerical flux is the kinetic energy preservation. The kinetic energy $\frac{1}{2}\rho v^2$ obeys (for smooth solutions)

$$\partial_t \left(\frac{1}{2} \rho v^2 \right) + \partial_x \left(\frac{1}{2} \rho v^2 v_x \right) + \partial_y \left(\frac{1}{2} \rho v^2 v_y \right) + v_x \partial_x p + v_y \partial_y p = 0. \quad (48)$$

In order to mimic this behaviour discretely in one space dimension, Jameson (2008) formulated the condition

$$f_{\rho v}^{\text{num}} = \{v\} f_{\rho}^{\text{num}} + p^{\text{num}}, \quad (49)$$

where p^{num} is a consistent numerical flux approximating the pressure. However, every consistent numerical flux $f_{\rho v}^{\text{num}}$ can be written in this form if some differences are accepted, i.e. if $p^{\text{num}} = f_{\rho v}^{\text{num}} - \{v\} f_{\rho}^{\text{num}}$ is accepted as numerical approximation of the pressure.

In the following, some entropy conservative numerical fluxes are presented. The fluxes of Roe (2006) and Chandrashekar (2013) in section 4.1 and 4.2 are well-known in the literature while the other ones are new.

4.1 $\sqrt{\frac{\rho}{p}}, \sqrt{\frac{\rho}{p}}v, \sqrt{\rho p}$ as variables

The entropy conservative flux of Ismail and Roe (2009); Roe (2006) can be derived using the variables

$$z_1 := \sqrt{\frac{\rho}{p}}, \quad z_2 := \sqrt{\frac{\rho}{p}}v_x, \quad z_3 := \sqrt{\frac{\rho}{p}}v_y, \quad z_5 := \sqrt{\rho p}. \quad (50)$$

In these variables, the flux potential (9) and the entropy variables (8) are given by

$$\psi_x = z_2 z_5, \quad \psi_y = z_3 z_5, \quad (51)$$

$$w = \left(\frac{\gamma}{\gamma-1} - \frac{s}{\gamma-1} - \frac{1}{2}z_2^2 - \frac{1}{2}z_3^2, z_1 z_2, z_1 z_3, -z_1^2 \right)^T, \quad s = -(\gamma+1) \log z_1 - (\gamma-1) \log z_5. \quad (52)$$

Thus, the jumps can be expressed using (45) and (47) as

$$\begin{aligned} [w_1] &= -\frac{1}{\gamma-1} [s] - \frac{1}{2} [z_2^2] - \frac{1}{2} [z_3^2] = \frac{\gamma+1}{\gamma-1} [\log z_1] + [\log z_5] - \frac{1}{2} [z_2^2] - \frac{1}{2} [z_3^2] \\ &= \frac{\gamma+1}{\gamma-1} \frac{1}{\{z_1\}_{\log}} [z_1] + \frac{1}{\{z_5\}_{\log}} [z_5] - \{z_2\} [z_2] - \{z_3\} [z_3], \\ [w_2] &= [z_1 z_2] = \{z_1\} [z_2] + \{z_2\} [z_1], \\ [w_3] &= [z_1 z_3] = \{z_1\} [z_3] + \{z_3\} [z_1], \\ [w_4] &= -[z_1^2] = -2\{z_1\} [z_1], \\ [\psi_x] &= [z_2 z_5] = \{z_2\} [z_5] + \{z_5\} [z_2], \\ [\psi_y] &= [z_3 z_5] = \{z_3\} [z_5] + \{z_5\} [z_3], \end{aligned} \quad (53)$$

and the entropy conservation conditions $[w] \cdot f^{\text{num},x/y} - [\psi_{x/y}] = 0$ (41) become

$$\begin{aligned} 0 &= \left(\frac{\gamma+1}{\gamma-1} \frac{1}{\{z_1\}_{\log}} f_{\rho}^{\text{num},x} + \{z_2\} f_{\rho v_x}^{\text{num},x} + \{z_3\} f_{\rho v_y}^{\text{num},x} - 2\{z_1\} f_{\rho e}^{\text{num},x} \right) [z_1] \\ &\quad + \left(-\{z_2\} f_{\rho}^{\text{num},x} + \{z_1\} f_{\rho v_x}^{\text{num},x} - \{z_5\} \right) [z_2] + \left(-\{z_3\} f_{\rho}^{\text{num},x} + \{z_1\} f_{\rho v_y}^{\text{num},x} - \{z_5\} \right) [z_3] \\ &\quad + \left(\frac{1}{\{z_5\}_{\log}} f_{\rho}^{\text{num},x} - \{z_2\} \right) [z_5], \\ 0 &= \left(\frac{\gamma+1}{\gamma-1} \frac{1}{\{z_1\}_{\log}} f_{\rho}^{\text{num},y} + \{z_2\} f_{\rho v_x}^{\text{num},y} + \{z_3\} f_{\rho v_y}^{\text{num},y} - 2\{z_1\} f_{\rho e}^{\text{num},y} \right) [z_1] \\ &\quad + \left(-\{z_2\} f_{\rho}^{\text{num},y} + \{z_1\} f_{\rho v_x}^{\text{num},y} \right) [z_2] + \left(-\{z_3\} f_{\rho}^{\text{num},y} + \{z_1\} f_{\rho v_y}^{\text{num},y} - \{z_5\} \right) [z_3] \\ &\quad + \left(\frac{1}{\{z_5\}_{\log}} f_{\rho}^{\text{num},y} - \{z_3\} \right) [z_5]. \end{aligned} \quad (54)$$

Thus, the fluxes

$$\begin{aligned}
f^{\text{num},x} & \begin{cases} f_{\varrho}^{\text{num},x} = \{\{z_2\}\}\{\{z_5\}\}_{\log}, \\ f_{\varrho v_x}^{\text{num},x} = \frac{\{\{z_2\}\}}{\{\{z_1\}\}} f_{\varrho}^{\text{num},x} + \frac{\{\{z_5\}\}}{\{\{z_1\}\}}, \\ f_{\varrho v_y}^{\text{num},x} = \frac{\{\{z_3\}\}}{\{\{z_1\}\}} f_{\varrho}^{\text{num},x}, \\ f_{\varrho e}^{\text{num},x} = \frac{1}{2} \frac{\gamma+1}{\gamma-1} \frac{1}{\{\{z_1\}\}\{\{z_1\}\}_{\log}} f_{\varrho}^{\text{num},x} + \frac{1}{2} \frac{\{\{z_2\}\}}{\{\{z_1\}\}} f_{\varrho v_x}^{\text{num},x} + \frac{1}{2} \frac{\{\{z_3\}\}}{\{\{z_1\}\}} f_{\varrho v_y}^{\text{num},x}, \end{cases} \\
f^{\text{num},y} & \begin{cases} f_{\varrho}^{\text{num},y} = \{\{z_3\}\}\{\{z_5\}\}_{\log}, \\ f_{\varrho v_x}^{\text{num},y} = \frac{\{\{z_2\}\}}{\{\{z_1\}\}} f_{\varrho}^{\text{num},y}, \\ f_{\varrho v_y}^{\text{num},y} = \frac{\{\{z_3\}\}}{\{\{z_1\}\}} f_{\varrho}^{\text{num},y} + \frac{\{\{z_5\}\}}{\{\{z_1\}\}}, \\ f_{\varrho e}^{\text{num},y} = \frac{1}{2} \frac{\gamma+1}{\gamma-1} \frac{1}{\{\{z_1\}\}\{\{z_1\}\}_{\log}} f_{\varrho}^{\text{num},y} + \frac{1}{2} \frac{\{\{z_2\}\}}{\{\{z_1\}\}} f_{\varrho v_x}^{\text{num},y} + \frac{1}{2} \frac{\{\{z_3\}\}}{\{\{z_1\}\}} f_{\varrho v_y}^{\text{num},y}, \end{cases}
\end{aligned} \tag{55}$$

proposed (in one space dimension) by Roe (2006) and Ismail and Roe (2009) can be seen to be entropy conservative and consistent.

However, by this choice of variables z , the pressure influences the numerical density flux. As explained by Derigs, Winters, Gassner, and Walch (2017), this can lead to problems if there are discontinuities in the pressure, see also the numerical tests in section 7.

4.2 ϱ, v, β as variables

Using the inverse of the temperature

$$\beta = \frac{1}{2RT} = \frac{\varrho}{2p}, \tag{56}$$

Chandrashekar (2013) derived some entropy conservative fluxes. The flux potential and the entropy variables are

$$\psi_x = \varrho v_x, \quad \psi_y = \varrho v_y, \tag{57}$$

$$w = \left(\frac{\gamma}{\gamma-1} - \frac{s}{\gamma-1} - \beta v^2, 2\beta v_x, 2\beta v_y, -2\beta \right)^T, \quad s = \log \frac{p}{\varrho^\gamma} = -\log \beta - (\gamma-1) \log \varrho - \log 2. \tag{58}$$

4.2.1 Variant 1

Writing the jumps using the chain rules (45) and (47) as

$$\begin{aligned}
\llbracket w_1 \rrbracket &= -\frac{1}{\gamma-1} \llbracket s \rrbracket - \llbracket \beta v^2 \rrbracket = \llbracket \log \varrho \rrbracket + \frac{1}{\gamma-1} \llbracket \log \beta \rrbracket - \llbracket \beta v^2 \rrbracket \\
&= \frac{1}{\{\{\varrho\}\}_{\log}} \llbracket \varrho \rrbracket + \frac{1}{\gamma-1} \frac{1}{\{\{\beta\}\}_{\log}} \llbracket \beta \rrbracket - \{\{v_x^2\}\} \llbracket \beta \rrbracket - \{\{v_y^2\}\} \llbracket \beta \rrbracket - 2\{\{\beta\}\} \{\{v_x\}\} \llbracket v_x \rrbracket - 2\{\{\beta\}\} \{\{v_y\}\} \llbracket v_y \rrbracket, \\
\llbracket w_2 \rrbracket &= 2\llbracket \beta v_x \rrbracket = 2\{\{\beta\}\} \llbracket v_x \rrbracket + 2\{\{v_x\}\} \llbracket \beta \rrbracket, \\
\llbracket w_3 \rrbracket &= 2\llbracket \beta v_y \rrbracket = 2\{\{\beta\}\} \llbracket v_y \rrbracket + 2\{\{v_y\}\} \llbracket \beta \rrbracket, \\
\llbracket w_4 \rrbracket &= -2\llbracket \beta \rrbracket, \\
\llbracket \psi_x \rrbracket &= \llbracket \varrho v_x \rrbracket = \{\{\varrho\}\} \llbracket v_x \rrbracket + \{\{v_x\}\} \llbracket \varrho \rrbracket, \\
\llbracket \psi_y \rrbracket &= \llbracket \varrho v_y \rrbracket = \{\{\varrho\}\} \llbracket v_y \rrbracket + \{\{v_y\}\} \llbracket \varrho \rrbracket,
\end{aligned} \tag{59}$$

the entropy conservation conditions $\llbracket w \rrbracket \cdot f^{\text{num},x/y} - \llbracket \psi_{x/y} \rrbracket = 0$ (41) become

$$\begin{aligned}
0 &= \left(\frac{1}{\llbracket \varrho \rrbracket_{\log}} f_{\varrho}^{\text{num},x} - \llbracket v_x \rrbracket \right) \llbracket \varrho \rrbracket + \left(-2\llbracket \beta \rrbracket \llbracket v_x \rrbracket f_{\varrho}^{\text{num},x} + 2\llbracket \beta \rrbracket f_{\varrho v_x}^{\text{num},x} - \llbracket \varrho \rrbracket \right) \llbracket v_x \rrbracket \\
&\quad + \left(-2\llbracket \beta \rrbracket \llbracket v_y \rrbracket f_{\varrho}^{\text{num},x} + 2\llbracket \beta \rrbracket f_{\varrho v_y}^{\text{num},x} \right) \llbracket v_y \rrbracket + \left(\frac{1}{\gamma-1} \frac{1}{\llbracket \beta \rrbracket_{\log}} f_{\varrho}^{\text{num},x} - \llbracket v_x^2 \rrbracket f_{\varrho}^{\text{num},x} \right. \\
&\quad \left. - \llbracket v_y^2 \rrbracket f_{\varrho}^{\text{num},x} + 2\llbracket v_x \rrbracket f_{\varrho v_x}^{\text{num},x} + 2\llbracket v_y \rrbracket f_{\varrho v_y}^{\text{num},x} - 2f_{\varrho e}^{\text{num},x} \right) \llbracket \beta \rrbracket, \\
0 &= \left(\frac{1}{\llbracket \varrho \rrbracket_{\log}} f_{\varrho}^{\text{num},y} - \llbracket v_y \rrbracket \right) \llbracket \varrho \rrbracket + \left(-2\llbracket \beta \rrbracket \llbracket v_x \rrbracket f_{\varrho}^{\text{num},y} + 2\llbracket \beta \rrbracket f_{\varrho v_x}^{\text{num},y} \right) \llbracket v_x \rrbracket \\
&\quad + \left(-2\llbracket \beta \rrbracket \llbracket v_y \rrbracket f_{\varrho}^{\text{num},y} + 2\llbracket \beta \rrbracket f_{\varrho v_y}^{\text{num},y} - \llbracket \varrho \rrbracket \right) \llbracket v_y \rrbracket + \left(\frac{1}{\gamma-1} \frac{1}{\llbracket \beta \rrbracket_{\log}} f_{\varrho}^{\text{num},y} - \llbracket v_x^2 \rrbracket f_{\varrho}^{\text{num},y} \right. \\
&\quad \left. - \llbracket v_y^2 \rrbracket f_{\varrho}^{\text{num},y} + 2\llbracket v_x \rrbracket f_{\varrho v_x}^{\text{num},y} + 2\llbracket v_y \rrbracket f_{\varrho v_y}^{\text{num},y} - 2f_{\varrho e}^{\text{num},y} \right) \llbracket \beta \rrbracket.
\end{aligned} \tag{60}$$

Thus, the fluxes

$$\begin{aligned}
f^{\text{num},x} &\begin{cases} f_{\varrho}^{\text{num},x} = \llbracket \varrho \rrbracket_{\log} \llbracket v_x \rrbracket, \\ f_{\varrho v_x}^{\text{num},x} = \llbracket v_x \rrbracket f_{\varrho}^{\text{num},x} + \frac{\llbracket \varrho \rrbracket}{2\llbracket \beta \rrbracket}, \\ f_{\varrho v_y}^{\text{num},x} = \llbracket v_y \rrbracket f_{\varrho}^{\text{num},x}, \\ f_{\varrho e}^{\text{num},x} = \frac{1}{2(\gamma-1)} \frac{1}{\llbracket \beta \rrbracket_{\log}} f_{\varrho}^{\text{num},x} - \frac{\llbracket v_x^2 \rrbracket + \llbracket v_y^2 \rrbracket}{2} f_{\varrho}^{\text{num},x} + \llbracket v_x \rrbracket f_{\varrho v_x}^{\text{num},x} + \llbracket v_y \rrbracket f_{\varrho v_y}^{\text{num},x}, \end{cases} \\
f^{\text{num},y} &\begin{cases} f_{\varrho}^{\text{num},y} = \llbracket \varrho \rrbracket_{\log} \llbracket v_y \rrbracket, \\ f_{\varrho v_x}^{\text{num},y} = \llbracket v_x \rrbracket f_{\varrho}^{\text{num},y}, \\ f_{\varrho v_y}^{\text{num},y} = \llbracket v_y \rrbracket f_{\varrho}^{\text{num},y} + \frac{\llbracket \varrho \rrbracket}{2\llbracket \beta \rrbracket}, \\ f_{\varrho e}^{\text{num},y} = \frac{1}{2(\gamma-1)} \frac{1}{\llbracket \beta \rrbracket_{\log}} f_{\varrho}^{\text{num},y} - \frac{\llbracket v_x^2 \rrbracket + \llbracket v_y^2 \rrbracket}{2} f_{\varrho}^{\text{num},y} + \llbracket v_x \rrbracket f_{\varrho v_x}^{\text{num},y} + \llbracket v_y \rrbracket f_{\varrho v_y}^{\text{num},y}, \end{cases}
\end{aligned} \tag{61}$$

proposed by Chandrashekar (2013) can be seen to be entropy conservative. Since $p = \frac{\varrho}{2\beta}$, they are consistent. Additionally, they are kinetic energy preserving with numerical pressure flux

$$p^{\text{num}} = \frac{\llbracket \varrho \rrbracket}{2\llbracket \beta \rrbracket}.$$

4.2.2 Variant 2

Choosing another possibility to split the jumps

$$\begin{aligned}
\llbracket \beta v_{x/y}^2 \rrbracket &= \llbracket \beta v_{x/y} \rrbracket \llbracket v_{x/y} \rrbracket + \llbracket v_{x/y} \rrbracket \llbracket \beta v_{x/y} \rrbracket \\
&= \llbracket \beta v_{x/y} \rrbracket \llbracket v_{x/y} \rrbracket + \llbracket \beta \rrbracket \llbracket v_{x/y} \rrbracket \llbracket v_{x/y} \rrbracket + \llbracket v_{x/y} \rrbracket^2 \llbracket \beta \rrbracket,
\end{aligned} \tag{62}$$

the entropy conservation conditions (41) can be written as

$$\begin{aligned}
0 = & \left(\frac{1}{\{\{\varrho\}\}_{\log}} f_{\varrho}^{\text{num},x} - \{\{v_x\}\} \right) [\varrho] \\
& + \left(-\{\{\beta v_x\}\} f_{\varrho}^{\text{num},x} - \{\{\beta\}\} \{\{v_x\}\} f_{\varrho}^{\text{num},x} + 2\{\{\beta\}\} f_{\varrho v_x}^{\text{num},x} - \{\{\varrho\}\} \right) [v_x] \\
& + \left(-\{\{\beta v_y\}\} f_{\varrho}^{\text{num},x} - \{\{\beta\}\} \{\{v_y\}\} f_{\varrho}^{\text{num},x} + 2\{\{\beta\}\} f_{\varrho v_y}^{\text{num},x} \right) [v_y] \\
& + \left(\frac{1}{\gamma-1} \frac{1}{\{\{\beta\}\}_{\log}} f_{\varrho}^{\text{num},x} - \{\{v_x^2\}\} f_{\varrho}^{\text{num},x} - \{\{v_y^2\}\} f_{\varrho}^{\text{num},x} \right. \\
& \quad \left. + 2\{\{v_x\}\} f_{\varrho v_x}^{\text{num},x} + 2\{\{v_y\}\} f_{\varrho v_y}^{\text{num},x} - 2f_{\varrho e}^{\text{num},x} \right) [\beta], \\
0 = & \left(\frac{1}{\{\{\varrho\}\}_{\log}} f_{\varrho}^{\text{num},y} - \{\{v_y\}\} \right) [\varrho] \\
& + \left(-\{\{\beta v_x\}\} f_{\varrho}^{\text{num},y} - \{\{\beta\}\} \{\{v_x\}\} f_{\varrho}^{\text{num},y} + 2\{\{\beta\}\} f_{\varrho v_x}^{\text{num},y} \right) [v_x] \\
& + \left(-\{\{\beta v_y\}\} f_{\varrho}^{\text{num},y} - \{\{\beta\}\} \{\{v_y\}\} f_{\varrho}^{\text{num},y} + 2\{\{\beta\}\} f_{\varrho v_y}^{\text{num},y} - \{\{\varrho\}\} \right) [v_y] \\
& + \left(\frac{1}{\gamma-1} \frac{1}{\{\{\beta\}\}_{\log}} f_{\varrho}^{\text{num},y} - \{\{v_x^2\}\} f_{\varrho}^{\text{num},y} - \{\{v_y^2\}\} f_{\varrho}^{\text{num},y} \right. \\
& \quad \left. + 2\{\{v_x\}\} f_{\varrho v_x}^{\text{num},y} + 2\{\{v_y\}\} f_{\varrho v_y}^{\text{num},y} - 2f_{\varrho e}^{\text{num},y} \right) [\beta].
\end{aligned} \tag{63}$$

Thus, the fluxes

$$\begin{aligned}
f^{\text{num},x} & \begin{cases} f_{\varrho}^{\text{num},x} = \{\{\varrho\}\}_{\log} \{\{v_x\}\}, \\ f_{\varrho v_x}^{\text{num},x} = \frac{\{\{\beta v_x\}\} + \{\{\beta\}\} \{\{v_x\}\}}{2\{\{\beta\}\}} f_{\varrho}^{\text{num},x} + \frac{\{\{\varrho\}\}}{2\{\{\beta\}\}}, \\ f_{\varrho v_y}^{\text{num},x} = \frac{\{\{\beta v_y\}\} + \{\{\beta\}\} \{\{v_y\}\}}{2\{\{\beta\}\}} f_{\varrho}^{\text{num},x}, \\ f_{\varrho e}^{\text{num},x} = \frac{1}{2(\gamma-1)} \frac{1}{\{\{\beta\}\}_{\log}} f_{\varrho}^{\text{num},x} - \frac{\{\{v_x^2\}\} + \{\{v_y^2\}\}}{2} f_{\varrho}^{\text{num},x} + \{\{v_x\}\} f_{\varrho v_x}^{\text{num},x} + \{\{v_y\}\} f_{\varrho v_y}^{\text{num},x}, \end{cases} \\
f^{\text{num},y} & \begin{cases} f_{\varrho}^{\text{num},y} = \{\{\varrho\}\}_{\log} \{\{v_y\}\}, \\ f_{\varrho v_x}^{\text{num},y} = \frac{\{\{\beta v_x\}\} + \{\{\beta\}\} \{\{v_x\}\}}{2\{\{\beta\}\}} f_{\varrho}^{\text{num},y}, \\ f_{\varrho v_y}^{\text{num},y} = \frac{\{\{\beta v_y\}\} + \{\{\beta\}\} \{\{v_y\}\}}{2\{\{\beta\}\}} f_{\varrho}^{\text{num},y} + \frac{\{\{\varrho\}\}}{2\{\{\beta\}\}}, \\ f_{\varrho e}^{\text{num},y} = \frac{1}{2(\gamma-1)} \frac{1}{\{\{\beta\}\}_{\log}} f_{\varrho}^{\text{num},y} - \frac{\{\{v_x^2\}\} + \{\{v_y^2\}\}}{2} f_{\varrho}^{\text{num},y} + \{\{v_x\}\} f_{\varrho v_x}^{\text{num},y} + \{\{v_y\}\} f_{\varrho v_y}^{\text{num},y}, \end{cases}
\end{aligned} \tag{64}$$

proposed by Chandrashekar (2013) can be seen to be entropy conservative. They are not directly kinetic energy preserving. However, considering

$$p^{\text{num}} = \frac{\{\{\varrho\}\}}{2\{\{\beta\}\}} + \frac{\{\{\beta v_{x/y}\}\} - \{\{\beta\}\} \{\{v_{x/y}\}\}}{2\{\{\beta\}\}} f_{\varrho}^{\text{num},x/y}, \tag{65}$$

they might be seen as kinetic energy preserving, since the second term is consistent with zero.

4.3 $\varrho, v, \frac{1}{p}$ as variables

Using the variables $\varrho, v, \frac{1}{p}$, the flux potentials (9) and the entropy variables (8) can be written as

$$\psi_x = \varrho v_x, \quad \psi_y = \varrho v_y, \quad (66)$$

$$w = \left(\frac{\gamma}{\gamma-1} - \frac{s}{\gamma-1} - \frac{\varrho v^2}{2p}, \frac{\varrho v_x}{p}, \frac{\varrho v_y}{p}, -\frac{\varrho}{p} \right)^T, \quad s = \log \frac{p}{\varrho^\gamma} = -\log \frac{1}{p} - \gamma \log \varrho. \quad (67)$$

4.3.1 Variant 1

One variant to write the jumps is given by setting

$$\begin{aligned} \llbracket w_1 \rrbracket &= -\frac{1}{\gamma-1} \llbracket s \rrbracket - \frac{1}{2} \left\llbracket \frac{\varrho v^2}{p} \right\rrbracket = \frac{1}{\gamma-1} \left\llbracket \log \frac{1}{p} + \gamma \log \varrho \right\rrbracket - \frac{1}{2} \left\llbracket \frac{\varrho v^2}{p} \right\rrbracket \\ &= \frac{1}{\gamma-1} \frac{1}{\llbracket p^{-1} \rrbracket_{\log}} \llbracket p^{-1} \rrbracket + \frac{\gamma}{\gamma-1} \frac{1}{\llbracket \varrho \rrbracket_{\log}} \llbracket \varrho \rrbracket - \left\llbracket \frac{\varrho}{p} \right\rrbracket \llbracket v_x \rrbracket \llbracket v_x \rrbracket \\ &\quad - \left\llbracket \frac{\varrho}{p} \right\rrbracket \llbracket v_y \rrbracket \llbracket v_y \rrbracket - \llbracket \varrho \rrbracket \frac{\llbracket v_x^2 \rrbracket + \llbracket v_y^2 \rrbracket}{2} \llbracket p^{-1} \rrbracket - \frac{\llbracket v_x^2 \rrbracket + \llbracket v_y^2 \rrbracket}{2} \llbracket p^{-1} \rrbracket \llbracket \varrho \rrbracket, \\ \llbracket w_2 \rrbracket &= \left\llbracket \frac{\varrho v_x}{p} \right\rrbracket = \left\llbracket \frac{\varrho}{p} \right\rrbracket \llbracket v_x \rrbracket + \llbracket \varrho \rrbracket \llbracket v_x \rrbracket \llbracket p^{-1} \rrbracket + \llbracket v_x \rrbracket \llbracket p^{-1} \rrbracket \llbracket \varrho \rrbracket, \\ \llbracket w_3 \rrbracket &= \left\llbracket \frac{\varrho v_y}{p} \right\rrbracket = \left\llbracket \frac{\varrho}{p} \right\rrbracket \llbracket v_y \rrbracket + \llbracket \varrho \rrbracket \llbracket v_y \rrbracket \llbracket p^{-1} \rrbracket + \llbracket v_y \rrbracket \llbracket p^{-1} \rrbracket \llbracket \varrho \rrbracket, \\ \llbracket w_4 \rrbracket &= -\left\llbracket \frac{\varrho}{p} \right\rrbracket = -\llbracket \varrho \rrbracket \llbracket p^{-1} \rrbracket - \llbracket p^{-1} \rrbracket \llbracket \varrho \rrbracket, \\ \llbracket \psi_x \rrbracket &= \llbracket \varrho v_x \rrbracket = \llbracket \varrho \rrbracket \llbracket v_x \rrbracket + \llbracket v_x \rrbracket \llbracket \varrho \rrbracket, \\ \llbracket \psi_y \rrbracket &= \llbracket \varrho v_y \rrbracket = \llbracket \varrho \rrbracket \llbracket v_y \rrbracket + \llbracket v_y \rrbracket \llbracket \varrho \rrbracket. \end{aligned} \quad (68)$$

Therefore, the entropy conservation conditions (41) can be written as

$$\begin{aligned} 0 &= \left(\frac{\gamma}{\gamma-1} \frac{1}{\llbracket \varrho \rrbracket_{\log}} f_{\varrho}^{\text{num},x} - \frac{\llbracket v_x^2 \rrbracket + \llbracket v_y^2 \rrbracket}{2} \llbracket p^{-1} \rrbracket f_{\varrho}^{\text{num},x} + \llbracket p^{-1} \rrbracket \llbracket v_x \rrbracket f_{\varrho v_x}^{\text{num},x} \right. \\ &\quad \left. + \llbracket p^{-1} \rrbracket \llbracket v_y \rrbracket f_{\varrho v_y}^{\text{num},x} - \llbracket p^{-1} \rrbracket f_{\varrho e}^{\text{num},x} - \llbracket v_x \rrbracket \right) \llbracket \varrho \rrbracket \\ &\quad + \left(-\left\llbracket \frac{\varrho}{p} \right\rrbracket \llbracket v_x \rrbracket f_{\varrho}^{\text{num},x} + \left\llbracket \frac{\varrho}{p} \right\rrbracket f_{\varrho v_x}^{\text{num},x} - \llbracket \varrho \rrbracket \right) \llbracket v_x \rrbracket + \left(-\left\llbracket \frac{\varrho}{p} \right\rrbracket \llbracket v_y \rrbracket f_{\varrho}^{\text{num},x} + \left\llbracket \frac{\varrho}{p} \right\rrbracket f_{\varrho v_y}^{\text{num},x} \right) \llbracket v_y \rrbracket \\ &\quad + \left(\frac{1}{\gamma-1} \frac{1}{\llbracket p^{-1} \rrbracket_{\log}} f_{\varrho}^{\text{num},x} - \llbracket \varrho \rrbracket \frac{\llbracket v_x^2 \rrbracket + \llbracket v_y^2 \rrbracket}{2} f_{\varrho}^{\text{num},x} + \llbracket \varrho \rrbracket \llbracket v_x \rrbracket f_{\varrho v_x}^{\text{num},x} \right. \\ &\quad \left. + \llbracket \varrho \rrbracket \llbracket v_y \rrbracket f_{\varrho v_y}^{\text{num},x} - \llbracket \varrho \rrbracket f_{\varrho e}^{\text{num},x} \right) \llbracket p^{-1} \rrbracket, \end{aligned} \quad (69)$$

$$\begin{aligned}
0 = & \left(\frac{\gamma}{\gamma-1} \frac{1}{\{\{\varrho\}\}_{\log}} f_{\varrho}^{\text{num},y} - \frac{\{\{v_x^2\}\} + \{\{v_y^2\}\}}{2} \{\{p^{-1}\}\} f_{\varrho}^{\text{num},y} + \{\{p^{-1}\}\} \{\{v_x\}\} f_{\varrho v_x}^{\text{num},y} \right. \\
& \left. + \{\{p^{-1}\}\} \{\{v_y\}\} f_{\varrho v_y}^{\text{num},y} - \{\{p^{-1}\}\} f_{\varrho e}^{\text{num},y} - \{\{v_y\}\} \right) [\varrho] \\
& + \left(-\{\{\frac{\varrho}{p}\}\} \{\{v_x\}\} f_{\varrho}^{\text{num},y} + \{\{\frac{\varrho}{p}\}\} f_{\varrho v_x}^{\text{num},y} \right) [v_x] + \left(-\{\{\frac{\varrho}{p}\}\} \{\{v_y\}\} f_{\varrho}^{\text{num},y} + \{\{\frac{\varrho}{p}\}\} f_{\varrho v_y}^{\text{num},y} - \{\{\varrho\}\} \right) [v_y] \\
& + \left(\frac{1}{\gamma-1} \frac{1}{\{\{p^{-1}\}\}_{\log}} f_{\varrho}^{\text{num},y} - \{\{\varrho\}\} \frac{\{\{v_x^2\}\} + \{\{v_y^2\}\}}{2} f_{\varrho}^{\text{num},y} + \{\{\varrho\}\} \{\{v_x\}\} f_{\varrho v_x}^{\text{num},y} \right. \\
& \left. + \{\{\varrho\}\} \{\{v_y\}\} f_{\varrho v_y}^{\text{num},y} - \{\{\varrho\}\} f_{\varrho e}^{\text{num},y} \right) [p^{-1}].
\end{aligned} \tag{70}$$

Thus, the fluxes

$$\begin{aligned}
f_{\text{num},x} & \begin{cases} f_{\varrho}^{\text{num},x} = (\gamma-1) \left(\frac{\gamma}{\{\{\varrho\}\}_{\log}} - \frac{\{\{p^{-1}\}\}}{\{\{p^{-1}\}\}_{\log} \{\{\varrho\}\}} \right)^{-1} \{\{v_x\}\}, \\ f_{\varrho v_x}^{\text{num},x} = \{\{v_x\}\} f_{\varrho}^{\text{num},x} + \frac{\{\{\varrho\}\}}{\{\{\varrho/p\}\}}, \\ f_{\varrho v_y}^{\text{num},x} = \{\{v_y\}\} f_{\varrho}^{\text{num},x}, \\ f_{\varrho e}^{\text{num},x} = \left(\frac{1}{\gamma-1} \frac{1}{\{\{p^{-1}\}\}_{\log} \{\{\varrho\}\}} + \{\{v_x\}\}^2 + \{\{v_y\}\}^2 - \frac{\{\{v_x^2\}\} + \{\{v_y^2\}\}}{2} \right) f_{\varrho}^{\text{num},x} + \frac{\{\{\varrho\}\} \{\{v_x\}\}}{\{\{\varrho/p\}\}}, \end{cases} \\
f_{\text{num},y} & \begin{cases} f_{\varrho}^{\text{num},y} = (\gamma-1) \left(\frac{\gamma}{\{\{\varrho\}\}_{\log}} - \frac{\{\{p^{-1}\}\}}{\{\{p^{-1}\}\}_{\log} \{\{\varrho\}\}} \right)^{-1} \{\{v_y\}\}, \\ f_{\varrho v_x}^{\text{num},y} = \{\{v_x\}\} f_{\varrho}^{\text{num},y}, \\ f_{\varrho v_y}^{\text{num},y} = \{\{v_y\}\} f_{\varrho}^{\text{num},y} + \frac{\{\{\varrho\}\}}{\{\{\varrho/p\}\}}, \\ f_{\varrho e}^{\text{num},y} = \left(\frac{1}{\gamma-1} \frac{1}{\{\{p^{-1}\}\}_{\log} \{\{\varrho\}\}} + \{\{v_x\}\}^2 + \{\{v_y\}\}^2 - \frac{\{\{v_x^2\}\} + \{\{v_y^2\}\}}{2} \right) f_{\varrho}^{\text{num},y} + \frac{\{\{\varrho\}\} \{\{v_y\}\}}{\{\{\varrho/p\}\}}, \end{cases}
\end{aligned} \tag{71}$$

can be seen to be entropy conservative and consistent. Additionally, they are kinetic energy preserving with numerical pressure flux $p^{\text{num}} = \frac{\{\{\varrho\}\}}{\{\{\varrho/p\}\}}$.

Again, similarly to the flux (55) of Ismail and Roe (2009); Roe (2006), the pressure influences the numerical density flux, leading to some problems as explained by Derigs, Winters, Gassner, and Walch (2017), see also the numerical tests in section 7.

4.4 ϱ, v, p as variables

Using the variables ϱ, v, p , the flux potentials (9) and the entropy variables (8) can be written as

$$\psi_x = \varrho v_x, \quad \psi_y = \varrho v_y, \tag{72}$$

$$w = \left(\frac{\gamma}{\gamma-1} - \frac{s}{\gamma-1} - \frac{\varrho v^2}{2p}, \frac{\varrho v_x}{p}, \frac{\varrho v_y}{p}, -\frac{\varrho}{p} \right)^T, \quad s = \log \frac{p}{\varrho^\gamma} = \log p - \gamma \log \varrho. \tag{73}$$

In order to handle the terms $\frac{1}{p}$, a new mean value has to be used. Since

$$\left[\left[\frac{1}{a}\right]\right] = \frac{1}{a_+} - \frac{1}{a_-} = \frac{a_- - a_+}{a_+ a_-}, \quad (74)$$

the *geometric mean*

$$\{a\}_{\text{geo}} := \sqrt{a_+ a_-}, \quad (75)$$

fulfils

$$\left[\left[\frac{1}{a}\right]\right] = -\frac{1}{\{a\}_{\text{geo}}^2} [a]. \quad (76)$$

4.4.1 Variant 1

One variant to write the jumps is

$$\begin{aligned} \llbracket w_1 \rrbracket &= -\frac{1}{\gamma-1} \llbracket s \rrbracket - \frac{1}{2} \left[\left[\frac{\varrho v^2}{p}\right]\right] = \frac{1}{\gamma-1} \llbracket -\log p + \gamma \log \varrho \rrbracket - \frac{1}{2} \left[\left[\frac{\varrho v^2}{p}\right]\right] \\ &= -\frac{1}{\gamma-1} \frac{1}{\{p\}_{\log}} \llbracket p \rrbracket + \frac{\gamma}{\gamma-1} \frac{1}{\{\varrho\}_{\log}} \llbracket \varrho \rrbracket - \left\{\left\{\frac{\varrho}{p}\right\}\right\} \{v_x\} \llbracket v_x \rrbracket \\ &\quad - \left\{\left\{\frac{\varrho}{p}\right\}\right\} \{v_y\} \llbracket v_y \rrbracket + \{\varrho\} \frac{\{v_x^2\} + \{v_y^2\}}{2\{p\}_{\text{geo}}^2} \llbracket p \rrbracket - \frac{\{v_x^2\} + \{v_y^2\}}{2} \{p^{-1}\} \llbracket \varrho \rrbracket, \\ \llbracket w_2 \rrbracket &= \left[\left[\frac{\varrho v_x}{p}\right]\right] = \left\{\left\{\frac{\varrho}{p}\right\}\right\} \{v_x\} - \frac{\{\varrho\} \{v_x\}}{\{p\}_{\text{geo}}^2} \llbracket p \rrbracket + \{p^{-1}\} \{v_x\} \llbracket \varrho \rrbracket, \\ \llbracket w_3 \rrbracket &= \left[\left[\frac{\varrho v_y}{p}\right]\right] = \left\{\left\{\frac{\varrho}{p}\right\}\right\} \{v_y\} - \frac{\{\varrho\} \{v_y\}}{\{p\}_{\text{geo}}^2} \llbracket p \rrbracket + \{p^{-1}\} \{v_y\} \llbracket \varrho \rrbracket, \\ \llbracket w_4 \rrbracket &= -\left[\left[\frac{\varrho}{p}\right]\right] = \frac{\{\varrho\}}{\{p\}_{\text{geo}}^2} \llbracket p \rrbracket - \{p^{-1}\} \llbracket \varrho \rrbracket, \\ \llbracket \psi \rrbracket &= \llbracket \varrho v \rrbracket = \{\varrho\} \llbracket v \rrbracket + \{v\} \llbracket \varrho \rrbracket. \end{aligned} \quad (77)$$

Therefore, the entropy conservation conditions (41) can be written as

$$\begin{aligned} 0 &= \left(\frac{\gamma}{\gamma-1} \frac{1}{\{\varrho\}_{\log}} f_{\varrho}^{\text{num},x} - \frac{\{v_x^2\} + \{v_y^2\}}{2} \{p^{-1}\} f_{\varrho}^{\text{num},x} + \{p^{-1}\} \{v_x\} f_{\varrho v_x}^{\text{num},x} \right. \\ &\quad \left. + \{p^{-1}\} \{v_y\} f_{\varrho v_y}^{\text{num},x} - \{p^{-1}\} f_{\varrho e}^{\text{num},x} - \{v_x\} \right) \llbracket \varrho \rrbracket \\ &\quad + \left(-\left\{\left\{\frac{\varrho}{p}\right\}\right\} \{v_x\} f_{\varrho}^{\text{num},x} + \left\{\left\{\frac{\varrho}{p}\right\}\right\} f_{\varrho v_x}^{\text{num},x} - \{\varrho\} \right) \llbracket v_x \rrbracket + \left(-\left\{\left\{\frac{\varrho}{p}\right\}\right\} \{v_y\} f_{\varrho}^{\text{num},x} + \left\{\left\{\frac{\varrho}{p}\right\}\right\} f_{\varrho v_y}^{\text{num},x} \right) \llbracket v_y \rrbracket \\ &\quad + \left(-\frac{1}{\gamma-1} \frac{1}{\{p\}_{\log}} f_{\varrho}^{\text{num},x} + \{\varrho\} \frac{\{v_x^2\} + \{v_y^2\}}{2\{p\}_{\text{geo}}^2} f_{\varrho}^{\text{num},x} - \frac{\{\varrho\} \{v_x\}}{\{p\}_{\text{geo}}^2} f_{\varrho v_x}^{\text{num},x} \right. \\ &\quad \left. - \frac{\{\varrho\} \{v_y\}}{\{p\}_{\text{geo}}^2} f_{\varrho v_y}^{\text{num},x} + \frac{\{\varrho\}}{\{p\}_{\text{geo}}^2} f_{\varrho e}^{\text{num},x} \right) \llbracket p \rrbracket, \end{aligned} \quad (78)$$

$$\begin{aligned}
0 = & \left(\frac{\gamma}{\gamma-1} \frac{1}{\{\varrho\}_{\log}} f_{\varrho}^{\text{num},y} - \frac{\{\{v_x^2\} + \{v_y^2\}\}}{2} \{\{p^{-1}\}\} f_{\varrho}^{\text{num},y} + \{\{p^{-1}\}\} \{\{v_x\}\} f_{\varrho v_x}^{\text{num},y} \right. \\
& \left. + \{\{p^{-1}\}\} \{\{v_y\}\} f_{\varrho v_y}^{\text{num},y} - \{\{p^{-1}\}\} f_{\varrho e}^{\text{num},y} - \{\{v_y\}\} \right) [\varrho] \\
& + \left(-\{\{\frac{\varrho}{p}\}\} \{\{v_x\}\} f_{\varrho}^{\text{num},y} + \{\{\frac{\varrho}{p}\}\} f_{\varrho v_x}^{\text{num},y} \right) [v_x] + \left(-\{\{\frac{\varrho}{p}\}\} \{\{v_y\}\} f_{\varrho}^{\text{num},y} + \{\{\frac{\varrho}{p}\}\} f_{\varrho v_y}^{\text{num},y} - \{\{\varrho\}\} \right) [v_y] \\
& + \left(-\frac{1}{\gamma-1} \frac{1}{\{\{p\}\}_{\log}} f_{\varrho}^{\text{num},y} + \{\{\varrho\}\} \frac{\{\{v_x^2\} + \{v_y^2\}\}}{2\{\{p\}\}_{\text{geo}}^2} f_{\varrho}^{\text{num},y} - \frac{\{\{\varrho\}\} \{\{v_x\}\}}{\{\{p\}\}_{\text{geo}}^2} f_{\varrho v_x}^{\text{num},y} \right. \\
& \left. - \frac{\{\{\varrho\}\} \{\{v_y\}\}}{\{\{p\}\}_{\text{geo}}^2} f_{\varrho v_y}^{\text{num},y} + \frac{\{\{\varrho\}\}}{\{\{p\}\}_{\text{geo}}^2} f_{\varrho e}^{\text{num},y} \right) [p].
\end{aligned} \tag{79}$$

Thus, the fluxes

$$\begin{aligned}
f_{\text{num},x} & \left\{ \begin{aligned} f_{\varrho}^{\text{num},x} &= (\gamma-1) \left(\frac{\gamma}{\{\{\varrho\}\}_{\log}} - \frac{\{\{p^{-1}\}\} \{\{p\}\}_{\text{geo}}^2}{\{\{\varrho\}\} \{\{p\}\}_{\log}} \right)^{-1} \{\{v_x\}\}, \\ f_{\varrho v_x}^{\text{num},x} &= \{\{v_x\}\} f_{\varrho}^{\text{num},x} + \frac{\{\{\varrho\}\}}{\{\{\varrho/p\}\}}, \\ f_{\varrho v_y}^{\text{num},x} &= \{\{v_y\}\} f_{\varrho}^{\text{num},x}, \\ f_{\varrho e}^{\text{num},x} &= \left(\frac{1}{\gamma-1} \frac{\{\{p\}\}_{\text{geo}}^2}{\{\{\varrho\}\} \{\{p\}\}_{\log}} + \{\{v_x\}\}^2 + \{\{v_y\}\}^2 - \frac{\{\{v_x^2\} + \{v_y^2\}\}}{2} \right) f_{\varrho}^{\text{num},x} + \frac{\{\{\varrho\}\} \{\{v\}\}}{\{\{\varrho/p\}\}}, \end{aligned} \right. \\
f_{\text{num},y} & \left\{ \begin{aligned} f_{\varrho}^{\text{num},y} &= (\gamma-1) \left(\frac{\gamma}{\{\{\varrho\}\}_{\log}} - \frac{\{\{p^{-1}\}\} \{\{p\}\}_{\text{geo}}^2}{\{\{\varrho\}\} \{\{p\}\}_{\log}} \right)^{-1} \{\{v_y\}\}, \\ f_{\varrho v_x}^{\text{num},y} &= \{\{v_x\}\} f_{\varrho}^{\text{num},y}, \\ f_{\varrho v_y}^{\text{num},y} &= \{\{v_y\}\} f_{\varrho}^{\text{num},y} + \frac{\{\{\varrho\}\}}{\{\{\varrho/p\}\}}, \\ f_{\varrho e}^{\text{num},y} &= \left(\frac{1}{\gamma-1} \frac{\{\{p\}\}_{\text{geo}}^2}{\{\{\varrho\}\} \{\{p\}\}_{\log}} + \{\{v_x\}\}^2 + \{\{v_y\}\}^2 - \frac{\{\{v_x^2\} + \{v_y^2\}\}}{2} \right) f_{\varrho}^{\text{num},y} + \frac{\{\{\varrho\}\} \{\{v\}\}}{\{\{\varrho/p\}\}}, \end{aligned} \right.
\end{aligned} \tag{80}$$

can be seen to be entropy conservative and consistent. Additionally, they are kinetic energy preserving with numerical pressure flux $p^{\text{num}} = \frac{\{\{\varrho\}\}}{\{\{\varrho/p\}\}}$.

As before, the pressure influences the numerical density flux, leading to some problems as explained by Derigs, Winters, Gassner, and Walch (2017), see also the numerical tests in section 7.

4.5 ϱ, v, T as variables

Using the variables ϱ, v , and $RT = \frac{p}{\varrho}$, the flux potentials (9) and the entropy variables (8) can be written as

$$\psi_x = \varrho v_x, \quad \psi_y = \varrho v_y, \tag{81}$$

$$w = \left(\frac{\gamma}{\gamma-1} - \frac{s}{\gamma-1} - \frac{v^2}{2RT}, \frac{v_x}{RT}, \frac{v_y}{RT}, -\frac{1}{RT} \right)^T, \quad s = \log \frac{p}{\varrho^\gamma} = \log RT - (\gamma-1) \log \varrho. \tag{82}$$

4.5.1 Variant 1

One way to write the jumps is

$$\begin{aligned}
\llbracket w_1 \rrbracket &= -\frac{1}{\gamma-1} \llbracket s \rrbracket - \frac{1}{2} \left\llbracket \frac{v^2}{RT} \right\rrbracket = -\frac{1}{\gamma-1} \llbracket \log RT \rrbracket + \llbracket \log \varrho \rrbracket - \frac{1}{2} \left\llbracket \frac{v^2}{RT} \right\rrbracket \\
&= -\frac{1}{\gamma-1} \frac{1}{\{\!\{RT\}\!\}_{\log}} \llbracket RT \rrbracket + \frac{1}{\{\!\{\varrho\}\!\}_{\log}} \llbracket \varrho \rrbracket - \left\{\!\left\{ \frac{1}{RT} \right\}\!\right\} \{\!\{v_x\}\!\} \llbracket v_x \rrbracket - \left\{\!\left\{ \frac{1}{RT} \right\}\!\right\} \{\!\{v_y\}\!\} \llbracket v_y \rrbracket \\
&\quad + \frac{\{\!\{v_x^2\}\!\} + \{\!\{v_y^2\}\!\}}{2\{\!\{RT\}\!\}_{\text{geo}}^2} \llbracket RT \rrbracket, \\
\llbracket w_2 \rrbracket &= \left\llbracket \frac{v_x}{RT} \right\rrbracket = \left\{\!\left\{ \frac{1}{RT} \right\}\!\right\} \llbracket v_x \rrbracket - \frac{\{\!\{v_x\}\!\}}{\{\!\{RT\}\!\}_{\text{geo}}^2} \llbracket RT \rrbracket, \\
\llbracket w_3 \rrbracket &= \left\llbracket \frac{v_y}{RT} \right\rrbracket = \left\{\!\left\{ \frac{1}{RT} \right\}\!\right\} \llbracket v_y \rrbracket - \frac{\{\!\{v_y\}\!\}}{\{\!\{RT\}\!\}_{\text{geo}}^2} \llbracket RT \rrbracket, \\
\llbracket w_4 \rrbracket &= -\left\llbracket \frac{1}{RT} \right\rrbracket = \frac{1}{\{\!\{RT\}\!\}_{\text{geo}}^2} \llbracket RT \rrbracket, \\
\llbracket \psi_x \rrbracket &= \llbracket \varrho v_x \rrbracket = \{\!\{\varrho\}\!\} \llbracket v_x \rrbracket + \{\!\{v_x\}\!\} \llbracket \varrho \rrbracket, \\
\llbracket \psi_y \rrbracket &= \llbracket \varrho v_y \rrbracket = \{\!\{\varrho\}\!\} \llbracket v_y \rrbracket + \{\!\{v_y\}\!\} \llbracket \varrho \rrbracket.
\end{aligned} \tag{83}$$

Therefore, the entropy conservation conditions (41) can be written as

$$\begin{aligned}
0 &= \left(\frac{1}{\{\!\{\varrho\}\!\}_{\log}} f_{\varrho}^{\text{num},x} - \{\!\{v_x\}\!\} \right) \llbracket \varrho \rrbracket + \left(-\left\{\!\left\{ \frac{1}{RT} \right\}\!\right\} \{\!\{v_x\}\!\} f_{\varrho}^{\text{num},x} + \left\{\!\left\{ \frac{1}{RT} \right\}\!\right\} f_{\varrho v_x}^{\text{num},x} - \{\!\{\varrho\}\!\} \right) \llbracket v_x \rrbracket \\
&\quad + \left(-\left\{\!\left\{ \frac{1}{RT} \right\}\!\right\} \{\!\{v_y\}\!\} f_{\varrho}^{\text{num},x} + \left\{\!\left\{ \frac{1}{RT} \right\}\!\right\} f_{\varrho v_y}^{\text{num},x} \right) \llbracket v_y \rrbracket \\
&\quad + \left(-\frac{1}{\gamma-1} \frac{1}{\{\!\{RT\}\!\}_{\log}} f_{\varrho}^{\text{num},x} + \frac{\{\!\{v_x^2\}\!\} + \{\!\{v_y^2\}\!\}}{2\{\!\{RT\}\!\}_{\text{geo}}^2} f_{\varrho}^{\text{num},x} - \frac{\{\!\{v_x\}\!\}}{\{\!\{RT\}\!\}_{\text{geo}}^2} f_{\varrho v_x}^{\text{num},x} \right. \\
&\quad \left. - \frac{\{\!\{v_y\}\!\}}{\{\!\{RT\}\!\}_{\text{geo}}^2} f_{\varrho v_y}^{\text{num},x} + \frac{1}{\{\!\{RT\}\!\}_{\text{geo}}^2} f_{\varrho e}^{\text{num},x} \right) \llbracket RT \rrbracket, \\
0 &= \left(\frac{1}{\{\!\{\varrho\}\!\}_{\log}} f_{\varrho}^{\text{num},y} - \{\!\{v_y\}\!\} \right) \llbracket \varrho \rrbracket + \left(-\left\{\!\left\{ \frac{1}{RT} \right\}\!\right\} \{\!\{v_x\}\!\} f_{\varrho}^{\text{num},y} + \left\{\!\left\{ \frac{1}{RT} \right\}\!\right\} f_{\varrho v_x}^{\text{num},y} \right) \llbracket v_x \rrbracket \\
&\quad + \left(-\left\{\!\left\{ \frac{1}{RT} \right\}\!\right\} \{\!\{v_y\}\!\} f_{\varrho}^{\text{num},y} + \left\{\!\left\{ \frac{1}{RT} \right\}\!\right\} f_{\varrho v_y}^{\text{num},y} - \{\!\{\varrho\}\!\} \right) \llbracket v_y \rrbracket \\
&\quad + \left(-\frac{1}{\gamma-1} \frac{1}{\{\!\{RT\}\!\}_{\log}} f_{\varrho}^{\text{num},y} + \frac{\{\!\{v_x^2\}\!\} + \{\!\{v_y^2\}\!\}}{2\{\!\{RT\}\!\}_{\text{geo}}^2} f_{\varrho}^{\text{num},y} - \frac{\{\!\{v_x\}\!\}}{\{\!\{RT\}\!\}_{\text{geo}}^2} f_{\varrho v_x}^{\text{num},y} \right. \\
&\quad \left. - \frac{\{\!\{v_y\}\!\}}{\{\!\{RT\}\!\}_{\text{geo}}^2} f_{\varrho v_y}^{\text{num},y} + \frac{1}{\{\!\{RT\}\!\}_{\text{geo}}^2} f_{\varrho e}^{\text{num},y} \right) \llbracket RT \rrbracket.
\end{aligned} \tag{84}$$

Thus, the fluxes

$$\begin{aligned}
f^{\text{num},x} & \begin{cases} f_{\varrho}^{\text{num},x} = \llbracket \varrho \rrbracket_{\log} \llbracket v_x \rrbracket, \\ f_{\varrho v_x}^{\text{num},x} = \llbracket v_x \rrbracket f_{\varrho}^{\text{num},x} + \frac{\llbracket \varrho \rrbracket}{\llbracket 1/RT \rrbracket}, \\ f_{\varrho v_y}^{\text{num},x} = \llbracket v_y \rrbracket f_{\varrho}^{\text{num},x}, \\ f_{\varrho e}^{\text{num},x} = \left(\frac{1}{\gamma-1} \frac{\llbracket RT \rrbracket_{\text{geo}}^2}{\llbracket RT \rrbracket_{\log}} - \frac{\llbracket v_x^2 \rrbracket + \llbracket v_y^2 \rrbracket}{2} \right) f_{\varrho}^{\text{num},x} + \llbracket v_x \rrbracket f_{\varrho v_x}^{\text{num},x} + \llbracket v_y \rrbracket f_{\varrho v_y}^{\text{num},x}, \end{cases} \\
f^{\text{num},y} & \begin{cases} f_{\varrho}^{\text{num},y} = \llbracket \varrho \rrbracket_{\log} \llbracket v_y \rrbracket, \\ f_{\varrho v_x}^{\text{num},y} = \llbracket v_x \rrbracket f_{\varrho}^{\text{num},y}, \\ f_{\varrho v_y}^{\text{num},y} = \llbracket v_y \rrbracket f_{\varrho}^{\text{num},y} + \frac{\llbracket \varrho \rrbracket}{\llbracket 1/RT \rrbracket}, \\ f_{\varrho e}^{\text{num},y} = \left(\frac{1}{\gamma-1} \frac{\llbracket RT \rrbracket_{\text{geo}}^2}{\llbracket RT \rrbracket_{\log}} - \frac{\llbracket v_x^2 \rrbracket + \llbracket v_y^2 \rrbracket}{2} \right) f_{\varrho}^{\text{num},y} + \llbracket v_x \rrbracket f_{\varrho v_x}^{\text{num},y} + \llbracket v_y \rrbracket f_{\varrho v_y}^{\text{num},y}, \end{cases}
\end{aligned} \tag{85}$$

can be seen to be entropy conservative and consistent. Additionally, they are kinetic energy preserving with numerical pressure flux $p^{\text{num}} = \frac{\llbracket \varrho \rrbracket}{\llbracket 1/RT \rrbracket}$, i.e. the same as for the entropy conservative and kinetic energy preserving flux (61) proposed by Chandrashekar (2013). Moreover, the density flux f_{ϱ}^{num} is the same. However, the energy fluxes $f_{\varrho e}^{\text{num}}$ are different.

4.5.2 Variant 2

Similarly to the derivation of (64), choosing another possibility to split the jump

$$\begin{aligned}
\left[\frac{v_{x/y}^2}{RT} \right] &= \left\{ \frac{v_{x/y}}{RT} \right\} \llbracket v_{x/y} \rrbracket + \left\{ v_{x/y} \right\} \left[\frac{v_{x/y}}{RT} \right] \\
&= \left\{ \frac{v_{x/y}}{RT} \right\} \llbracket v_{x/y} \rrbracket + \left\{ \frac{1}{RT} \right\} \left\{ v_{x/y} \right\} \llbracket v_{x/y} \rrbracket - \frac{\left\{ v_{x/y} \right\}^2}{\llbracket RT \rrbracket_{\text{geo}}^2} \llbracket RT \rrbracket,
\end{aligned} \tag{86}$$

the entropy conservation conditions (41) can be written as

$$\begin{aligned}
0 &= \left(\frac{1}{\llbracket \varrho \rrbracket_{\log}} f_{\varrho}^{\text{num},x} - \llbracket v_x \rrbracket \right) \llbracket \varrho \rrbracket \\
&+ \left(-\frac{1}{2} \left\{ \frac{v_x}{RT} \right\} f_{\varrho}^{\text{num},x} - \frac{1}{2} \left\{ \frac{1}{RT} \right\} \left\{ v_x \right\} f_{\varrho}^{\text{num},x} + \left\{ \frac{1}{RT} \right\} f_{\varrho v_x}^{\text{num},x} - \llbracket \varrho \rrbracket \right) \llbracket v_x \rrbracket \\
&+ \left(-\frac{1}{2} \left\{ \frac{v_y}{RT} \right\} f_{\varrho}^{\text{num},x} - \frac{1}{2} \left\{ \frac{1}{RT} \right\} \left\{ v_y \right\} f_{\varrho}^{\text{num},x} + \left\{ \frac{1}{RT} \right\} f_{\varrho v_y}^{\text{num},x} \right) \llbracket v_y \rrbracket \\
&+ \left(-\frac{1}{\gamma-1} \frac{1}{\llbracket RT \rrbracket_{\log}} f_{\varrho}^{\text{num},x} + \frac{\llbracket v_x \rrbracket^2 + \llbracket v_y \rrbracket^2}{2 \llbracket RT \rrbracket_{\text{geo}}^2} f_{\varrho}^{\text{num},x} - \frac{\llbracket v_x \rrbracket}{\llbracket RT \rrbracket_{\text{geo}}^2} f_{\varrho v_x}^{\text{num},x} \right. \\
&\quad \left. - \frac{\llbracket v_y \rrbracket}{\llbracket RT \rrbracket_{\text{geo}}^2} f_{\varrho v_y}^{\text{num},x} + \frac{1}{\llbracket RT \rrbracket_{\text{geo}}^2} f_{\varrho e}^{\text{num},x} \right) \llbracket RT \rrbracket,
\end{aligned} \tag{87}$$

$$\begin{aligned}
0 = & \left(\frac{1}{\{\{\varrho\}\}_{\log}} f_{\varrho}^{\text{num},y} - \{\{v_y\}\} \right) [\varrho] \\
& + \left(-\frac{1}{2} \left\{ \frac{v_x}{RT} \right\} f_{\varrho}^{\text{num},y} - \frac{1}{2} \left\{ \frac{1}{RT} \right\} \{\{v_x\}\} f_{\varrho}^{\text{num},y} + \left\{ \frac{1}{RT} \right\} f_{\varrho v_x}^{\text{num},y} \right) [v_x] \\
& + \left(-\frac{1}{2} \left\{ \frac{v_y}{RT} \right\} f_{\varrho}^{\text{num},y} - \frac{1}{2} \left\{ \frac{1}{RT} \right\} \{\{v_y\}\} f_{\varrho}^{\text{num},y} + \left\{ \frac{1}{RT} \right\} f_{\varrho v_y}^{\text{num},y} - \{\{\varrho\}\} \right) [v_y] \quad (88) \\
& + \left(-\frac{1}{\gamma-1} \frac{1}{\{\{RT\}\}_{\log}} f_{\varrho}^{\text{num},y} + \frac{\{\{v_x\}\}^2 + \{\{v_y\}\}^2}{2\{\{RT\}\}_{\text{geo}}^2} f_{\varrho}^{\text{num},y} - \frac{\{\{v_x\}\}}{\{\{RT\}\}_{\text{geo}}^2} f_{\varrho v_x}^{\text{num},y} \right. \\
& \quad \left. - \frac{\{\{v_y\}\}}{\{\{RT\}\}_{\text{geo}}^2} f_{\varrho v_y}^{\text{num},y} + \frac{1}{\{\{RT\}\}_{\text{geo}}^2} f_{\varrho e}^{\text{num},y} \right) [RT].
\end{aligned}$$

Thus, the fluxes

$$\begin{aligned}
f^{\text{num},x} & \begin{cases} f_{\varrho}^{\text{num},x} = \{\{\varrho\}\}_{\log} \{\{v_x\}\}, \\ f_{\varrho v_x}^{\text{num},x} = \frac{\{\{v_x/RT\}\} + \{\{1/RT\}\} \{\{v_x\}\}}{2\{\{1/RT\}\}} f_{\varrho}^{\text{num},x} + \frac{\{\{\varrho\}\}}{\{\{1/RT\}\}}, \\ f_{\varrho v_y}^{\text{num},x} = \frac{\{\{v_y/RT\}\} + \{\{1/RT\}\} \{\{v_y\}\}}{2\{\{1/RT\}\}} f_{\varrho}^{\text{num},x}, \\ f_{\varrho e}^{\text{num},x} = \left(\frac{1}{\gamma-1} \frac{\{\{RT\}\}_{\text{geo}}^2}{\{\{RT\}\}_{\log}} - \frac{\{\{v_x\}\}^2 + \{\{v_y\}\}^2}{2} \right) f_{\varrho}^{\text{num},x} + \{\{v_x\}\} f_{\varrho v_x}^{\text{num},x} + \{\{v_y\}\} f_{\varrho v_y}^{\text{num},x}, \end{cases} \\
f^{\text{num},y} & \begin{cases} f_{\varrho}^{\text{num},y} = \{\{\varrho\}\}_{\log} \{\{v_y\}\}, \\ f_{\varrho v_x}^{\text{num},y} = \frac{\{\{v_x/RT\}\} + \{\{1/RT\}\} \{\{v_x\}\}}{2\{\{1/RT\}\}} f_{\varrho}^{\text{num},y}, \\ f_{\varrho v_y}^{\text{num},y} = \frac{\{\{v_y/RT\}\} + \{\{1/RT\}\} \{\{v_y\}\}}{2\{\{1/RT\}\}} f_{\varrho}^{\text{num},y} + \frac{\{\{\varrho\}\}}{\{\{1/RT\}\}}, \\ f_{\varrho e}^{\text{num},y} = \left(\frac{1}{\gamma-1} \frac{\{\{RT\}\}_{\text{geo}}^2}{\{\{RT\}\}_{\log}} - \frac{\{\{v_x\}\}^2 + \{\{v_y\}\}^2}{2} \right) f_{\varrho}^{\text{num},y} + \{\{v_x\}\} f_{\varrho v_x}^{\text{num},y} + \{\{v_y\}\} f_{\varrho v_y}^{\text{num},y}, \end{cases} \quad (89)
\end{aligned}$$

can be seen to be entropy conservative. They are not directly kinetic energy preserving. However, considering

$$p^{\text{num}} = \frac{\{\{\varrho\}\}}{\{\{1/RT\}\}} + \frac{\{\{v/RT\}\} - \{\{1/RT\}\} \{\{v\}\}}{2\{\{1/RT\}\}} f_{\varrho}^{\text{num}}, \quad (90)$$

they might be seen as kinetic energy preserving, since the second term is consistent with zero.

4.6 $\varrho, v, g^{-1}(\varrho/p)$ as variables

As can be seen in the previous subsections, there are many entropy conservative and kinetic energy preserving numerical fluxes in the sense described at the beginning of section 4, obtained using the general procedure described there. However, they are different and will thus have advantages or disadvantages compared to each other. Looking at the entropy variables (8)

$$w = \left(\frac{\gamma}{\gamma-1} - \frac{s}{\gamma-1} - \frac{\varrho v^2}{2p}, \frac{\varrho v_x}{p}, \frac{\varrho v_y}{p}, -\frac{\varrho}{p} \right)^T, \quad s = \log \frac{p}{\varrho^\gamma}, \quad (91)$$

it can be seen that the term $\frac{\varrho}{p}$ has a crucial role. If the variables ϱ, v, χ are chosen (where χ is some third variable), and the expression $\frac{\varrho}{p} = g(\chi)$ depends only on this third variable χ , a

kinetic energy preserving flux can be constructed using a density flux depending only on ϱ, v . Indeed, writing the jumps as

$$\begin{aligned}
[[w_1]] &= -\frac{1}{\gamma-1}[[s]] - \frac{1}{2}\left[\left[\frac{\varrho}{p}v^2\right]\right] = [[\log \varrho]] + \frac{1}{\gamma-1}\left[\left[\log \frac{\varrho}{p}\right]\right] - \frac{1}{2}\left[\left[\frac{\varrho}{p}v^2\right]\right] \\
&= \frac{1}{\{\{\varrho\}\}_{\log}}[[\varrho]] + \frac{1}{\gamma-1}\left[\left[\log \frac{\varrho}{p}\right]\right] - \frac{\{\{v_x^2\}\} + \{\{v_y^2\}\}}{2}\left[\left[\frac{\varrho}{p}\right]\right] - \left\{\left\{\frac{\varrho}{p}\right\}\right\}\{\{v_x\}\}[[v_x]] - \left\{\left\{\frac{\varrho}{p}\right\}\right\}\{\{v_y\}\}[[v_y]], \\
[[w_2]] &= \left[\left[\frac{\varrho}{p}v_x\right]\right] = \left\{\left\{\frac{\varrho}{p}\right\}\right\}[[v_x]] + \{\{v_x\}\}\left[\left[\frac{\varrho}{p}\right]\right], \\
[[w_3]] &= \left[\left[\frac{\varrho}{p}v_y\right]\right] = \left\{\left\{\frac{\varrho}{p}\right\}\right\}[[v_y]] + \{\{v_y\}\}\left[\left[\frac{\varrho}{p}\right]\right], \\
[[w_4]] &= -\left[\left[\frac{\varrho}{p}\right]\right], \\
[[\psi_x]] &= [[\varrho v_x]] = \{\{\varrho\}\}[[v_x]] + \{\{v_x\}\}[[\varrho]], \\
[[\psi_y]] &= [[\varrho v_y]] = \{\{\varrho\}\}[[v_y]] + \{\{v_y\}\}[[\varrho]],
\end{aligned} \tag{92}$$

the entropy conservation conditions $[[w]] \cdot f^{\text{num},x/y} - [[\psi_{x/y}]] = 0$ (41) become

$$\begin{aligned}
0 &= \left(\frac{1}{\{\{\varrho\}\}_{\log}} f_{\varrho}^{\text{num},x} - \{\{v_x\}\} \right) [[\varrho]] + \left(-\left\{\left\{\frac{\varrho}{p}\right\}\right\}\{\{v_x\}\} f_{\varrho}^{\text{num},x} + \left\{\left\{\frac{\varrho}{p}\right\}\right\} f_{\varrho v_x}^{\text{num},x} - \{\{\varrho\}\} \right) [[v_x]] \\
&\quad + \left(-\left\{\left\{\frac{\varrho}{p}\right\}\right\}\{\{v_y\}\} f_{\varrho}^{\text{num},x} + \left\{\left\{\frac{\varrho}{p}\right\}\right\} f_{\varrho v_y}^{\text{num},x} \right) [[v_y]] \\
&\quad + \left(\frac{1}{\gamma-1} \left[\left[\log \frac{\varrho}{p}\right]\right] f_{\varrho}^{\text{num},x} - \frac{\{\{v_x^2\}\} + \{\{v_y^2\}\}}{2} \left[\left[\frac{\varrho}{p}\right]\right] f_{\varrho}^{\text{num},x} + \{\{v_x\}\} \left[\left[\frac{\varrho}{p}\right]\right] f_{\varrho v_x}^{\text{num},x} \right. \\
&\quad \left. + \{\{v_y\}\} \left[\left[\frac{\varrho}{p}\right]\right] f_{\varrho v_y}^{\text{num},x} - \left[\left[\frac{\varrho}{p}\right]\right] f_{\varrho e}^{\text{num},x} \right), \\
0 &= \left(\frac{1}{\{\{\varrho\}\}_{\log}} f_{\varrho}^{\text{num},y} - \{\{v_y\}\} \right) [[\varrho]] + \left(-\left\{\left\{\frac{\varrho}{p}\right\}\right\}\{\{v_x\}\} f_{\varrho}^{\text{num},y} + \left\{\left\{\frac{\varrho}{p}\right\}\right\} f_{\varrho v_x}^{\text{num},y} \right) [[v_x]] \\
&\quad + \left(-\left\{\left\{\frac{\varrho}{p}\right\}\right\}\{\{v_y\}\} f_{\varrho}^{\text{num},y} + \left\{\left\{\frac{\varrho}{p}\right\}\right\} f_{\varrho v_y}^{\text{num},y} - \{\{\varrho\}\} \right) [[v_y]] \\
&\quad + \left(\frac{1}{\gamma-1} \left[\left[\log \frac{\varrho}{p}\right]\right] f_{\varrho}^{\text{num},y} - \frac{\{\{v_x^2\}\} + \{\{v_y^2\}\}}{2} \left[\left[\frac{\varrho}{p}\right]\right] f_{\varrho}^{\text{num},y} + \{\{v_x\}\} \left[\left[\frac{\varrho}{p}\right]\right] f_{\varrho v_x}^{\text{num},y} \right. \\
&\quad \left. + \{\{v_y\}\} \left[\left[\frac{\varrho}{p}\right]\right] f_{\varrho v_y}^{\text{num},y} - \left[\left[\frac{\varrho}{p}\right]\right] f_{\varrho e}^{\text{num},y} \right).
\end{aligned} \tag{93}$$

Thus, the density and momentum fluxes

$$\begin{aligned}
f^{\text{num},x} &\begin{cases} f_{\varrho}^{\text{num},x} = \{\{\varrho\}\}_{\log} \{\{v_x\}\}, \\ f_{\varrho v_x}^{\text{num},x} = \{\{v_x\}\} f_{\varrho}^{\text{num},x} + \frac{\{\{\varrho\}\}}{\{\{\varrho/p\}\}}, \\ f_{\varrho v_y}^{\text{num},x} = \{\{v_y\}\} f_{\varrho}^{\text{num},x}, \end{cases} \\
f^{\text{num},y} &\begin{cases} f_{\varrho}^{\text{num},y} = \{\{\varrho\}\}_{\log} \{\{v_y\}\}, \\ f_{\varrho v_y}^{\text{num},y} = \{\{v_y\}\} f_{\varrho}^{\text{num},y}, \\ f_{\varrho v_x}^{\text{num},y} = \{\{v_x\}\} f_{\varrho}^{\text{num},y} + \frac{\{\{\varrho\}\}}{\{\{\varrho/p\}\}}, \end{cases}
\end{aligned} \tag{94}$$

set the two terms to zero. These fluxes are the same as in (61) and (85), i.e. the same as the ones used by Chandrashekar (2013). However, depending on the expression of $\left[\left[\log \frac{\varrho}{p}\right]\right]$, different

energy fluxes can be constructed, resulting in entropy conservative and kinetic energy preserving schemes.

Choosing $\chi = \beta \propto \frac{\varrho}{p}$, Chandrashekar (2013) set $\left\llbracket \log \frac{\varrho}{p} \right\rrbracket = \frac{1}{\{\!\!\{\chi}\!\!\}_{\log}} \llbracket \chi \rrbracket$ and derived his EC and KEP flux (61).

Choosing $\chi = RT = \left(\frac{\varrho}{p}\right)^{-1}$ and setting $\left\llbracket \log \frac{\varrho}{p} \right\rrbracket = -\frac{1}{\{\!\!\{\chi}\!\!\}_{\log}} \llbracket \chi \rrbracket$, the flux (85) has been derived in section 4.5.

4.6.1 Variant 1

More generally, choosing $r \in \mathbb{R} \setminus \{0\}$, and setting $\frac{\varrho}{p} = \chi^r$, the jumps become

$$\left\llbracket \log \frac{\varrho}{p} \right\rrbracket = \llbracket \log \chi^r \rrbracket = r \llbracket \log \chi \rrbracket = \frac{r}{\{\!\!\{\chi}\!\!\}_{\log}} \llbracket \chi \rrbracket, \quad \left\llbracket \frac{\varrho}{p} \right\rrbracket = \llbracket \chi^r \rrbracket = \frac{\chi_+^r - \chi_-^r}{\chi_+ - \chi_-} \llbracket \chi \rrbracket, \quad (95)$$

where the mean value

$$\{\!\!\{\chi}\!\!\}_{x \mapsto x^r} := \left(\frac{1}{r} \frac{\chi_+^r - \chi_-^r}{\chi_+ - \chi_-} \right)^{1/(r-1)} \quad (96)$$

can be introduced to yield

$$\llbracket \chi^r \rrbracket = r \{\!\!\{\chi}\!\!\}_{x \mapsto x^r}^{r-1} \llbracket \chi \rrbracket. \quad (97)$$

Thus, the arithmetic mean (44) becomes $\{\!\!\{a}\!\!\} = \{\!\!\{a}\!\!\}_{x \mapsto x^2}$ and the geometric mean (75) becomes $\{\!\!\{a}\!\!\}_{\text{geo}} = \{\!\!\{a}\!\!\}_{x \mapsto 1/x}$.

Using this mean value, entropy conservative, kinetic energy preserving, and consistent numerical fluxes are

$$\begin{aligned} f^{\text{num},x} & \begin{cases} f_{\varrho}^{\text{num},x} = \{\!\!\{\varrho}\!\!\}_{\log} \{\!\!\{v_x}\!\!\}, \\ f_{\varrho v_x}^{\text{num},x} = \{\!\!\{v_x}\!\!\} f_{\varrho}^{\text{num},x} + \frac{\{\!\!\{\varrho}\!\!\}}{\{\!\!\{\varrho/p}\!\!\}}, \\ f_{\varrho v_y}^{\text{num},x} = \{\!\!\{v_y}\!\!\} f_{\varrho}^{\text{num},x}, \\ f_{\varrho e}^{\text{num},x} = \left(\frac{1}{\gamma - 1} \frac{1}{\{\!\!\{\chi}\!\!\}_{x \mapsto x^r}^{r-1} \{\!\!\{\chi}\!\!\}_{\log}} - \frac{\{\!\!\{v_x^2}\!\!\} + \{\!\!\{v_y^2}\!\!\}}{2} \right) f_{\varrho}^{\text{num},x} + \{\!\!\{v_x}\!\!\} f_{\varrho v_x}^{\text{num},x} + \{\!\!\{v_y}\!\!\} f_{\varrho v_y}^{\text{num},x}, \end{cases} \\ f^{\text{num},y} & \begin{cases} f_{\varrho}^{\text{num},y} = \{\!\!\{\varrho}\!\!\}_{\log} \{\!\!\{v_y}\!\!\}, \\ f_{\varrho v_y}^{\text{num},y} = \{\!\!\{v_y}\!\!\} f_{\varrho}^{\text{num},y}, \\ f_{\varrho v_x}^{\text{num},y} = \{\!\!\{v_x}\!\!\} f_{\varrho}^{\text{num},y} + \frac{\{\!\!\{\varrho}\!\!\}}{\{\!\!\{\varrho/p}\!\!\}}, \\ f_{\varrho e}^{\text{num},y} = \left(\frac{1}{\gamma - 1} \frac{1}{\{\!\!\{\chi}\!\!\}_{x \mapsto x^r}^{r-1} \{\!\!\{\chi}\!\!\}_{\log}} - \frac{\{\!\!\{v_x^2}\!\!\} + \{\!\!\{v_y^2}\!\!\}}{2} \right) f_{\varrho}^{\text{num},y} + \{\!\!\{v_x}\!\!\} f_{\varrho v_x}^{\text{num},y} + \{\!\!\{v_y}\!\!\} f_{\varrho v_y}^{\text{num},y}. \end{cases} \end{aligned} \quad (98)$$

Of course, some numerically stable procedure to compute $\{\!\!\{\chi}\!\!\}_{x \mapsto x^r}^{r-1} = \frac{1}{r} \frac{\chi_+^r - \chi_-^r}{\chi_+ - \chi_-}$ has to be derived.

4.6.2 Variant 2

The choice $\frac{\varrho}{p} = \exp \chi$ results in

$$\left\llbracket \log \frac{\varrho}{p} \right\rrbracket = \llbracket \log \exp \chi \rrbracket = \llbracket \chi \rrbracket, \quad \left\llbracket \frac{\varrho}{p} \right\rrbracket = \llbracket \exp \chi \rrbracket = \frac{\exp \chi_+ - \exp \chi_-}{\chi_+ - \chi_-} \llbracket \chi \rrbracket, \quad (99)$$

where the mean value

$$\{\!\!\{\chi}\!\!\}_{x \mapsto \exp x} := \log \frac{\exp \chi_+ - \exp \chi_-}{\chi_+ - \chi_-} \quad (100)$$

can be introduced to yield

$$\llbracket \exp \chi \rrbracket = \exp \left(\llbracket \chi \rrbracket_{x \mapsto \exp x} \right) \llbracket \chi \rrbracket. \quad (101)$$

Using this mean value, an entropy conservative, kinetic energy preserving, and consistent numerical flux is

$$f^{\text{num},x} \begin{cases} f_{\varrho}^{\text{num},x} = \llbracket \varrho \rrbracket_{\log} \llbracket v_x \rrbracket, \\ f_{\varrho v_x}^{\text{num},x} = \llbracket v_x \rrbracket f_{\varrho}^{\text{num},x} + \frac{\llbracket \varrho \rrbracket}{\llbracket \varrho/p \rrbracket}, \\ f_{\varrho v_y}^{\text{num},x} = \llbracket v_y \rrbracket f_{\varrho}^{\text{num},x}, \\ f_{\varrho e}^{\text{num},x} = \left(\frac{1}{\gamma - 1} \frac{1}{\exp \llbracket \chi \rrbracket_{x \mapsto \exp x}} - \frac{\llbracket v_x^2 \rrbracket + \llbracket v_y^2 \rrbracket}{2} \right) f_{\varrho}^{\text{num},x} + \llbracket v_x \rrbracket f_{\varrho v_x}^{\text{num},x} + \llbracket v_y \rrbracket f_{\varrho v_y}^{\text{num},x}, \end{cases}$$

$$f^{\text{num},y} \begin{cases} f_{\varrho}^{\text{num},y} = \llbracket \varrho \rrbracket_{\log} \llbracket v_y \rrbracket, \\ f_{\varrho v_y}^{\text{num},y} = \llbracket v_y \rrbracket f_{\varrho}^{\text{num},y}, \\ f_{\varrho v_x}^{\text{num},y} = \llbracket v_x \rrbracket f_{\varrho}^{\text{num},y} + \frac{\llbracket \varrho \rrbracket}{\llbracket \varrho/p \rrbracket}, \\ f_{\varrho e}^{\text{num},y} = \left(\frac{1}{\gamma - 1} \frac{1}{\exp \llbracket \chi \rrbracket_{x \mapsto \exp x}} - \frac{\llbracket v_x^2 \rrbracket + \llbracket v_y^2 \rrbracket}{2} \right) f_{\varrho}^{\text{num},y} + \llbracket v_x \rrbracket f_{\varrho v_x}^{\text{num},y} + \llbracket v_y \rrbracket f_{\varrho v_y}^{\text{num},y}. \end{cases} \quad (102)$$

Again, some numerically stable procedure to compute $\exp \llbracket \chi \rrbracket_{x \mapsto \exp x} = \frac{\exp \chi_+ - \exp \chi_-}{\chi_+ - \chi_-}$ has to be derived.

4.7 Other variables

Of course, some other sets of variables can be used to derive entropy conservative numerical fluxes similar to the previous sections. However, since there is no clear intuition which choice of variables might be “good”, this is not carried out in detail here.

As noted by Derigs, Winters, Gassner, and Walch (2017), an influence of the pressure in the numerical density flux should be avoided, see also the numerical tests in section 7.

5 Reversing the role of energy and entropy

As proposed by Coquel, Godlewski, Perthame, In, and Rascle (2001) and used by Bouchut (2004, Section 2.4.6) to derive an approximate Riemann solver based on the Suliciu relaxation approach, the role of energy and entropy for the Euler equations can be reversed, i.e. a conservation law for the entropy and an inequality for the energy can be considered. Then, the system reads

$$\underbrace{\partial_t \begin{pmatrix} \varrho \\ \varrho v_x \\ \varrho v_y \\ \varrho s \end{pmatrix}}_{=u} + \partial_x \underbrace{\begin{pmatrix} \varrho v_x \\ \varrho v_x^2 + p \\ \varrho v_x v_y \\ \varrho s v_x \end{pmatrix}}_{=f_x(u)} + \partial_y \underbrace{\begin{pmatrix} \varrho v_y \\ \varrho v_x v_y \\ \varrho v_y^2 + p \\ \varrho s v_y \end{pmatrix}}_{=f_y(u)} = 0, \quad (103)$$

and the ‘entropy’ condition becomes

$$\underbrace{\partial_t (\varrho e)}_{=U} + \partial_x \underbrace{((\varrho e + p)v_x)}_{=F_x} + \partial_y \underbrace{((\varrho e + p)v_y)}_{=F_y} \leq 0. \quad (104)$$

Since smooth solutions satisfy (104) with equality, they are also smooth solutions of the Euler equations (1) with equality in the usual entropy condition (7). In the same spirit, an ‘entropy’

conserving numerical flux for (103), (104) is an entropy conserving flux for (1), (7) and vice versa.

In order to express the energy $\varrho e = \frac{1}{2}\varrho v^2 + \varrho \varepsilon$ (2) as a function of the new conserved variables $\varrho, \varrho v, \varrho s$, the pressure $p = (\gamma - 1)\varrho \varepsilon$ (3) can be inserted into the specific entropy $s = \log \frac{p}{\varrho^\gamma}$ (5) to yield

$$\varrho \varepsilon = \frac{\varrho^\gamma}{\gamma - 1} \exp s. \quad (105)$$

Thus, the energy can be written as

$$\varrho e = \frac{1}{2} \frac{(\varrho v)^2}{\varrho} + \frac{1}{\gamma - 1} \varrho^\gamma \exp \left(\frac{\varrho s}{\varrho} \right). \quad (106)$$

Therefore, the new 'entropy' variables are

$$w = \frac{\partial(\varrho e)}{\partial(\varrho, \varrho v_x, \varrho v_y, \varrho s)} = \begin{pmatrix} -\frac{1}{2} \frac{(\varrho v)^2}{\varrho^2} + \frac{\gamma}{\gamma - 1} \varrho^{\gamma-1} \exp \left(\frac{\varrho s}{\varrho} \right) - \frac{1}{\gamma - 1} \varrho^\gamma \frac{\varrho s}{\varrho^2} \exp \left(\frac{\varrho s}{\varrho} \right) \\ \frac{\varrho v_x}{\varrho} \\ \frac{\varrho v_y}{\varrho} \\ \frac{1}{\gamma - 1} \varrho^{\gamma-1} \exp \left(\frac{\varrho s}{\varrho} \right) \end{pmatrix} \quad (107)$$

$$= \begin{pmatrix} -\frac{1}{2} v^2 + \frac{\gamma}{\gamma - 1} \varrho^{\gamma-1} \exp(s) - \frac{1}{\gamma - 1} \varrho^{\gamma-1} s \exp(s) \\ v_x \\ v_y \\ \frac{1}{\gamma - 1} \varrho^{\gamma-1} \exp(s) \end{pmatrix}.$$

The new 'entropy' fluxes are

$$\begin{aligned} F_x &= (\varrho e + p)v_x = \frac{1}{2} \varrho v^2 v_x + \gamma \varrho \varepsilon v_x = \frac{1}{2} \varrho v^2 v_x + \frac{\gamma}{\gamma - 1} \varrho^\gamma v_x \exp(s), \\ F_y &= (\varrho e + p)v_y = \frac{1}{2} \varrho v^2 v_y + \gamma \varrho \varepsilon v_y = \frac{1}{2} \varrho v^2 v_y + \frac{\gamma}{\gamma - 1} \varrho^\gamma v_y \exp(s), \end{aligned} \quad (108)$$

so that the new flux potentials $\psi_{x/y}$ fulfilling $\partial_w \psi_{x/y} = f_{x/y}(u(w))$ become

$$\begin{aligned} \psi_{x/y} &= w \cdot f_{x/y} - F_{x/y} = \left(-\frac{1}{2} v^2 + \frac{\gamma}{\gamma - 1} \varrho^{\gamma-1} \exp(s) - \frac{1}{\gamma - 1} \varrho^{\gamma-1} s \exp(s) \right) \varrho v_{x/y} \\ &\quad + v_{x/y} \left(\varrho v_{x/y}^2 + \varrho^\gamma \exp(s) \right) + v_{y/x} \varrho v_{x/y} v_{y/x} \\ &\quad + \frac{1}{\gamma - 1} \varrho^{\gamma-1} \exp(s) \varrho s v_{x/y} - \frac{1}{2} \varrho v^2 v_{x/y} - \frac{\gamma}{\gamma - 1} \varrho^\gamma v_{x/y} \exp(s) \\ &= \varrho^\gamma v_{x/y} \exp(s). \end{aligned} \quad (109)$$

As before, the conditions for 'entropy' conservation in the semidiscrete setting of Tadmor (1987, 2003) are $\llbracket w \rrbracket \cdot f^{\text{num}, x/y} - \llbracket \psi_{x/y} \rrbracket = 0$ (41). The corresponding 'entropy' fluxes are $F_{x/y}^{\text{num}} = \llbracket w \rrbracket \cdot f^{\text{num}, x/y} - \llbracket \psi_{x/y} \rrbracket$, i.e. the numerical energy fluxes corresponding to an 'entropy' conservative flux $f^{\text{num}, x/y}$ for (103) are

$$f_{\varrho e}^{\text{num}, x/y} = \llbracket w \rrbracket \cdot f^{\text{num}, x/y} - \llbracket \psi_{x/y} \rrbracket, \quad (110)$$

with w as in (107) and $\psi_{x/y}$ as in (109).

Choosing v as variable and writing the jumps using the product rule (45) as

$$\begin{aligned} \llbracket w_1 \rrbracket &= -\llbracket v_x \rrbracket \llbracket v_x \rrbracket - \llbracket v_y \rrbracket \llbracket v_y \rrbracket + \frac{\gamma}{\gamma - 1} \llbracket \varrho^{\gamma-1} \exp(s) \rrbracket - \frac{1}{\gamma - 1} \llbracket \varrho^{\gamma-1} s \exp(s) \rrbracket, \\ \llbracket w_2 \rrbracket &= \llbracket v_x \rrbracket, \\ \llbracket w_3 \rrbracket &= \llbracket v_y \rrbracket, \\ \llbracket w_4 \rrbracket &= \frac{1}{\gamma - 1} \llbracket \varrho^{\gamma-1} \exp(s) \rrbracket, \\ \llbracket \psi_x \rrbracket &= \llbracket \varrho^\gamma \exp(s) \rrbracket \llbracket v_x \rrbracket + \llbracket v_x \rrbracket \llbracket \varrho^\gamma \exp(s) \rrbracket, \\ \llbracket \psi_y \rrbracket &= \llbracket \varrho^\gamma \exp(s) \rrbracket \llbracket v_y \rrbracket + \llbracket v_y \rrbracket \llbracket \varrho^\gamma \exp(s) \rrbracket, \end{aligned} \quad (111)$$

the coefficients of $\llbracket v_{x/y} \rrbracket$ in the entropy conditions $\llbracket w \rrbracket \cdot f^{\text{num},x/y} - \llbracket \psi_{x/y} \rrbracket = 0$ become

$$-\llbracket v_x \rrbracket f_{\varrho}^{\text{num},x} + f_{\varrho v_x}^{\text{num},x} - \llbracket \varrho^\gamma \exp(s) \rrbracket, \quad -\llbracket v_y \rrbracket f_{\varrho}^{\text{num},y} + f_{\varrho v_y}^{\text{num},y} - \llbracket \varrho^\gamma \exp(s) \rrbracket. \quad (112)$$

Thus, general momentum fluxes for entropy conservative numerical fluxes can be written as

$$\begin{aligned} f^{\text{num},x} & \begin{cases} f_{\varrho v_x}^{\text{num},x} = \llbracket v_x \rrbracket f_{\varrho}^{\text{num},x} + \llbracket \varrho^\gamma \exp(s) \rrbracket = \llbracket v_x \rrbracket f_{\varrho}^{\text{num},x} + \llbracket p \rrbracket, \\ f_{\varrho v_y}^{\text{num},x} = \llbracket v_y \rrbracket f_{\varrho}^{\text{num},x}, \end{cases} \\ f^{\text{num},y} & \begin{cases} f_{\varrho v_x}^{\text{num},y} = \llbracket v_x \rrbracket f_{\varrho}^{\text{num},y}, \\ f_{\varrho v_y}^{\text{num},y} = \llbracket v_y \rrbracket f_{\varrho}^{\text{num},y} + \llbracket \varrho^\gamma \exp(s) \rrbracket = \llbracket v_y \rrbracket f_{\varrho}^{\text{num},y} + \llbracket p \rrbracket, \end{cases} \end{aligned} \quad (113)$$

i.e. in the form proposed by Jameson (2008) for a kinetic energy preserving flux (in one space dimension). Another possibility would be to split the jump of $\psi_{x/y}$ in some other way, resulting in a numerical pressure flux p^{num} different from $\llbracket p \rrbracket$.

5.1 ϱ, v, T as variables

Using the variables ϱ, v , and $RT = \frac{p}{\varrho} = \varrho^{\gamma-1} \exp(s)$, the flux potentials $\psi_{x/y} = \varrho^\gamma v_{x/y} \exp(s)$ (109) and the entropy variables (107) can be written as

$$\psi_{x/y} = \varrho RT v_{x/y}, \quad w = \begin{pmatrix} -\frac{1}{2}v^2 + \frac{\gamma}{\gamma-1}RT - \frac{1}{\gamma-1}sRT \\ v_x \\ v_y \\ \frac{1}{\gamma-1}RT \end{pmatrix}, \quad s = \log RT - (\gamma-1) \log \varrho. \quad (114)$$

5.1.1 Variant 1

Using these variables, the jumps can be written using the chain rules (45) and (47) as

$$\begin{aligned} \llbracket w_1 \rrbracket &= -\frac{1}{2}\llbracket v^2 \rrbracket + \frac{\gamma}{\gamma-1}\llbracket RT \rrbracket - \frac{1}{\gamma-1}\llbracket RT \log RT \rrbracket + \llbracket RT \log \varrho \rrbracket \\ &= -\llbracket v_x \rrbracket \llbracket v_x \rrbracket - \llbracket v_y \rrbracket \llbracket v_y \rrbracket + \frac{\gamma}{\gamma-1}\llbracket RT \rrbracket - \frac{1}{\gamma-1} \frac{\llbracket RT \rrbracket}{\llbracket RT \rrbracket_{\log}} \llbracket RT \rrbracket \\ &\quad - \frac{1}{\gamma-1} \llbracket \log RT \rrbracket \llbracket RT \rrbracket + \llbracket \log \varrho \rrbracket \llbracket RT \rrbracket + \frac{\llbracket RT \rrbracket}{\llbracket \varrho \rrbracket_{\log}} \llbracket \varrho \rrbracket, \\ \llbracket w_2 \rrbracket &= \llbracket v_x \rrbracket, \\ \llbracket w_3 \rrbracket &= \llbracket v_y \rrbracket, \\ \llbracket w_4 \rrbracket &= \frac{1}{\gamma-1} \llbracket RT \rrbracket, \\ \llbracket \psi_x \rrbracket &= \llbracket \varrho RT \rrbracket \llbracket v_x \rrbracket + \llbracket v_x \rrbracket \llbracket \varrho RT \rrbracket = \llbracket \varrho RT \rrbracket \llbracket v_x \rrbracket + \llbracket \varrho \rrbracket \llbracket v_x \rrbracket \llbracket RT \rrbracket + \llbracket v_x \rrbracket \llbracket RT \rrbracket \llbracket \varrho \rrbracket, \\ \llbracket \psi_y \rrbracket &= \llbracket \varrho RT \rrbracket \llbracket v_y \rrbracket + \llbracket v_y \rrbracket \llbracket \varrho RT \rrbracket = \llbracket \varrho RT \rrbracket \llbracket v_y \rrbracket + \llbracket \varrho \rrbracket \llbracket v_y \rrbracket \llbracket RT \rrbracket + \llbracket v_y \rrbracket \llbracket RT \rrbracket \llbracket \varrho \rrbracket. \end{aligned} \quad (115)$$

Inserting this in the entropy conditions $\llbracket w \rrbracket \cdot f^{\text{num},x/y} - \llbracket \psi_{x/y} \rrbracket = 0$,

$$\begin{aligned}
0 &= \left(\frac{\llbracket RT \rrbracket}{\llbracket \varrho \rrbracket_{\log}} f_{\varrho}^{\text{num},x} - \llbracket v_x \rrbracket \llbracket RT \rrbracket \right) \llbracket \varrho \rrbracket \\
&+ \left(-\llbracket v_x \rrbracket f_{\varrho}^{\text{num},x} + f_{\varrho v_x}^{\text{num},x} - \llbracket \varrho RT \rrbracket \right) \llbracket v_x \rrbracket + \left(-\llbracket v_y \rrbracket f_{\varrho}^{\text{num},x} + f_{\varrho v_y}^{\text{num},x} \right) \llbracket v_y \rrbracket \\
&+ \left(\left(\frac{\gamma}{\gamma-1} - \frac{1}{\gamma-1} \frac{\llbracket RT \rrbracket}{\llbracket RT \rrbracket_{\log}} - \frac{1}{\gamma-1} \llbracket \log RT \rrbracket + \llbracket \log \varrho \rrbracket \right) f_{\varrho}^{\text{num},x} \right. \\
&\quad \left. + \frac{1}{\gamma-1} f_{\varrho s}^{\text{num},x} - \llbracket \varrho \rrbracket \llbracket v_x \rrbracket \right) \llbracket RT \rrbracket, \\
0 &= \left(\frac{\llbracket RT \rrbracket}{\llbracket \varrho \rrbracket_{\log}} f_{\varrho}^{\text{num},y} - \llbracket v_y \rrbracket \llbracket RT \rrbracket \right) \llbracket \varrho \rrbracket \\
&+ \left(-\llbracket v_x \rrbracket f_{\varrho}^{\text{num},y} + f_{\varrho v_x}^{\text{num},y} \right) \llbracket v_x \rrbracket + \left(-\llbracket v_y \rrbracket f_{\varrho}^{\text{num},y} + f_{\varrho v_y}^{\text{num},y} - \llbracket \varrho RT \rrbracket \right) \llbracket v_y \rrbracket \\
&+ \left(\left(\frac{\gamma}{\gamma-1} - \frac{1}{\gamma-1} \frac{\llbracket RT \rrbracket}{\llbracket RT \rrbracket_{\log}} - \frac{1}{\gamma-1} \llbracket \log RT \rrbracket + \llbracket \log \varrho \rrbracket \right) f_{\varrho}^{\text{num},y} \right. \\
&\quad \left. + \frac{1}{\gamma-1} f_{\varrho s}^{\text{num},y} - \llbracket \varrho \rrbracket \llbracket v_y \rrbracket \right) \llbracket RT \rrbracket,
\end{aligned} \tag{116}$$

the fluxes

$$\begin{aligned}
f^{\text{num},x} &\left\{ \begin{aligned} f_{\varrho}^{\text{num},x} &= \llbracket \varrho \rrbracket_{\log} \llbracket v_x \rrbracket, \\ f_{\varrho v_x}^{\text{num},x} &= \llbracket v_x \rrbracket f_{\varrho}^{\text{num},x} + \llbracket \varrho RT \rrbracket = \llbracket v_x \rrbracket f_{\varrho}^{\text{num},x} + \llbracket p \rrbracket, \\ f_{\varrho v_y}^{\text{num},x} &= \llbracket v_y \rrbracket f_{\varrho}^{\text{num},x}, \\ f_{\varrho s}^{\text{num},x} &= \left(\frac{\llbracket RT \rrbracket}{\llbracket RT \rrbracket_{\log}} - \gamma + \llbracket \log RT \rrbracket - (\gamma-1) \llbracket \log \varrho \rrbracket \right) f_{\varrho}^{\text{num},x} + (\gamma-1) \llbracket \varrho \rrbracket \llbracket v_x \rrbracket, \\ f_{\varrho e}^{\text{num},x} &= \left(-\frac{\llbracket v_x^2 \rrbracket + \llbracket v_y^2 \rrbracket}{2} + \frac{\gamma}{\gamma-1} \llbracket RT \rrbracket - \frac{1}{\gamma-1} \llbracket sRT \rrbracket \right) f_{\varrho}^{\text{num},x} \\ &\quad + \llbracket v_x \rrbracket f_{\varrho v_x}^{\text{num},x} + \llbracket v_y \rrbracket f_{\varrho v_y}^{\text{num},x} + \frac{1}{\gamma-1} \llbracket RT \rrbracket f_{\varrho s}^{\text{num},x} - \llbracket \varrho RT v_x \rrbracket, \end{aligned} \right. \\
f^{\text{num},y} &\left\{ \begin{aligned} f_{\varrho}^{\text{num},y} &= \llbracket \varrho \rrbracket_{\log} \llbracket v_y \rrbracket, \\ f_{\varrho v_x}^{\text{num},y} &= \llbracket v_x \rrbracket f_{\varrho}^{\text{num},y}, \\ f_{\varrho v_y}^{\text{num},y} &= \llbracket v_y \rrbracket f_{\varrho}^{\text{num},y} + \llbracket \varrho RT \rrbracket = \llbracket v_y \rrbracket f_{\varrho}^{\text{num},y} + \llbracket p \rrbracket, \\ f_{\varrho s}^{\text{num},y} &= \left(\frac{\llbracket RT \rrbracket}{\llbracket RT \rrbracket_{\log}} - \gamma + \llbracket \log RT \rrbracket - (\gamma-1) \llbracket \log \varrho \rrbracket \right) f_{\varrho}^{\text{num},y} + (\gamma-1) \llbracket \varrho \rrbracket \llbracket v_y \rrbracket, \\ f_{\varrho e}^{\text{num},y} &= \left(-\frac{\llbracket v_x^2 \rrbracket + \llbracket v_y^2 \rrbracket}{2} + \frac{\gamma}{\gamma-1} \llbracket RT \rrbracket - \frac{1}{\gamma-1} \llbracket sRT \rrbracket \right) f_{\varrho}^{\text{num},y} \\ &\quad + \llbracket v_x \rrbracket f_{\varrho v_x}^{\text{num},y} + \llbracket v_y \rrbracket f_{\varrho v_y}^{\text{num},y} + \frac{1}{\gamma-1} \llbracket RT \rrbracket f_{\varrho s}^{\text{num},y} - \llbracket \varrho RT v_y \rrbracket, \end{aligned} \right.
\end{aligned} \tag{117}$$

can be seen to be consistent, entropy conservative, and kinetic energy preserving fluxes for the Euler equations (1), where the energy fluxes $f_{\varrho e}^{\text{num},x/y}$ have been computed as $\llbracket w \rrbracket \cdot f^{\text{num},x/y} - \llbracket \psi_{x/y} \rrbracket$.

Inserting the numerical fluxes into the definition of the energy fluxes $f_{\varrho e}^{\text{num},x}, f_{\varrho e}^{\text{num},y}$ yields

$$\begin{aligned}
f_{\varrho e}^{\text{num},x} &= \left(-\frac{\langle v_x^2 \rangle + \langle v_y^2 \rangle}{2} + \frac{\gamma}{\gamma-1} \langle RT \rangle - \frac{1}{\gamma-1} \langle sRT \rangle \right) \langle \varrho \rangle_{\log} \langle v_x \rangle \\
&\quad + \langle v_x \rangle \left(\langle \varrho \rangle_{\log} \langle v_x \rangle^2 + \langle \varrho RT \rangle \right) + \langle v_y \rangle \left(\langle \varrho \rangle_{\log} \langle v_x \rangle \langle v_y \rangle \right) \\
&\quad + \frac{1}{\gamma-1} \langle RT \rangle \left(\frac{\langle RT \rangle}{\langle RT \rangle_{\log}} - \gamma + \langle \log RT \rangle - (\gamma-1) \langle \log \varrho \rangle \right) \langle \varrho \rangle_{\log} \langle v_x \rangle \\
&\quad + \langle RT \rangle \langle \varrho \rangle \langle v_x \rangle - \langle \varrho v_x RT \rangle \\
&= \langle \varrho \rangle_{\log} \langle v_x \rangle \left(\langle v_x \rangle^2 + \langle v_y \rangle^2 - \frac{\langle v_x^2 \rangle + \langle v_y^2 \rangle}{2} \right) \\
&\quad + \langle \varrho \rangle \langle v_x \rangle \langle RT \rangle + \langle \varrho RT \rangle \langle v_x \rangle - \langle \varrho v_x RT \rangle + \frac{1}{\gamma-1} \langle \varrho \rangle_{\log} \langle v_x \rangle \frac{\langle RT \rangle^2}{\langle RT \rangle_{\log}} \\
&\quad + \langle \varrho \rangle_{\log} \langle v_x \rangle \left(\frac{1}{\gamma-1} \langle RT \rangle \langle \log RT \rangle - \langle \log \varrho \rangle \langle RT \rangle - \frac{1}{\gamma-1} \langle sRT \rangle \right), \\
f_{\varrho e}^{\text{num},y} &= \left(-\frac{\langle v_x^2 \rangle + \langle v_y^2 \rangle}{2} + \frac{\gamma}{\gamma-1} \langle RT \rangle - \frac{1}{\gamma-1} \langle sRT \rangle \right) \langle \varrho \rangle_{\log} \langle v_y \rangle \\
&\quad + \langle v_x \rangle \left(\langle \varrho \rangle_{\log} \langle v_x \rangle \langle v_y \rangle \right) + \langle v_y \rangle \left(\langle \varrho \rangle_{\log} \langle v_y \rangle^2 + \langle \varrho RT \rangle \right) \\
&\quad + \frac{1}{\gamma-1} \langle RT \rangle \left(\frac{\langle RT \rangle}{\langle RT \rangle_{\log}} - \gamma + \langle \log RT \rangle - (\gamma-1) \langle \log \varrho \rangle \right) \langle \varrho \rangle_{\log} \langle v_y \rangle \\
&\quad + \langle RT \rangle \langle \varrho \rangle \langle v_y \rangle - \langle \varrho v_y RT \rangle \\
&= \langle \varrho \rangle_{\log} \langle v_y \rangle \left(\langle v_x \rangle^2 + \langle v_y \rangle^2 - \frac{\langle v_x^2 \rangle + \langle v_y^2 \rangle}{2} \right) \\
&\quad + \langle \varrho \rangle \langle v_y \rangle \langle RT \rangle + \langle \varrho RT \rangle \langle v_y \rangle - \langle \varrho v_y RT \rangle + \frac{1}{\gamma-1} \langle \varrho \rangle_{\log} \langle v_y \rangle \frac{\langle RT \rangle^2}{\langle RT \rangle_{\log}} \\
&\quad + \langle \varrho \rangle_{\log} \langle v_y \rangle \left(\frac{1}{\gamma-1} \langle RT \rangle \langle \log RT \rangle - \langle \log \varrho \rangle \langle RT \rangle - \frac{1}{\gamma-1} \langle sRT \rangle \right). \tag{118}
\end{aligned}$$

Here, the first two lines of the results are consistent approximations of the fluxes $\frac{1}{2} \varrho v^2 v_{x/y} + \frac{\gamma}{\gamma-1} p$ with additional terms that are consistent with zero, since $s = \log RT - (\gamma-1) \log \varrho$.

5.2 Other variables

As in section 4, other choices of variables are possible, e.g. ϱ, v, χ with $\frac{p}{\varrho} = g(\chi)$. However, this approach is not further pursued here, since there does not seem to be a clear intuition, which choice is preferable.

6 Numerical surface fluxes / Riemann solvers

The numerical surface fluxes are an important ingredient for stability and robustness of the method. In a first order finite volume setting, they determine the method completely. Here, some choices of the fluxes will be presented and compared.

6.1 Adding dissipation to entropy conservative fluxes

Similarly to the local Lax-Friedrichs flux

$$f_{\text{LLF}}^{\text{num}}(u_-, u_+) = \frac{f(u_+) + f(u_-)}{2} - \frac{\lambda}{2}(u_+ - u_-), \tag{119}$$

an entropy stable flux can be constructed as an entropy conservative central flux plus an additional dissipation term.

The simplest choice is to add a local Lax-Friedrichs type dissipation of the form $-\frac{\lambda}{2}[\![u]\!]$. The resulting flux is entropy stable, since multiplication with the jump of the entropy variables results in

$$\begin{aligned} -\frac{\lambda}{2}[\![w]\!] \cdot [\![u]\!] &= -\frac{\lambda}{2}[\![w]\!] \cdot \int_0^1 \frac{\partial u}{\partial w} (w_- + \sigma(w_+ - w_-)) \cdot (w_+ - w_-) d\sigma \\ &= -\frac{\lambda}{2}[\![w]\!] \cdot \int_0^1 \frac{\partial u}{\partial w} (w_- + \sigma(w_+ - w_-)) d\sigma \cdot [\![w]\!], \end{aligned} \quad (120)$$

and $\frac{\partial u}{\partial w} = \left(\frac{\partial w}{\partial u}\right)^{-1}$ is positive definite, since $w = \partial_u U$ and the entropy U is convex.

Another construction uses a dissipation term of the form $-\frac{1}{2}|f'(u)|[\![u]\!] \approx -\frac{1}{2}|f'(u)| \partial_w u \cdot [\![w]\!]$. Using the scaling of the eigenvectors proposed by Barth (1999, Theorem 4) results in $|f'(u)| = R|\Lambda|R^{-1}$ and $\partial_w u = RR^T$, where Λ contains the eigenvalues of $f'(u)$ on the diagonal. Thus, $-|f'(u)|[\![u]\!] \approx -R|\Lambda|R^T \cdot [\![w]\!]$ and the matrix $R|\Lambda|R^T$ is positive definite.

Using this form, choosing $|\Lambda| = \lambda I$ and some intermediate value $H = RR^T = \partial_w u$ results in a scalar dissipation term (SD) $-\frac{\lambda}{2}H[\![w]\!]$. A matrix dissipation term (MD) is obtained by setting $|\lambda| = \text{diag}(|\lambda_i|)$.

Of course, the matrices $H, R, |\Lambda|$ have to be evaluated at some suitable intermediate values. Derigs, Winters, Gassner, and Walch (2017); Winters, Derigs, Gassner, and Walch (2016) investigated this problem for ideal MHD and the Euler equations using the entropy conservative flux (61) of Chandrashekar (2013) and derived scalar and matrix dissipation operators of the forms described above. Additionally, they proposed to use the convex combination $-\Xi \frac{\lambda}{2}H[\![w]\!] - (1 - \Xi) \frac{1}{2}R|\Lambda|R^T \cdot [\![w]\!]$, where $\Xi = \left|\frac{p_+ - p_-}{p_+ + p_-}\right|^{\frac{1}{2}}$ is the indicator of the shock strength also used by Chandrashekar (2013).

6.2 Preserving positivity of the density

The Euler equations are valid for positive density ϱ and pressure p . In order to be robust, the numerical flux f^{num} should preserve these invariant regions of the Euler equations in a first order finite volume update procedure using an explicit Euler step in time

$$u_i^+ = u_i - \frac{\Delta t}{\Delta x} (f^{\text{num}}(u_i, u_{i+1}) - f^{\text{num}}(u_{i-1}, u_i)). \quad (121)$$

Extensions of this property to higher order methods can be constructed using the framework of Zhang and Shu (2011).

As described inter alia by Zhang and Shu (2010, Remark 2.4), the (local) Lax-Friedrichs flux preserves positivity of both density and pressure.

The same result can be obtained – at least heuristically – for the density, if the numerical flux is of the form $f_\varrho^{\text{num}} = \{\!\!\{\varrho\}\!\!\}_{\log} \{\!\!\{v\}\!\!\} - \frac{\lambda}{2}[\![\varrho]\!]$, i.e. if one of the entropy conservative fluxes described above containing no contribution of the pressure in the density flux is used and the dissipation is of LLF type in the variable ϱ . This is also fulfilled for the scalar dissipation operator SD of Derigs, Winters, Gassner, and Walch (2017).

The FV step (121) for the density can be separated into two similar parts as

$$\varrho_i^+ = \left(\frac{1}{2}\varrho_i - \frac{\Delta t}{\Delta x} f_\varrho^{\text{num}}(u_i, u_{i+1})\right) + \left(\frac{1}{2}\varrho_i + \frac{\Delta t}{\Delta x} f_\varrho^{\text{num}}(u_{i-1}, u_i)\right). \quad (122)$$

Since both can be handled similarly, only the first one will be analysed. Using the numerical flux $f_\varrho^{\text{num}} = \{\!\!\{\varrho\}\!\!\}_{\log} \{\!\!\{v\}\!\!\} - \frac{\lambda}{2}[\![\varrho]\!]$, the logarithmic mean value can be written as a convex combination $\{\!\!\{\varrho\}\!\!\}_{\log} = \alpha\varrho_i + (1 - \alpha)\varrho_{i+1}$, $\alpha \in [0, 1]$. Thus, the first term becomes

$$\frac{1}{2}\varrho_i - \frac{\Delta t}{\Delta x} \left(\{\!\!\{\varrho\}\!\!\}_{\log} \{\!\!\{v\}\!\!\} - \frac{\lambda}{2}[\![\varrho]\!]\right) = \varrho_i \left(\frac{1}{2} - \frac{\lambda}{2} \frac{\Delta t}{\Delta x} - \alpha \{\!\!\{v\}\!\!\} \frac{\Delta t}{\Delta x}\right) + \varrho_{i+1} \frac{\Delta t}{\Delta x} \left(\frac{\lambda}{2} - (1 - \alpha) \{\!\!\{v\}\!\!\}\right). \quad (123)$$

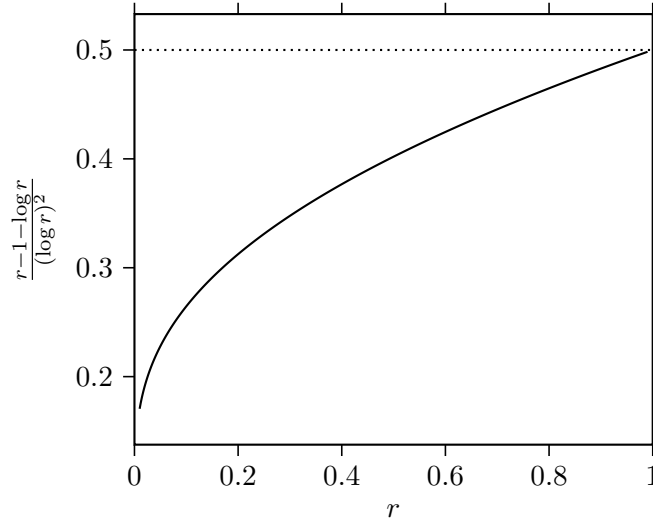


Figure 1: Visualisation of the function $(0, 1) \ni r \mapsto \frac{r-1-\log r}{(\log r)^2}$.

If α was guaranteed to be $\frac{1}{2}$, the second term becomes non-negative for $\lambda \geq \max\{|v_i|, |v_{i+1}|\}$ and the first one is controlled under a reasonable CFL condition. This is the case for the local Lax-Friedrichs flux.

However, if $\alpha \neq \frac{1}{2}$, the analysis is more complicated. Since the first term contains a factor $\frac{1}{2}\varrho_i$, it is the “good one” and can be controlled by some CFL condition. The only “bad case” occurs, if the second term becomes negative and the first term cannot compensate for this, e.g. $\varrho_i \rightarrow 0$. Nevertheless, if $\alpha > \frac{1}{2}$ for $\varrho_i < \varrho_{i+1}$, i.e. $\{\varrho\}_{\log} \leq \{\varrho\}$, this cannot happen and the density remains positive under a reasonable CFL condition.

This is indeed the case: Comparing the logarithmic and arithmetic mean of two positive numbers a, b , the desired result is

$$\frac{a-b}{\log a - \log b} \stackrel{!}{\leq} \frac{a+b}{2}. \quad (124)$$

Since

$$\frac{a-b}{\log a - \log b} = \frac{a+b}{2} - \frac{(b-a)^2}{12a} + \frac{(b-a)^3}{24a^2} + \dots, \quad (125)$$

both means are equal for $a = b$. Fixing the smaller value, say a , the derivative with respect to b is

$$\frac{d}{db} \frac{a-b}{\log a - \log b} = \frac{-1}{\log a - \log b} + \frac{a-b}{(\log a - \log b)^2} \frac{1}{b} = \frac{-1}{\log \frac{a}{b}} + \frac{\frac{a}{b} - 1}{(\log \frac{a}{b})^2} = \frac{\frac{a}{b} - 1 - \log \frac{a}{b}}{(\log \frac{a}{b})^2}. \quad (126)$$

This depends only on the ratio $r = \frac{a}{b}$. As can be seen in Figure 1, the function $(0, 1) \ni r \mapsto \frac{r-1-\log r}{(\log r)^2}$ has values $\leq \frac{1}{2}$. Thus, for $b > a$, the derivative of the logarithmic mean value is less than the derivative of the arithmetic mean value. Consequently, the desired inequality (124) holds and the density remains positive under a reasonable CFL condition.

6.3 Preserving positivity of the pressure

Preserving the positivity of the pressure / internal energy is more complicated than the corresponding property of the density. For the (local) Lax-Friedrichs flux, it can be proved as described inter alia by Zhang and Shu (2010, Remark 2.4). Further investigations have to be conducted for the case of the numerical fluxes considered here.

As a general procedure, the reversed roles of entropy and energy as in section 5 can be used to get entropy stable fluxes that preserve the positivity of the internal energy as described by Bouchut (2004). This corresponds to a computation of the pressure via the entropy, which has also been used by Derigs, Winters, Gassner, and Walch (2016) in an *a posteriori* manner. However, this direction of further research will not be pursued here.

6.4 Suliciu relaxation solver

The Suliciu relaxation solver described by Bouchut (2004, Section 2.4) for the two-dimensional Euler equations in x direction can be summed up as follows.

At first, intermediate wave speeds are computed via

$$\begin{aligned} \text{if } p_+ \geq p_-, & \begin{cases} \frac{c_-}{\varrho_-} = \sqrt{\gamma \frac{p_-}{\varrho_-}} + \frac{\gamma+1}{2} \max \left\{ \frac{p_+ - p_-}{\varrho_+ \sqrt{\gamma p_+ / \varrho_+}} + v_{x-} - v_{x+}, 0 \right\}, \\ \frac{c_+}{\varrho_+} = \sqrt{\gamma \frac{p_+}{\varrho_+}} + \frac{\gamma+1}{2} \max \left\{ \frac{p_- - p_+}{c_-} + v_{x-} - v_{x+}, 0 \right\}, \end{cases} \\ \text{if } p_+ \leq p_-, & \begin{cases} \frac{c_+}{\varrho_+} = \sqrt{\gamma \frac{p_+}{\varrho_+}} + \frac{\gamma+1}{2} \max \left\{ \frac{p_- - p_+}{\varrho_- \sqrt{\gamma p_- / \varrho_-}} + v_{x-} - v_{x+}, 0 \right\}, \\ \frac{c_-}{\varrho_-} = \sqrt{\gamma \frac{p_-}{\varrho_-}} + \frac{\gamma+1}{2} \max \left\{ \frac{p_+ - p_-}{c_+} + v_{x-} - v_{x+}, 0 \right\}. \end{cases} \end{aligned} \quad (127)$$

Then, intermediate values are computed using $c_{\pm} = \varrho_{\pm} \frac{c_{\pm}}{c_{\pm}}$ as

$$\begin{aligned} v_{x-}^* &= v_{x+}^* = \frac{c_- v_{x-} + c_+ v_{x+} + p_- - p_+}{c_- + c_+}, & p_-^* &= p_+^* = \frac{c_+ p_- + c_- p_+ - c_- c_+ (v_{x+} - v_{x-})}{c_- + c_+}, \\ \frac{1}{\varrho_-^*} &= \frac{1}{\varrho_-} + \frac{c_+ (v_{x+} - v_{x-}) + p_- - p_+}{c_- (c_- + c_+)}, & \frac{1}{\varrho_+^*} &= \frac{1}{\varrho_+} + \frac{c_- (v_{x+} - v_{x-}) + p_+ - p_-}{c_+ (c_- + c_+)}, \\ \varepsilon_-^* &= \varepsilon_- + \frac{(p_-^*)^2 - p_-^2}{2c_-^2}, & \varepsilon_+^* &= \varepsilon_+ + \frac{(p_+^*)^2 - p_+^2}{2c_+^2}. \end{aligned} \quad (128)$$

Finally, the numerical fluxes are given by

$$\begin{pmatrix} f_{\varrho}^{\text{num}} \\ f_{\varrho v_x}^{\text{num}} \\ f_{\varrho v_y}^{\text{num}} \\ f_{\varrho e}^{\text{num}} \end{pmatrix} = \begin{cases} \begin{pmatrix} \varrho_- v_{x-} \\ \varrho_- v_{x-}^2 + p_- \\ \varrho_- v_{x-} v_{y,-} \\ \left(\frac{1}{2} \varrho_- v_{x-}^2 + \frac{1}{2} \varrho_- v_{y,-}^2 + \varrho_- \varepsilon_- + p_- \right) v_{x-} \end{pmatrix}, & \text{if } 0 \leq v_{x-} - \frac{c_-}{\varrho_-}, \\ \begin{pmatrix} \varrho_-^* v_{x-}^* \\ \varrho_-^* (v_{x-}^*)^2 + p_-^* \\ \varrho_-^* v_{x-}^* v_{y,-} \\ \left(\frac{1}{2} \varrho_-^* (v_{x-}^*)^2 + \frac{1}{2} \varrho_-^* (v_{y,-}^*)^2 + \varrho_-^* \varepsilon_-^* + p_-^* \right) v_{x-}^* \end{pmatrix}, & \text{if } v_{x-} - \frac{c_-}{\varrho_-} < 0 \leq v_{x-}^* \equiv v_{x+}^*, \\ \begin{pmatrix} \varrho_+^* v_{x+}^* \\ \varrho_+^* (v_{x+}^*)^2 + p_+^* \\ \varrho_+^* v_{x+}^* v_{y,+} \\ \left(\frac{1}{2} \varrho_+^* (v_{x+}^*)^2 + \frac{1}{2} \varrho_+^* (v_{y,+}^*)^2 + \varrho_+^* \varepsilon_+^* + p_+^* \right) v_{x+}^* \end{pmatrix}, & \text{if } v_{x-}^* \equiv v_{x+}^* < 0 \leq v_{x+} + \frac{c_+}{\varrho_+}, \\ \begin{pmatrix} \varrho_+ v_{x+} \\ \varrho_+ v_{x+}^2 + p_+ \\ \varrho_+ v_{x+} v_{y,+} \\ \left(\frac{1}{2} \varrho_+ v_{x+}^2 + \frac{1}{2} \varrho_+ v_{y,+}^2 + \varrho_+ \varepsilon_+ + p_+ \right) v_{x+} \end{pmatrix}, & \text{else.} \end{cases} \quad (129)$$

The numerical flux in y direction is computed analogously.

This flux is entropy stable and positivity preserving for ϱ and p , with corresponding CFL condition

$$\frac{\Delta t}{\Delta x} \max \left\{ \left| v_{x-} - \frac{c_-}{\varrho_-} \right|, \left| v_{x+} - \frac{c_+}{\varrho_+} \right| \right\} \leq \frac{1}{2}. \quad (130)$$

Additionally, it satisfies the maximum principle on the specific entropy s and resolves stationary contact discontinuities with $v_x \equiv 0, p \equiv \text{const}$ exactly.

7 Numerical tests

In this section, some numerical experiments using the methods described in the previous sections will be conducted. Unless stated otherwise, the ratio of specific heats is set to $\gamma = 1.4$ and the three stage, third-order, strong stability preserving Runge-Kutta method of Gottlieb and Shu (1998) will be used as time integration method.

If a one-dimensional Riemann problem is considered, the exact solution is computed as described by Toro (2009, Section 4).

7.1 Isentropic vortex

At first, the isentropic vortex problem of Shu (1997, Problem 8 in section 5.1) will be used to test the methods for a smooth solution. The initial condition is given by

$$\begin{pmatrix} \varrho_0 \\ \varrho v_{x,0} \\ \varrho v_{y,0} \\ \varrho e_0 \end{pmatrix} = \begin{pmatrix} \varrho_\infty \left(\frac{RT_0}{RT_\infty} \right)^{1/(\gamma-1)} \\ \varrho_0 v_{x,0} \\ \varrho_0 v_{y,0} \\ \varrho \frac{v_{x,0}^2 + v_{y,0}^2}{2} + \frac{p_0}{\gamma-1} \end{pmatrix}, \quad (131)$$

where

$$v_{x,0} = v_{x,\infty} + \delta v_x, \quad v_{y,0} = v_{y,\infty} + \delta v_y, \quad p_0 = \varrho_0 RT_0, \quad RT_0 = RT_\infty + \delta RT, \quad (132)$$

and

$$\delta v_x(x, y) = -y \frac{\beta}{2\pi} \exp\left(\frac{1-x^2-y^2}{2r}\right), \quad \delta v_y(x, y) = x \frac{\beta}{2\pi} \exp\left(\frac{1-x^2-y^2}{2r}\right), \quad (133)$$

$$\delta RT(x, y) = -\frac{\gamma-1}{\gamma} \frac{\beta}{8\pi^2} \exp\left(\frac{1-x^2-y^2}{r}\right). \quad (134)$$

The parameters have been chosen as

$$\varrho_\infty = 1, \quad v_{x,\infty} = 1, \quad v_{y,\infty} = 0, \quad RT_\infty = 1, \quad \beta = 5, \quad r = \frac{1}{4}. \quad (135)$$

The solution is computed on the domain $[-5, 5]^2$ during the time interval $[0, 10]$. Thus, the perturbation is of the order of magnitude $\exp\left(\frac{1-5^2}{2r}\right) \approx 10^{-21}$ at the boundary and should be approximately negligible for 64 bit floating point values. Therefore, the isentropic vortex should be advected with the free stream velocity and reach its initial position at $t = 10$.

The Suliciu relaxation solver has been used as numerical flux and several volume fluxes have been used for the subcell flux differencing form:

- Central: The central flux $\{f\}$ resulting in a standard nodal DG method as described by Gassner, Winters, and Kopriva (2016).
- Morinishi: The flux resulting in the split form of Morinishi (2010) as described by Gassner, Winters, and Kopriva (2016).
- Ducros: The flux resulting in the split form of Ducros, Laporte, Souleres, Guinot, Moinat, and Caruelle (2000) as described by Gassner, Winters, and Kopriva (2016).
- KG: The flux resulting in the split form of Kennedy and Gruber (2008) as described by Gassner, Winters, and Kopriva (2016).
- Pirozzoli: The flux resulting in the split form of Pirozzoli (2011) as described by Gassner, Winters, and Kopriva (2016).
- IR: The entropy conservative flux (55) of Roe (2006) and Ismail and Roe (2009).
- Ch: The entropy conservative flux (61) of Chandrashekar (2013).

- ϱ, v, β (2): The flux (64).
- $\varrho, v, \frac{1}{p}$: The flux (71).
- ϱ, v, p : The flux (80).
- ϱ, v, T (1): The flux (85).
- ϱ, v, T (2): The flux (89).
- ϱ, v, T (rev): The flux (117).

The errors (computed via the mass matrix \underline{M} , i.e. Lobatto quadrature) in the density for varying polynomial degrees p on a mesh using 10×10 elements are shown in Table 1. As can be seen there, there is not much variance in the error for $p = 1$. For $p \in \{2, 3\}$, there are variations up to approximately 15% [e.g. $p = 2$, Ducros, Morinishi and $p = 3$, Ducros, ϱ, v, T (rev)]. There does not seem to be any advantage of the entropy stable formulations compared to the other ones in this test case, similar to the results of Gassner, Winters, and Kopriva (2016) for the Taylor Green vortex.

Table 1: Errors for the isentropic vortex problem (131) using 10×10 elements of varying polynomial degrees p , several volume fluxes and the Suliciu relaxation solver as numerical flux.

p	Central $\ \text{err}_\varrho\ _M$	Morinishi $\ \text{err}_\varrho\ _M$	Ducros $\ \text{err}_\varrho\ _M$	KG $\ \text{err}_\varrho\ _M$	Pirozzoli $\ \text{err}_\varrho\ _M$	IR $\ \text{err}_\varrho\ _M$	Ch $\ \text{err}_\varrho\ _M$
1	1.20e−1	1.21e−1	1.20e−1	1.20e−1	1.20e−1	1.20e−1	1.21e−1
2	4.28e−2	4.36e−2	3.79e−2	3.83e−2	3.83e−2	3.93e−2	4.11e−2
3	1.73e−2	1.81e−2	1.60e−2	1.62e−2	1.62e−2	1.64e−2	1.80e−2

p	ϱ, v, β (2) $\ \text{err}_\varrho\ _M$	$\varrho, v, \frac{1}{p}$ $\ \text{err}_\varrho\ _M$	ϱ, v, p $\ \text{err}_\varrho\ _M$	ϱ, v, T (1) $\ \text{err}_\varrho\ _M$	ϱ, v, T (2) $\ \text{err}_\varrho\ _M$	ϱ, V, T (rev) $\ \text{err}_\varrho\ _M$
1	1.21e−1	1.21e−1	1.21e−1	1.21e−1	1.20e−1	1.20e−1
2	4.13e−2	4.11e−2	4.11e−2	4.11e−2	3.93e−2	4.12e−2
3	1.81e−2	1.79e−2	1.79e−2	1.80e−2	1.64e−2	1.89e−2

7.2 Sod shock tube: Subcell flux differencing

In this section, the classical shock tube of Sod (1978) will be used. The initial condition is given in primitive variables by

$$\varrho_0(x) = \begin{cases} 1, & x < \frac{1}{2}, \\ 0.125, & \text{else,} \end{cases}, \quad v_0(x) = 0, \quad p_0(x) = \begin{cases} 1, & x < \frac{1}{2}, \\ 0.1, & \text{else,} \end{cases} \quad (136)$$

and the conservative variables are computed via $\varrho v_0 = \varrho_0 v_0$ and $\varrho e_0 = \frac{1}{2} \varrho_0 v_0^2 + \frac{p_0}{\gamma-1}$. The solution is computed on the domain $[-0.5, 1.5]$ from $t = 0$ until $t = 0.25$ using 3000 time steps.

The error of the numerical solution for the density ϱ is calculated using Lobatto quadrature, i.e. the diagonal mass matrix \underline{M} of the SBP operator, for varying numbers of elements N and polynomial degrees p . The results using the Suliciu relaxation solver and the local Lax-Friedrichs flux as numerical flux are shown in Tables 2 and 3, respectively.

There is some variance across the results for different volume fluxes up to approximately 25% [e.g. for $p = 1$, $N = 10$, (ϱ, v, p) vs. $\varrho, v, T(\text{rev})$]. However, there is no clear bias towards one volume flux across all combinations of the polynomial degree p and the number of elements N [e.g. for $p = 1$ and $N = 320$, (ϱ, v, p) has a smaller error than $\varrho, v, T(\text{rev})$].

Contrary, comparing the numerical surface fluxes, there is some clear bias. Although the local Lax-Friedrichs flux yields a smaller error in some cases [e.g. $p = 1$, $N = 10$, (ϱ, v, p)], the Suliciu relaxation solver results in smaller errors if the resolution is good enough. Therefore, it can be considered superior to the LLF flux in this test case.

Additionally, the volume fluxes recovering the central form as well as the split forms of Morinishi (2010), Ducros, Laporte, Souleres, Guinot, Moinat, and Caruelle (2000), Kennedy and Gruber (2008), and Pirozzoli (2011) have been used. The relevant results are shown in

the Tables 4 (Suliciu) and 5 (LLF). As can be seen there, the central flux and the splitting of Morinishi (2010) are unstable. The splitting of Ducros, Laporte, Souleres, Guinot, Moinat, and Caruelle (2000) crashes for polynomial degree $p = 5$ whereas the other splittings remain stable. There is not much variance in the error for the stable calculations.

As for the entropy conservative volume fluxes, the Suliciu relaxation solver yields less error if the resolution is good enough.

Table 2: Errors and experimental order of convergence (EOC) for varying polynomial degrees p and number of elements N for the Sod shock tube problem (136) using the Suliciu relaxation solver as numerical flux and entropy conserving volume fluxes.

p	N	IR		Ch		ρ, v, β (2)		ρ, v, p		ρ, v, T (1)		ρ, v, T (2)		ρ, V, T (rev)	
		$\ \text{err}_\rho\ _M$	EOC	$\ \text{err}_\rho\ _M$	EOC	$\ \text{err}_\rho\ _M$	EOC	$\ \text{err}_\rho\ _M$	EOC	$\ \text{err}_\rho\ _M$	EOC	$\ \text{err}_\rho\ _M$	EOC	$\ \text{err}_\rho\ _M$	EOC
1	10	1.07e-1		1.06e-1		1.07e-1		1.37e-1		1.06e-1		1.06e-1		1.03e-1	
	20	6.90e-2	0.64	6.85e-2	0.63	7.07e-2	0.60	6.94e-2	0.98	6.85e-2	0.63	6.87e-2	0.62	6.83e-2	0.60
	40	4.79e-2	0.53	4.83e-2	0.51	5.15e-2	0.46	4.38e-2	0.66	4.83e-2	0.51	4.86e-2	0.50	4.79e-2	0.51
	80	3.54e-2	0.43	3.62e-2	0.42	3.76e-2	0.45	3.38e-2	0.38	3.62e-2	0.42	3.61e-2	0.43	3.64e-2	0.40
	160	2.64e-2	0.42	2.67e-2	0.44	2.79e-2	0.43	2.55e-2	0.40	2.67e-2	0.44	2.69e-2	0.42	2.70e-2	0.43
	320	1.98e-2	0.42	1.98e-2	0.43	2.01e-2	0.47	1.91e-2	0.42	1.98e-2	0.43	1.99e-2	0.44	2.03e-2	0.41
2	10	6.37e-2		6.26e-2		6.28e-2		6.39e-2		6.26e-2		6.31e-2		6.51e-2	
	20	3.37e-2	0.92	3.34e-2	0.91	3.35e-2	0.90	3.60e-2	0.83	3.34e-2	0.91	3.32e-2	0.92	3.30e-2	0.98
	40	2.84e-2	0.24	2.86e-2	0.22	2.88e-2	0.22	2.77e-2	0.38	2.86e-2	0.22	2.85e-2	0.22	2.86e-2	0.21
	80	2.14e-2	0.41	2.12e-2	0.43	2.14e-2	0.43	2.09e-2	0.40	2.12e-2	0.43	2.13e-2	0.42	2.13e-2	0.43
	160	1.23e-2	0.80	1.22e-2	0.81	1.22e-2	0.81	1.21e-2	0.79	1.22e-2	0.81	1.22e-2	0.80	1.26e-2	0.76
	320	6.65e-3	0.88	6.61e-3	0.88	6.66e-3	0.88	6.81e-3	0.83	6.61e-3	0.88	6.60e-3	0.89	6.70e-3	0.91
3	10	3.30e-2		3.33e-2		3.35e-2		3.69e-2		3.33e-2		3.24e-2		3.18e-2	
	20	2.93e-2	0.17	2.91e-2	0.19	2.92e-2	0.20	2.84e-2	0.38	2.91e-2	0.19	2.87e-2	0.18	2.91e-2	0.12
	40	2.14e-2	0.46	2.10e-2	0.47	2.14e-2	0.45	2.25e-2	0.34	2.10e-2	0.47	2.11e-2	0.44	2.07e-2	0.49
	80	1.08e-2	0.98	1.09e-2	0.95	1.11e-2	0.95	1.16e-2	0.96	1.09e-2	0.95	1.09e-2	0.95	1.03e-2	1.01
	160	6.48e-3	0.74	6.45e-3	0.76	6.51e-3	0.77	7.10e-3	0.71	6.45e-3	0.76	6.42e-3	0.77	6.68e-3	0.62
	320	5.00e-3	0.38	4.97e-3	0.38	4.98e-3	0.39	5.32e-3	0.42	4.97e-3	0.38	4.93e-3	0.38	5.15e-3	0.37
4	10	3.98e-2		3.97e-2		4.01e-2		4.18e-2		3.97e-2		3.94e-2		3.70e-2	
	20	1.32e-2	1.59	1.29e-2	1.63	1.29e-2	1.64	1.46e-2	1.52	1.29e-2	1.63	1.27e-2	1.63	1.35e-2	1.45
	40	1.06e-2	0.32	1.03e-2	0.32	1.02e-2	0.33	1.18e-2	0.31	1.03e-2	0.32	1.05e-2	0.29	1.14e-2	0.25
	80	1.30e-2	-0.30	1.27e-2	-0.30	1.28e-2	-0.32	1.27e-2	-0.10	1.27e-2	-0.30	1.26e-2	-0.27	1.27e-2	-0.16
	160	7.10e-3	0.88	6.95e-3	0.87	6.95e-3	0.88	7.47e-3	0.76	6.95e-3	0.87	6.97e-3	0.86	7.38e-3	0.78
	320	4.59e-3	0.63	4.49e-3	0.63	4.46e-3	0.64	4.90e-3	0.61	4.49e-3	0.63	4.48e-3	0.64	4.85e-3	0.61
5	10	2.97e-2		2.87e-2		2.88e-2		2.87e-2		2.87e-2		2.86e-2		2.70e-2	
	20	2.24e-2	0.41	2.19e-2	0.39	2.24e-2	0.36	2.47e-2	0.22	2.19e-2	0.39	2.21e-2	0.37	2.05e-2	0.40
	40	1.10e-2	1.02	1.10e-2	0.99	1.15e-2	0.96	1.28e-2	0.95	1.10e-2	0.99	1.11e-2	0.99	1.03e-2	0.99
	80	6.34e-3	0.79	6.22e-3	0.82	6.36e-3	0.86	7.39e-3	0.79	6.22e-3	0.82	6.24e-3	0.83	6.48e-3	0.67
	160	5.56e-3	0.19	5.39e-3	0.21	5.43e-3	0.23	6.10e-3	0.28	5.39e-3	0.21	5.46e-3	0.19	5.73e-3	0.18
	320	4.66e-3	0.26	4.43e-3	0.28	4.37e-3	0.31	4.92e-3	0.31	4.43e-3	0.28	4.50e-3	0.28	4.96e-3	0.21

Table 3: Errors and experimental order of convergence (EOC) for varying polynomial degrees p and number of elements N for the Sod shock tube problem (136) using the local Lax-Friedrichs numerical flux and entropy conserving volume fluxes.

p	N	IR		Ch		q, v, β (2)		q, v, p		q, v, T (1)		q, v, T (2)		q, V, T (rev)	
		$\ err_e\ _M$	EOC	$\ err_e\ _M$	EOC	$\ err_e\ _M$	EOC	$\ err_e\ _M$	EOC	$\ err_e\ _M$	EOC	$\ err_e\ _M$	EOC	$\ err_e\ _M$	EOC
1	10	1.02e-1		1.02e-1		1.22e-1		1.22e-1		1.02e-1		1.03e-1		1.04e-1	
	20	6.94e-2	0.55	6.87e-2	0.58	7.25e-2	0.75	7.25e-2	0.75	6.87e-2	0.58	6.96e-2	0.56	7.18e-2	0.53
	40	5.13e-2	0.44	5.22e-2	0.40	4.61e-2	0.65	4.61e-2	0.65	5.22e-2	0.40	5.14e-2	0.44	5.00e-2	0.52
	80	3.75e-2	0.45	3.81e-2	0.45	3.53e-2	0.38	3.53e-2	0.38	3.81e-2	0.45	3.82e-2	0.43	3.82e-2	0.39
	160	2.83e-2	0.40	2.86e-2	0.41	2.60e-2	0.44	2.60e-2	0.44	2.86e-2	0.41	2.90e-2	0.40	2.90e-2	0.40
	320	2.10e-2	0.43	2.10e-2	0.44	1.94e-2	0.42	1.94e-2	0.42	2.10e-2	0.44	2.13e-2	0.44	2.17e-2	0.42
2	10	6.45e-2		6.30e-2		6.32e-2		6.32e-2		6.30e-2		6.37e-2		6.76e-2	
	20	3.66e-2	0.82	3.65e-2	0.79	3.85e-2	0.71	3.85e-2	0.71	3.65e-2	0.79	3.58e-2	0.83	3.52e-2	0.94
	40	3.01e-2	0.29	3.04e-2	0.26	2.92e-2	0.40	2.92e-2	0.40	3.04e-2	0.26	3.01e-2	0.25	3.01e-2	0.23
	80	2.19e-2	0.46	2.18e-2	0.48	2.19e-2	0.42	2.19e-2	0.42	2.18e-2	0.48	2.16e-2	0.48	2.16e-2	0.47
	160	1.29e-2	0.76	1.29e-2	0.76	1.27e-2	0.79	1.27e-2	0.79	1.29e-2	0.76	1.29e-2	0.75	1.33e-2	0.70
	320	6.91e-3	0.90	6.89e-3	0.90	7.12e-3	0.83	7.12e-3	0.83	6.89e-3	0.90	6.87e-3	0.91	6.98e-3	0.93
3	10	3.48e-2		3.48e-2		3.79e-2		3.79e-2		3.48e-2		3.41e-2		3.30e-2	
	20	3.10e-2	0.17	3.09e-2	0.17	3.21e-2	0.24	3.21e-2	0.24	3.09e-2	0.17	3.02e-2	0.18	3.04e-2	0.12
	40	2.19e-2	0.50	2.16e-2	0.52	2.17e-2	0.17	2.85e-2	0.17	2.16e-2	0.52	2.13e-2	0.50	2.09e-2	0.54
	80	1.16e-2	0.91	1.17e-2	0.89	1.16e-2	0.40	2.16e-2	0.40	1.17e-2	0.89	1.14e-2	0.90	1.09e-2	0.94
	160	7.23e-3	0.69	7.09e-3	0.72	6.93e-3	0.74	2.00e-2	0.11	7.09e-3	0.72	6.87e-3	0.73	7.67e-3	0.50
	320	5.77e-3	0.32	5.63e-3	0.33	5.50e-3	0.32	1.60e-2	0.32	5.63e-3	0.33	5.52e-3	0.32	6.36e-3	0.27
4	10	4.03e-2		4.03e-2		4.24e-2		4.24e-2		4.03e-2		3.98e-2		3.79e-2	
	20	1.43e-2	1.50	1.40e-2	1.52	1.96e-2	1.11	1.96e-2	1.11	1.40e-2	1.52	1.32e-2	1.60	1.37e-2	1.47
	40	1.05e-2	0.44	1.01e-2	0.47	2.40e-2	-0.29	2.40e-2	-0.29	1.01e-2	0.47	1.02e-2	0.36	1.16e-2	0.24
	80	1.30e-2	-0.30	1.28e-2	-0.34	3.48e-2	-0.54	3.48e-2	-0.54	1.28e-2	-0.34	1.27e-2	-0.31	1.25e-2	-0.10
	160	7.43e-3	0.81	7.28e-3	0.81	2.58e-2	0.43	2.58e-2	0.43	7.28e-3	0.81	7.32e-3	0.79	7.87e-3	0.67
	320	4.90e-3	0.60	4.78e-3	0.61	1.77e-2	0.55	1.77e-2	0.55	4.78e-3	0.61	4.80e-3	0.61	5.49e-3	0.52
5	10	3.02e-2		2.93e-2		3.02e-2		3.02e-2		2.93e-2		2.91e-2		2.73e-2	
	20	2.31e-2	0.39	2.26e-2	0.37	3.05e-2	-0.02	3.05e-2	-0.02	2.26e-2	0.37	2.24e-2	0.38	2.11e-2	0.37
	40	1.20e-2	0.95	1.17e-2	0.96	3.24e-2	-0.09	3.24e-2	-0.09	1.17e-2	0.96	1.19e-2	0.91	1.08e-2	0.96
	80	7.29e-3	0.71	6.82e-3	0.78	2.85e-2	0.18	2.85e-2	0.18	6.82e-3	0.78	7.08e-3	0.75	7.14e-3	0.60
	160	6.48e-3	0.17	6.04e-3	0.18	1.81e-2	0.66	1.81e-2	0.66	6.04e-3	0.18	6.34e-3	0.16	6.50e-3	0.14
	320	5.41e-3	0.26	4.92e-3	0.29	1.20e-2	0.59	1.20e-2	0.59	4.92e-3	0.29	5.22e-3	0.28	5.66e-3	0.20

Table 4: Errors and experimental order of convergence (EOC) for varying polynomial degrees p and number of elements N for the Sod shock tube problem (136) using the Suliciu relaxation solver as numerical flux and "simple" volume fluxes.

p	N	Central		Morinishi		Ducros		KG		Pirozzoli	
		$\ \text{err}_\ell\ _M$	EOC	$\ \text{err}_\ell\ _M$	EOC	$\ \text{err}_\ell\ _M$	EOC	$\ \text{err}_\ell\ _M$	EOC	$\ \text{err}_\ell\ _M$	EOC
1	10	*		*		1.04e-1		1.05e-1		1.06e-1	
	20	*	*	*	*	6.66e-2	0.65	6.64e-2	0.66	6.68e-2	0.66
	40	*	*	*	*	4.20e-2	0.67	4.51e-2	0.56	4.59e-2	0.54
	80	*	*	*	*	3.26e-2	0.36	3.48e-2	0.37	3.50e-2	0.39
	160	*	*	*	*	2.45e-2	0.41	2.59e-2	0.43	2.58e-2	0.44
	320	*	*	*	*	1.86e-2	0.40	1.95e-2	0.41	1.95e-2	0.40
2	10	*		8.74e-2		6.38e-2		6.40e-2		6.39e-2	
	20	*	*	*	*	3.36e-2	0.93	3.41e-2	0.91	3.41e-2	0.91
	40	*	*	*	*	2.56e-2	0.39	2.66e-2	0.36	2.69e-2	0.34
	80	*	*	*	*	1.93e-2	0.41	2.00e-2	0.41	2.00e-2	0.43
	160	*	*	*	*	1.18e-2	0.71	1.22e-2	0.71	1.24e-2	0.69
	320	*	*	*	*	6.32e-3	0.90	6.47e-3	0.91	6.55e-3	0.92
3	10	*		*		3.29e-2		3.30e-2		3.33e-2	
	20	*	*	*	*	2.51e-2	0.39	2.56e-2	0.36	2.60e-2	0.36
	40	*	*	*	*	1.74e-2	0.52	1.93e-2	0.41	1.93e-2	0.43
	80	*	*	*	*	9.93e-3	0.81	9.89e-3	0.97	9.79e-3	0.98
	160	*	*	*	*	6.05e-3	0.72	5.97e-3	0.73	6.04e-3	0.70
	320	*	*	*	*	5.03e-3	0.27	4.83e-3	0.31	4.85e-3	0.32
4	10	*		*		3.48e-2		3.62e-2		3.63e-2	
	20	*	*	*	*	1.35e-2	1.37	1.26e-2	1.52	1.27e-2	1.51
	40	*	*	*	*	1.21e-2	0.15	1.17e-2	0.11	1.17e-2	0.12
	80	*	*	*	*	1.03e-2	0.23	1.13e-2	0.05	1.15e-2	0.03
	160	*	*	*	*	7.13e-3	0.53	7.04e-3	0.68	7.15e-3	0.68
	320	*	*	*	*	5.17e-3	0.46	4.77e-3	0.56	4.74e-3	0.59
5	10	*		*		*		2.53e-2		2.59e-2	
	20	*	*	*	*	*	*	1.92e-2	0.40	1.92e-2	0.43
	40	*	*	*	*	*	*	9.55e-3	1.00	9.40e-3	1.03
	80	*	*	*	*	*	*	6.47e-3	0.56	6.47e-3	0.54
	160	*	*	*	*	*	*	5.68e-3	0.19	5.68e-3	0.19
	320	*	*	*	*	*	*	5.24e-3	0.12	5.19e-3	0.13

Table 5: Errors and experimental order of convergence (EOC) for varying polynomial degrees p and number of elements N for the Sod shock tube problem (136) using the local Lax-Friedrichs numerical flux and "simple" volume fluxes.

p	N	Central		Morinishi		Ducros		KG		Pirozzoli	
		$\ \text{err}_\varrho\ _M$	EOC	$\ \text{err}_\varrho\ _M$	EOC	$\ \text{err}_\varrho\ _M$	EOC	$\ \text{err}_\varrho\ _M$	EOC	$\ \text{err}_\varrho\ _M$	EOC
1	10	*		*		1.03e-1		1.02e-1		1.02e-1	
	20	*	*	*	*	6.74e-2	0.61	6.75e-2	0.60	6.75e-2	0.60
	40	*	*	*	*	4.38e-2	0.62	4.82e-2	0.49	4.94e-2	0.45
	80	*	*	*	*	3.38e-2	0.37	3.63e-2	0.41	3.68e-2	0.42
	160	*	*	*	*	2.60e-2	0.38	2.76e-2	0.39	2.77e-2	0.41
	320	*	*	*	*	*	*	2.09e-2	0.40	2.08e-2	0.41
2	10	8.35e-2		5.87e-2		6.60e-2		6.54e-2		6.46e-2	
	20	*	*	*	*	3.42e-2	0.95	3.52e-2	0.90	3.53e-2	0.87
	40	*	*	*	*	2.67e-2	0.36	2.78e-2	0.34	2.82e-2	0.33
	80	*	*	*	*	1.93e-2	0.47	2.02e-2	0.47	2.02e-2	0.48
	160	*	*	*	*	1.24e-2	0.65	1.27e-2	0.66	1.29e-2	0.65
	320	*	*	*	*	6.54e-3	0.92	6.66e-3	0.94	6.73e-3	0.94
3	10	*		*		3.31e-2		3.44e-2		3.50e-2	
	20	*	*	*	*	2.58e-2	0.36	2.72e-2	0.34	2.78e-2	0.34
	40	*	*	*	*	1.74e-2	0.57	1.93e-2	0.50	1.93e-2	0.52
	80	*	*	*	*	1.05e-2	0.74	1.04e-2	0.88	1.04e-2	0.89
	160	*	*	*	*	6.91e-3	0.60	6.57e-3	0.67	6.63e-3	0.65
	320	*	*	*	*	6.08e-3	0.19	5.58e-3	0.24	5.59e-3	0.25
4	10	*		*		3.49e-2		3.68e-2		3.70e-2	
	20	*	*	*	*	1.27e-2	1.46	1.23e-2	1.58	1.26e-2	1.56
	40	*	*	*	*	1.18e-2	0.11	1.13e-2	0.13	1.14e-2	0.15
	80	*	*	*	*	1.02e-2	0.21	1.13e-2	0.00	1.15e-2	-0.01
	160	*	*	*	*	7.43e-3	0.46	7.49e-3	0.59	7.57e-3	0.60
	320	*	*	*	*	5.47e-3	0.44	5.22e-3	0.52	5.15e-3	0.56
5	10	*		*		*		2.57e-2		2.65e-2	
	20	*	*	*	*	*	*	1.93e-2	0.41	1.93e-2	0.46
	40	*	*	*	*	*	*	1.11e-2	0.80	1.08e-2	0.84
	80	*	*	*	*	*	*	7.68e-3	0.54	7.53e-3	0.52
	160	*	*	*	*	*	*	6.94e-3	0.15	6.82e-3	0.14
	320	*	*	*	*	*	*	6.35e-3	0.13	6.18e-3	0.14

7.3 Modified version of Sod's shock tube: Subcell flux differencing

In this section, the modified version of the shock tube of Sod (1978) as described by Toro (2009, Section 6.4, Test 1) will be used to test the methods. The initial condition is given in primitive variables by

$$\varrho_0(x) = \begin{cases} 1, & x < \frac{3}{10}, \\ 0.125 & \text{else,} \end{cases}, \quad v_0(x) = \begin{cases} 0.75, & x < \frac{3}{10}, \\ 0 & \text{else,} \end{cases}, \quad p_0(x) = \begin{cases} 1, & x < \frac{3}{10}, \\ 0.1, & \text{else,} \end{cases} \quad (137)$$

and the conservative variables are again computed via $\varrho v_0 = \varrho_0 v_0$ and $\varrho e_0 = \frac{1}{2} \varrho_0 v_0^2 + \frac{p_0}{\gamma-1}$. The solution is computed on the domain $[0, 1]$ from $t = 0$ until $t = 0.2$ using 15 000 steps and the error is computed as in section 7.2.

The results using the Suliciu relaxation solver and the local Lax-Friedrichs flux for varying polynomial degrees p and number of elements N are shown in Table 6 and 7, respectively. Again, there are some variances across the volume fluxes of up to 33% [e.g. $p = 4$, $N = 10$, (ϱ, v, p) vs. $(\varrho, v, \beta(2))$] but no flux seems to be clearly superior. As in the previous test case in section 7.2, the Suliciu solver performs better than the LLF flux – at least, if the resolution is good enough.

As in the previous section 7.2, the volume fluxes recovering the central form as well as the split forms of Morinishi (2010), Ducros, Laporte, Souleres, Guinot, Moinat, and Caruelle (2000), Kennedy and Gruber (2008), and Pirozzoli (2011) have been used. The relevant results are shown in the Tables 8 (Suliciu) and 9 (LLF).

Contrary to the results of the unmodified shock tube of Sod, all calculations are stable for low resolution. The splitting of Morinishi (2010) blows up at first if the Suliciu solver is used, while the central flux crashes at first for the LLF flux. Moreover, even the splittings of Kennedy and Gruber (2008); Pirozzoli (2011) that remained stable in the previous section 7.2 blow up for higher polynomial degrees.

Table 6: Errors and experimental order of convergence (EOC) for varying polynomial degrees p and number of elements N for the modified Sod shock tube problem (137) using the Suliciu relaxation solver as numerical flux and entropy conservative volume fluxes.

p	N	IR		Ch		q, v, β (2)		$q, v, \frac{1}{p}$		q, v, p		q, v, T (1)		q, v, T (2)		q, V, T (rev)	
		$\ err_e\ _M$	EOC	$\ err_e\ _M$	EOC	$\ err_e\ _M$	EOC	$\ err_e\ _M$	EOC	$\ err_e\ _M$	EOC	$\ err_e\ _M$	EOC	$\ err_e\ _M$	EOC	$\ err_e\ _M$	EOC
1	10	1.40e-1		1.42e-1		1.42e-1		1.43e-1		1.43e-1		1.42e-1		1.42e-1		1.42e-1	
	20	7.93e-2	0.82	7.74e-2	0.88	7.85e-2	0.86	8.82e-2	0.70	8.82e-2	0.70	7.74e-2	0.88	7.67e-2	0.89	7.55e-2	0.91
	40	6.46e-2	0.30	6.49e-2	0.25	6.69e-2	0.23	6.13e-2	0.53	6.13e-2	0.53	6.49e-2	0.25	6.44e-2	0.25	6.49e-2	0.22
	80	5.20e-2	0.31	5.24e-2	0.31	5.42e-2	0.30	5.27e-2	0.22	5.27e-2	0.22	5.24e-2	0.31	5.20e-2	0.31	5.20e-2	0.32
	160	3.63e-2	0.52	3.67e-2	0.51	3.80e-2	0.51	3.59e-2	0.56	3.59e-2	0.56	3.67e-2	0.51	3.66e-2	0.51	3.65e-2	0.51
	320	2.47e-2	0.56	2.48e-2	0.56	2.56e-2	0.57	2.43e-2	0.56	2.43e-2	0.56	2.48e-2	0.56	2.48e-2	0.56	2.51e-2	0.54
2	10	8.31e-2		8.28e-2		8.31e-2		8.73e-2		8.73e-2		8.28e-2		8.18e-2		8.24e-2	
	20	4.89e-2	0.76	4.84e-2	0.78	4.80e-2	0.79	5.27e-2	0.73	5.27e-2	0.73	4.84e-2	0.78	4.76e-2	0.78	5.05e-2	0.71
	40	4.84e-2	0.02	4.85e-2	0.00	4.87e-2	-0.02	4.53e-2	0.22	4.53e-2	0.22	4.85e-2	0.00	4.83e-2	-0.02	4.77e-2	0.08
	80	2.17e-2	1.16	2.17e-2	1.16	2.18e-2	1.16	2.46e-2	0.88	2.46e-2	0.88	2.17e-2	1.16	2.13e-2	1.18	2.22e-2	1.10
	160	1.88e-2	0.21	1.88e-2	0.21	1.86e-2	0.23	2.15e-2	0.20	2.15e-2	0.20	1.88e-2	0.21	1.87e-2	0.19	1.94e-2	0.19
	320	1.55e-2	0.28	1.57e-2	0.26	1.58e-2	0.23	1.57e-2	0.45	1.57e-2	0.45	1.57e-2	0.26	1.56e-2	0.26	1.56e-2	0.32
3	10	5.76e-2		5.53e-2		5.21e-2		6.96e-2		6.96e-2		5.53e-2		5.40e-2		5.96e-2	
	20	5.42e-2	0.09	5.26e-2	0.07	5.18e-2	0.01	6.15e-2	0.18	6.15e-2	0.18	5.26e-2	0.07	5.15e-2	0.07	5.24e-2	0.19
	40	2.45e-2	1.14	2.29e-2	1.20	2.22e-2	1.22	3.98e-2	0.63	3.98e-2	0.63	2.29e-2	1.20	2.18e-2	1.24	2.77e-2	0.92
	80	2.06e-2	0.25	1.94e-2	0.24	1.87e-2	0.24	3.17e-2	0.33	3.17e-2	0.33	1.94e-2	0.24	1.87e-2	0.22	2.39e-2	0.21
	160	1.60e-2	0.37	1.62e-2	0.26	1.67e-2	0.17	2.77e-2	0.19	2.77e-2	0.19	1.62e-2	0.26	1.64e-2	0.19	1.56e-2	0.62
	320	1.25e-2	0.35	1.22e-2	0.40	1.25e-2	0.42	2.35e-2	0.24	2.35e-2	0.24	1.22e-2	0.40	1.18e-2	0.48	1.43e-2	0.12
4	10	4.22e-2		3.89e-2		3.79e-2		5.65e-2		5.65e-2		3.89e-2		3.82e-2		4.11e-2	
	20	3.60e-2	0.23	3.36e-2	0.21	3.42e-2	0.15	3.97e-2	0.51	3.97e-2	0.51	3.36e-2	0.21	3.35e-2	0.19	3.08e-2	0.42
	40	2.74e-2	0.39	2.66e-2	0.33	2.71e-2	0.33	3.03e-2	0.39	3.03e-2	0.39	2.66e-2	0.33	2.64e-2	0.35	2.39e-2	0.37
	80	2.33e-2	0.23	2.29e-2	0.22	2.33e-2	0.22	2.35e-2	0.37	2.35e-2	0.37	2.29e-2	0.22	2.27e-2	0.21	2.08e-2	0.20
	160	1.53e-2	0.60	1.40e-2	0.71	1.36e-2	0.78	1.49e-2	0.66	1.49e-2	0.66	1.40e-2	0.71	1.31e-2	0.79	1.66e-2	0.32
	320	1.27e-2	0.27	1.25e-2	0.16	1.26e-2	0.10	1.59e-2	-0.10	1.59e-2	-0.10	1.25e-2	0.16	1.20e-2	0.12	1.29e-2	0.36
5	10	5.95e-2		5.85e-2		5.91e-2		6.27e-2		6.27e-2		5.85e-2		5.62e-2		5.57e-2	
	20	2.98e-2	1.00	2.84e-2	1.04	2.85e-2	1.05	3.35e-2	0.90	3.35e-2	0.90	2.84e-2	1.04	2.71e-2	1.05	2.79e-2	1.00
	40	2.62e-2	0.19	2.24e-2	0.34	2.33e-2	0.29	2.67e-2	0.33	2.67e-2	0.33	2.24e-2	0.34	2.41e-2	0.17	2.52e-2	0.15
	80	2.08e-2	0.33	2.03e-2	0.14	2.12e-2	0.13	2.17e-2	0.30	2.17e-2	0.30	2.03e-2	0.14	2.04e-2	0.24	1.93e-2	0.39
	160	1.66e-2	0.33	1.61e-2	0.34	1.72e-2	0.30	1.85e-2	0.23	1.85e-2	0.23	1.61e-2	0.34	1.66e-2	0.29	1.52e-2	0.34
	320	1.45e-2	0.19	1.43e-2	0.17	1.60e-2	0.10	1.96e-2	-0.08	1.96e-2	-0.08	1.43e-2	0.17	1.47e-2	0.18	1.33e-2	0.19

Table 7: Errors and experimental order of convergence (EOC) for varying polynomial degrees p and number of elements N for the modified Sod shock tube problem (137) using the local Lax-Friedrichs numerical flux and entropy conservative volume fluxes.

p	N	IR		Ch		ρ, v, β (2)		$\rho, v, \frac{1}{p}$		ρ, v, p		ρ, v, T (1)		ρ, v, T (2)		ρ, V, T (rev)	
		$\ \text{err}_e\ _M$	EOC	$\ \text{err}_e\ _M$	EOC	$\ \text{err}_e\ _M$	EOC	$\ \text{err}_e\ _M$	EOC	$\ \text{err}_e\ _M$	EOC	$\ \text{err}_e\ _M$	EOC	$\ \text{err}_e\ _M$	EOC	$\ \text{err}_e\ _M$	EOC
1	10	1.42e-1		1.44e-1		1.44e-1		1.39e-1		1.39e-1		1.44e-1		1.45e-1		1.45e-1	
	20	7.61e-2	0.90	7.47e-2	0.95	7.53e-2	0.94	9.05e-2	0.62	9.05e-2	0.62	7.47e-2	0.95	7.44e-2	0.96	7.37e-2	0.97
	40	6.67e-2	0.19	6.69e-2	0.16	6.87e-2	0.13	6.23e-2	0.54	6.23e-2	0.54	6.69e-2	0.16	6.65e-2	0.16	6.68e-2	0.14
	80	5.38e-2	0.31	5.42e-2	0.30	5.63e-2	0.29	5.35e-2	0.22	5.35e-2	0.22	5.42e-2	0.30	5.41e-2	0.30	5.40e-2	0.31
	160	3.78e-2	0.51	3.83e-2	0.50	3.97e-2	0.51	3.66e-2	0.55	3.66e-2	0.55	3.83e-2	0.50	3.82e-2	0.50	3.80e-2	0.51
	320	2.58e-2	0.55	2.60e-2	0.56	2.68e-2	0.57	2.49e-2	0.55	2.49e-2	0.55	2.60e-2	0.56	2.60e-2	0.55	2.63e-2	0.53
2	10	8.77e-2		8.72e-2		8.74e-2		9.15e-2		9.15e-2		8.72e-2		8.63e-2		8.62e-2	
	20	5.26e-2	0.74	5.22e-2	0.74	5.18e-2	0.75	5.37e-2	0.77	5.37e-2	0.77	5.22e-2	0.74	5.21e-2	0.73	5.43e-2	0.67
	40	4.83e-2	0.12	4.88e-2	0.10	4.90e-2	0.08	4.77e-2	0.17	4.77e-2	0.17	4.88e-2	0.10	4.84e-2	0.11	4.76e-2	0.19
	80	2.26e-2	1.10	2.31e-2	1.08	2.30e-2	1.09	2.53e-2	0.92	2.53e-2	0.92	2.31e-2	1.08	2.28e-2	1.09	2.38e-2	1.00
	160	1.95e-2	0.21	2.01e-2	0.20	1.96e-2	0.23	2.12e-2	0.25	2.12e-2	0.25	2.01e-2	0.20	2.01e-2	0.18	2.10e-2	0.18
	320	1.56e-2	0.32	1.61e-2	0.32	1.63e-2	0.27	1.43e-2	0.57	1.43e-2	0.57	1.61e-2	0.32	1.60e-2	0.33	1.61e-2	0.39
3	10	5.78e-2		5.57e-2		5.31e-2		6.41e-2		6.41e-2		5.57e-2		5.57e-2		5.96e-2	
	20	5.41e-2	0.10	5.33e-2	0.07	5.29e-2	0.01	6.01e-2	0.09	6.01e-2	0.09	5.33e-2	0.07	5.19e-2	0.10	5.24e-2	0.19
	40	2.50e-2	1.12	2.39e-2	1.16	2.34e-2	1.18	3.64e-2	0.72	3.64e-2	0.72	2.39e-2	1.16	2.28e-2	1.18	2.70e-2	0.96
	80	2.10e-2	0.25	2.02e-2	0.24	1.94e-2	0.26	2.88e-2	0.34	2.88e-2	0.34	2.02e-2	0.24	1.95e-2	0.23	2.37e-2	0.19
	160	1.73e-2	0.28	1.72e-2	0.23	1.73e-2	0.17	2.27e-2	0.34	2.27e-2	0.34	1.72e-2	0.23	1.71e-2	0.19	1.69e-2	0.49
	320	1.24e-2	0.48	1.25e-2	0.47	1.28e-2	0.44	2.30e-2	-0.02	2.30e-2	-0.02	1.25e-2	0.47	1.19e-2	0.51	1.37e-2	0.30
4	10	3.85e-2		3.71e-2		3.65e-2		5.28e-2		5.28e-2		3.71e-2		3.54e-2		3.98e-2	
	20	3.48e-2	0.14	3.37e-2	0.14	3.43e-2	0.09	3.73e-2	0.50	3.73e-2	0.50	3.37e-2	0.14	3.41e-2	0.06	2.99e-2	0.42
	40	2.69e-2	0.37	2.59e-2	0.38	2.69e-2	0.35	2.98e-2	0.32	2.98e-2	0.32	2.59e-2	0.38	2.65e-2	0.36	2.42e-2	0.30
	80	2.44e-2	0.14	2.38e-2	0.12	2.40e-2	0.17	2.53e-2	0.24	2.53e-2	0.24	2.38e-2	0.12	2.42e-2	0.13	2.40e-2	0.01
	160	1.39e-2	0.81	1.35e-2	0.82	1.37e-2	0.80	1.66e-2	0.61	1.66e-2	0.61	1.35e-2	0.82	1.42e-2	0.77	1.64e-2	0.55
	320	1.40e-2	-0.01	1.37e-2	-0.02	1.40e-2	-0.03	1.94e-2	-0.22	1.94e-2	-0.22	1.37e-2	-0.02	1.40e-2	0.03	1.50e-2	0.13
5	10	6.49e-2		6.49e-2		6.41e-2		6.53e-2		6.53e-2		6.49e-2		6.21e-2		5.83e-2	
	20	3.44e-2	0.92	3.39e-2	0.94	3.25e-2	0.98	3.49e-2	0.91	3.49e-2	0.91	3.39e-2	0.94	3.21e-2	0.95	3.25e-2	0.84
	40	3.10e-2	0.15	2.85e-2	0.25	2.55e-2	0.35	2.75e-2	0.34	2.75e-2	0.34	2.85e-2	0.25	2.85e-2	0.17	2.92e-2	0.15
	80	2.46e-2	0.33	2.47e-2	0.20	2.35e-2	0.12	2.19e-2	0.33	2.19e-2	0.33	2.47e-2	0.20	2.44e-2	0.23	2.32e-2	0.33
	160	1.84e-2	0.42	1.83e-2	0.43	1.78e-2	0.40	1.62e-2	0.43	1.62e-2	0.43	1.83e-2	0.43	1.86e-2	0.39	1.71e-2	0.44
	320	1.70e-2	0.12	1.72e-2	0.09	1.70e-2	0.07	1.62e-2	0.00	1.62e-2	0.00	1.72e-2	0.09	1.67e-2	0.15	1.56e-2	0.14

Table 8: Errors and experimental order of convergence (EOC) for varying polynomial degrees p and number of elements N for the modified Sod shock tube problem (137) using the Suliciu relaxation solver as numerical flux and "simple" volume fluxes.

p	N	Central		Morinishi		Ducros		KG		Pirozzoli	
		$\ \text{err}_\varrho\ _M$	EOC	$\ \text{err}_\varrho\ _M$	EOC	$\ \text{err}_\varrho\ _M$	EOC	$\ \text{err}_\varrho\ _M$	EOC	$\ \text{err}_\varrho\ _M$	EOC
1	10	1.42e-1		1.42e-1		1.34e-1		1.33e-1		1.33e-1	
	20	7.46e-2	0.93	8.55e-2	0.74	7.21e-2	0.89	7.41e-2	0.85	7.48e-2	0.83
	40	6.63e-2	0.17	1.05e-1	-0.29	5.71e-2	0.34	6.07e-2	0.29	6.17e-2	0.28
	80	6.00e-2	0.14	*	*	4.49e-2	0.35	4.79e-2	0.34	4.86e-2	0.34
	160	5.25e-2	0.19	*	*	3.10e-2	0.53	3.35e-2	0.52	3.42e-2	0.51
	320	4.86e-2	0.11	*	*	2.14e-2	0.53	2.34e-2	0.52	2.40e-2	0.51
2	10	*		8.38e-2		7.83e-2		8.03e-2		8.02e-2	
	20	*	*	4.62e-2	0.86	4.97e-2	0.66	5.10e-2	0.66	5.20e-2	0.63
	40	*	*	4.17e-2	0.15	4.00e-2	0.31	4.20e-2	0.28	4.21e-2	0.30
	80	*	*	2.73e-2	0.61	2.10e-2	0.93	2.14e-2	0.98	2.18e-2	0.95
	160	*	*	*	*	2.05e-2	0.04	2.09e-2	0.03	2.11e-2	0.04
	320	*	*	*	*	1.27e-2	0.69	1.41e-2	0.57	1.45e-2	0.54
3	10	*		*		*		*		6.02e-2	
	20	*	*	*	*	*	*	*	*	*	*
	40	*	*	*	*	*	*	*	*	*	*
	80	*	*	*	*	*	*	*	*	*	*
	160	*	*	*	*	*	*	*	*	*	*
	320	*	*	*	*	*	*	*	*	*	*
4	10	*		*		*		*		*	
	20	*	*	*	*	*	*	*	*	*	*
	40	*	*	*	*	*	*	*	*	*	*
	80	*	*	*	*	*	*	*	*	*	*
	160	*	*	*	*	*	*	*	*	*	*
	320	*	*	*	*	*	*	*	*	*	*
5	10	*		*		*		*		*	
	20	*	*	*	*	*	*	*	*	*	*
	40	*	*	*	*	*	*	*	*	*	*
	80	*	*	*	*	*	*	*	*	*	*
	160	*	*	*	*	*	*	*	*	*	*
	320	*	*	*	*	*	*	*	*	*	*

Table 9: Errors and experimental order of convergence (EOC) for varying polynomial degrees p and number of elements N for the modified Sod shock tube problem (137) using the local Lax-Friedrichs numerical flux and "simple" volume fluxes.

p	N	Central		Morinishi		Ducros		KG		Pirozzoli	
		$\ \text{err}_\varrho\ _M$	EOC	$\ \text{err}_\varrho\ _M$	EOC	$\ \text{err}_\varrho\ _M$	EOC	$\ \text{err}_\varrho\ _M$	EOC	$\ \text{err}_\varrho\ _M$	EOC
1	10	1.44e-1		1.45e-1		1.35e-1		1.34e-1		1.34e-1	
	20	7.30e-2	0.98	8.23e-2	0.81	6.95e-2	0.96	7.18e-2	0.90	7.23e-2	0.89
	40	6.68e-2	0.13	9.44e-2	-0.20	5.91e-2	0.23	6.30e-2	0.19	6.44e-2	0.17
	80	6.08e-2	0.13	*	*	4.62e-2	0.36	4.94e-2	0.35	5.04e-2	0.35
	160	5.16e-2	0.24	*	*	3.22e-2	0.52	3.48e-2	0.50	3.58e-2	0.49
	320	4.72e-2	0.13	*	*	2.25e-2	0.52	2.46e-2	0.50	2.53e-2	0.50
2	10	8.42e-2		8.46e-2		8.62e-2		8.67e-2		8.67e-2	
	20	5.08e-2	0.73	5.23e-2	0.69	5.36e-2	0.68	5.43e-2	0.68	5.50e-2	0.66
	40	3.78e-2	0.42	4.92e-2	0.09	3.99e-2	0.43	4.20e-2	0.37	4.22e-2	0.38
	80	2.30e-2	0.72	*	*	2.25e-2	0.82	2.21e-2	0.93	2.25e-2	0.90
	160	2.14e-2	0.10	*	*	2.11e-2	0.10	2.08e-2	0.09	2.10e-2	0.10
	320	1.43e-2	0.59	*	*	1.32e-2	0.67	1.40e-2	0.56	1.44e-2	0.54
3	10	*		*		*		6.11e-2		6.22e-2	
	20	*	*	*	*	*	*	4.53e-2	0.43	4.58e-2	0.44
	40	*	*	*	*	*	*	2.48e-2	0.87	2.51e-2	0.87
	80	*	*	*	*	*	*	2.28e-2	0.12	2.29e-2	0.13
	160	*	*	*	*	*	*	1.52e-2	0.58	1.55e-2	0.57
	320	*	*	*	*	*	*	1.16e-2	0.39	1.17e-2	0.40
4	10	*		*		*		*		*	
	20	*	*	*	*	*	*	*	*	*	*
	40	*	*	*	*	*	*	*	*	*	*
	80	*	*	*	*	*	*	*	*	*	*
	160	*	*	*	*	*	*	*	*	*	*
	320	*	*	*	*	*	*	*	*	*	*
5	10	*		*		*		*		*	
	20	*	*	*	*	*	*	*	*	*	*
	40	*	*	*	*	*	*	*	*	*	*
	80	*	*	*	*	*	*	*	*	*	*
	160	*	*	*	*	*	*	*	*	*	*
	320	*	*	*	*	*	*	*	*	*	*

7.4 Sod shock tube: Finite volume setting

Here, the classical shock tube of Sod (1978) with initial condition (136) of section 7.2 will be used again, but in the context of first order finite volume methods.

The entropy conservative flux (61) of Chandrashekar (2013) has been used with the scalar dissipation (SD) of Derigs, Winters, Gassner, and Walch (2017), the matrix (MD) and hybrid (HD) dissipation of Winters, Derigs, Gassner, and Walch (2016) and the local Lax-Friedrichs (LLF) dissipation operator. The last one has also been used for the other entropy conservative fluxes. Additionally, the classical LLF flux and Suliciu relaxation solver of Bouchut (2004) are tested.

The results are shown in Table 10. Here, the matrix dissipation (MD) and the Suliciu solver perform equally good and yield less error than the other fluxes. Additionally, there is nearly no variance across the solvers using the LLF or scalar dissipation operator.

Table 10: Errors and experimental order of convergence (EOC) for varying number of elements N for the Sod shock tube problem (136) using several numerical fluxes.

N	Ch + SD DWGW		Ch + MD DWGW		Ch + HD DWGW		Ch + LLF	
	$\ \text{err}_\varrho\ _M$	EOC	$\ \text{err}_\varrho\ _M$	EOC	$\ \text{err}_\varrho\ _M$	EOC	$\ \text{err}_\varrho\ _M$	EOC
100	4.62e-2		3.97e-2		4.22e-2		4.62e-2	
200	3.75e-2	0.30	3.04e-2	0.38	3.23e-2	0.38	3.75e-2	0.30
400	2.80e-2	0.42	2.19e-2	0.47	2.31e-2	0.49	2.80e-2	0.42
800	2.08e-2	0.43	1.62e-2	0.43	1.69e-2	0.45	2.08e-2	0.43
1600	1.56e-2	0.42	1.23e-2	0.40	1.26e-2	0.42	1.56e-2	0.42
3200	1.18e-2	0.40	9.33e-3	0.40	9.49e-3	0.41	1.18e-2	0.40
6400	9.24e-3	0.35	7.35e-3	0.34	7.42e-3	0.36	9.24e-3	0.35
12800	7.22e-3	0.36	5.60e-3	0.39	5.64e-3	0.40	7.22e-3	0.36

N	ϱ, v, β (2) + LLF		$\varrho, v, \frac{1}{p}$ + LLF		ϱ, v, p + LLF		ϱ, v, T (1) + LLF	
	$\ \text{err}_\varrho\ _M$	EOC	$\ \text{err}_\varrho\ _M$	EOC	$\ \text{err}_\varrho\ _M$	EOC	$\ \text{err}_\varrho\ _M$	EOC
100	4.62e-2		4.61e-2		4.61e-2		4.62e-2	
200	3.75e-2	0.30	3.74e-2	0.30	3.74e-2	0.30	3.75e-2	0.30
400	2.80e-2	0.42	2.80e-2	0.42	2.80e-2	0.42	2.80e-2	0.42
800	2.08e-2	0.43	2.08e-2	0.43	2.08e-2	0.43	2.08e-2	0.43
1600	1.56e-2	0.42	1.56e-2	0.42	1.56e-2	0.42	1.56e-2	0.42
3200	1.18e-2	0.40	1.18e-2	0.40	1.18e-2	0.40	1.18e-2	0.40
6400	9.24e-3	0.35	9.24e-3	0.35	9.24e-3	0.35	9.24e-3	0.35
12800	7.22e-3	0.36	7.22e-3	0.36	7.22e-3	0.36	7.22e-3	0.36

N	ϱ, v, T (2) + LLF		ϱ, V, T (rev) + LLF		LLF		Suliciu	
	$\ \text{err}_\varrho\ _M$	EOC	$\ \text{err}_\varrho\ _M$	EOC	$\ \text{err}_\varrho\ _M$	EOC	$\ \text{err}_\varrho\ _M$	EOC
100	4.62e-2		4.63e-2		4.58e-2		3.95e-2	
200	3.75e-2	0.30	3.76e-2	0.30	3.72e-2	0.30	3.03e-2	0.38
400	2.80e-2	0.42	2.80e-2	0.42	2.79e-2	0.42	2.19e-2	0.47
800	2.08e-2	0.43	2.08e-2	0.43	2.07e-2	0.43	1.63e-2	0.43
1600	1.56e-2	0.42	1.56e-2	0.42	1.56e-2	0.41	1.23e-2	0.40
3200	1.18e-2	0.40	1.18e-2	0.40	1.18e-2	0.40	9.36e-3	0.39
6400	9.24e-3	0.35	9.24e-3	0.35	9.25e-3	0.35	7.36e-3	0.35
12800	7.22e-3	0.36	7.22e-3	0.36	7.23e-3	0.36	5.63e-3	0.39

7.5 Modified version of Sod's shock tube: Finite volume setting

Similar to the previous section, the modified Sod shock tube problem of section 7.3 is used to test the finite volume fluxes. The results are shown in Table 11. Again, the matrix dissipation and the Suliciu solver perform equally good and are superior to the other fluxes. As in section 7.4, there is nearly no variance across the methods with matrix / LLF dissipation.

Table 11: Errors and experimental order of convergence (EOC) for varying number of elements N for the modified Sod shock tube problem (137) using several numerical fluxes.

N	Ch + SD DWGW		Ch + MD DWGW		Ch + HD DWGW		Ch + LLF	
	$\ \text{err}_\varrho\ _M$	EOC	$\ \text{err}_\varrho\ _M$	EOC	$\ \text{err}_\varrho\ _M$	EOC	$\ \text{err}_\varrho\ _M$	EOC
100	5.55e-2		4.03e-2		4.59e-2		5.55e-2	
200	4.67e-2	0.25	3.31e-2	0.28	3.61e-2	0.35	4.67e-2	0.25
400	3.70e-2	0.34	2.65e-2	0.32	2.80e-2	0.37	3.70e-2	0.34
800	2.90e-2	0.35	2.14e-2	0.31	2.21e-2	0.34	2.90e-2	0.35
1600	2.23e-2	0.38	1.68e-2	0.35	1.72e-2	0.37	2.23e-2	0.38
3200	1.76e-2	0.34	1.37e-2	0.29	1.39e-2	0.31	1.76e-2	0.34
6400	1.39e-2	0.34	1.10e-2	0.32	1.11e-2	0.32	1.39e-2	0.34
12800	1.10e-2	0.34	8.51e-3	0.37	8.57e-3	0.37	1.10e-2	0.34

N	ϱ, v, β (2) + LLF		$\varrho, v, \frac{1}{p}$ + LLF		ϱ, v, p + LLF		ϱ, v, T (1) + LLF	
	$\ \text{err}_\varrho\ _M$	EOC	$\ \text{err}_\varrho\ _M$	EOC	$\ \text{err}_\varrho\ _M$	EOC	$\ \text{err}_\varrho\ _M$	EOC
100	5.55e-2		5.53e-2		5.53e-2		5.55e-2	
200	4.67e-2	0.25	4.67e-2	0.25	4.67e-2	0.25	4.67e-2	0.25
400	3.70e-2	0.34	3.70e-2	0.33	3.70e-2	0.33	3.70e-2	0.34
800	2.90e-2	0.35	2.90e-2	0.35	2.90e-2	0.35	2.90e-2	0.35
1600	2.23e-2	0.38	2.23e-2	0.38	2.23e-2	0.38	2.23e-2	0.38
3200	1.76e-2	0.34	1.76e-2	0.34	1.76e-2	0.34	1.76e-2	0.34
6400	1.39e-2	0.34	1.39e-2	0.34	1.39e-2	0.34	1.39e-2	0.34
12800	1.10e-2	0.34	1.10e-2	0.34	1.10e-2	0.34	1.10e-2	0.34

N	ϱ, v, T (2) + LLF		ϱ, V, T (rev) + LLF		LLF		Suliciu	
	$\ \text{err}_\varrho\ _M$	EOC	$\ \text{err}_\varrho\ _M$	EOC	$\ \text{err}_\varrho\ _M$	EOC	$\ \text{err}_\varrho\ _M$	EOC
100	5.55e-2		5.55e-2		5.58e-2		4.13e-2	
200	4.67e-2	0.25	4.67e-2	0.25	4.69e-2	0.25	3.34e-2	0.31
400	3.70e-2	0.34	3.70e-2	0.34	3.71e-2	0.34	2.66e-2	0.33
800	2.90e-2	0.35	2.90e-2	0.35	2.91e-2	0.35	2.15e-2	0.31
1600	2.23e-2	0.38	2.23e-2	0.38	2.24e-2	0.38	1.69e-2	0.35
3200	1.76e-2	0.34	1.76e-2	0.34	1.76e-2	0.34	1.38e-2	0.29
6400	1.39e-2	0.34	1.39e-2	0.34	1.40e-2	0.34	1.11e-2	0.32
12800	1.10e-2	0.34	1.10e-2	0.34	1.10e-2	0.34	8.61e-3	0.36

7.6 Near vacuum rarefaction

In this section, the rarefaction waves near vacuum as described by Toro (2009, Section 4.3.3, Test 2) will be used to test the methods. The initial condition is given in primitive variables by

$$\varrho_0(x) = 1, \quad v_0(x) = \begin{cases} -2, & x < \frac{1}{2}, \\ 2, & \text{else,} \end{cases}, \quad p_0(x) = 0.4, \quad (138)$$

and the conservative variables are again computed via $\varrho v_0 = \varrho_0 v_0$ and $\varrho e_0 = \frac{1}{2} \varrho_0 v_0^2 + \frac{p_0}{\gamma-1}$. The solution is computed on the domain $[0, 1]$ from $t = 0$ until $t = 0.15$.

Using the same finite volume methods as in section 7.4, the results are shown in Table 12. Across the varying number of elements N , no flux is clearly superior.

Table 12: Errors and experimental order of convergence (EOC) for varying number of elements N for the near vacuum rarefaction problem (138) using several numerical fluxes.

N	Ch + SD DWGW $\ \text{err}_\varrho\ _M$	EOC	Ch + MD DWGW $\ \text{err}_\varrho\ _M$	EOC	Ch + HD DWGW $\ \text{err}_\varrho\ _M$	EOC	Ch + LLF $\ \text{err}_\varrho\ _M$	EOC
100	8.83e-2		7.94e-2		7.98e-2		8.84e-2	
200	5.66e-2	0.64	5.67e-2	0.49	5.62e-2	0.51	5.66e-2	0.64
400	4.01e-2	0.50	4.18e-2	0.44	4.14e-2	0.44	4.01e-2	0.50
800	2.91e-2	0.46	2.99e-2	0.48	2.98e-2	0.47	2.91e-2	0.46
1600	2.02e-2	0.52	2.05e-2	0.54	2.05e-2	0.54	2.03e-2	0.52
3200	1.32e-2	0.61	1.33e-2	0.62	1.33e-2	0.62	1.33e-2	0.61
6400	8.04e-3	0.72	8.08e-3	0.72	8.06e-3	0.72	8.04e-3	0.72
12800	4.25e-3	0.92	4.22e-3	0.94	4.20e-3	0.94	4.26e-3	0.92

N	ϱ, v, β (2) + LLF $\ \text{err}_\varrho\ _M$	EOC	$\varrho, v, \frac{1}{p}$ + LLF $\ \text{err}_\varrho\ _M$	EOC	ϱ, v, p + LLF $\ \text{err}_\varrho\ _M$	EOC	ϱ, v, T (1) + LLF $\ \text{err}_\varrho\ _M$	EOC
100	8.80e-2		8.87e-2		8.87e-2		8.84e-2	
200	5.65e-2	0.64	5.68e-2	0.64	5.68e-2	0.64	5.66e-2	0.64
400	4.01e-2	0.49	4.04e-2	0.49	4.04e-2	0.49	4.01e-2	0.50
800	2.91e-2	0.46	2.93e-2	0.46	2.93e-2	0.46	2.91e-2	0.46
1600	2.03e-2	0.52	2.03e-2	0.53	2.03e-2	0.53	2.03e-2	0.52
3200	1.32e-2	0.61	1.33e-2	0.61	1.33e-2	0.61	1.33e-2	0.61
6400	8.04e-3	0.72	8.07e-3	0.72	8.07e-3	0.72	8.04e-3	0.72
12800	4.25e-3	0.92	4.29e-3	0.91	4.29e-3	0.91	4.26e-3	0.92

N	ϱ, v, T (2) + LLF $\ \text{err}_\varrho\ _M$	EOC	ϱ, V, T (rev) + LLF $\ \text{err}_\varrho\ _M$	EOC	LLF $\ \text{err}_\varrho\ _M$	EOC	Suliciu $\ \text{err}_\varrho\ _M$	EOC
100	8.80e-2		8.84e-2		8.07e-2		7.72e-2	
200	5.63e-2	0.64	5.67e-2	0.64	5.52e-2	0.55	5.55e-2	0.47
400	3.99e-2	0.50	4.02e-2	0.50	4.00e-2	0.46	4.10e-2	0.44
800	2.90e-2	0.46	2.92e-2	0.46	2.89e-2	0.47	2.95e-2	0.48
1600	2.02e-2	0.52	2.03e-2	0.52	2.01e-2	0.53	2.02e-2	0.54
3200	1.32e-2	0.61	1.33e-2	0.61	1.31e-2	0.61	1.32e-2	0.62
6400	8.02e-3	0.72	8.05e-3	0.72	7.92e-3	0.73	7.98e-3	0.72
12800	4.23e-3	0.92	4.26e-3	0.92	4.05e-3	0.97	4.12e-3	0.95

7.7 Left half of the blast wave problem of Woodward and Colella

In this section, the left half of the blast wave problem of Woodward and Colella (1984, Section IV.a) as described by Toro (2009, Section 4.3.3, Test 3) is considered. In primitive variables, it is given by

$$\varrho_0(x) = 1, \quad v_0(x) = 0, \quad p_0(x) = \begin{cases} 1000, & x < \frac{1}{2}, \\ 0.01, & \text{else,} \end{cases} \quad (139)$$

and the conservative variables are again computed via $\varrho v_0 = \varrho_0 v_0$ and $\varrho e_0 = \frac{1}{2} \varrho_0 v_0^2 + \frac{p_0}{\gamma-1}$. The solution is computed on the domain $[0, 1]$ from $t = 0$ until $t = 0.012$ using the finite volume methods described in section 7.4.

The results are shown in table 13. The simulations using the fluxes with variables ϱ, v and p or $\frac{1}{p}$ crashed since they left the invariant region for the Euler equations. As described by Derigs, Winters, Gassner, and Walch (2017), the reason is the appearance of the pressure in the density flux as in the entropy conservative flux of Roe (2006).

The Suliciu solver and the matrix dissipation (MD) yielded similar errors until the last one crashed using 12800 elements. There is a bit more variance across the other fluxes than in the previous sections 7.4, 7.5 and 7.6. However, in the end, the Suliciu relaxation solver performs better than the others.

Table 13: Errors and experimental order of convergence (EOC) for varying number of elements N for the left half (139) of the blast wave problem of Woodward and Colella (1984) using several numerical fluxes.

N	Ch + SD DWGW		Ch + MD DWGW		Ch + HD DWGW		Ch + LLF	
	$\ \text{err}_\varrho\ _M$	EOC	$\ \text{err}_\varrho\ _M$	EOC	$\ \text{err}_\varrho\ _M$	EOC	$\ \text{err}_\varrho\ _M$	EOC
100	7.35e-1		7.09e-1		7.03e-1		7.35e-1	
200	6.60e-1	0.16	6.33e-1	0.16	6.24e-1	0.17	6.59e-1	0.16
400	5.32e-1	0.31	4.92e-1	0.36	4.89e-1	0.35	5.32e-1	0.31
800	4.33e-1	0.30	3.92e-1	0.33	3.91e-1	0.32	4.33e-1	0.30
1600	3.51e-1	0.30	3.12e-1	0.33	3.12e-1	0.33	3.51e-1	0.30
3200	2.91e-1	0.27	2.58e-1	0.27	2.57e-1	0.28	2.91e-1	0.27
6400	2.38e-1	0.29	2.06e-1	0.32	2.07e-1	0.31	2.38e-1	0.29
12800	1.92e-1	0.31	*		1.62e-1	0.36	1.92e-1	0.31

N	ϱ, v, β (2) + LLF		$\varrho, v, \frac{1}{p}$ + LLF		ϱ, v, p + LLF		ϱ, v, T (1) + LLF	
	$\ \text{err}_\varrho\ _M$	EOC	$\ \text{err}_\varrho\ _M$	EOC	$\ \text{err}_\varrho\ _M$	EOC	$\ \text{err}_\varrho\ _M$	EOC
100	7.34e-1		*		*		7.35e-1	
200	6.59e-1	0.16	*		*		6.59e-1	0.16
400	5.32e-1	0.31	*		*		5.32e-1	0.31
800	4.33e-1	0.30	*		*		4.33e-1	0.30
1600	3.51e-1	0.30	*		*		3.51e-1	0.30
3200	2.91e-1	0.27	*		*		2.91e-1	0.27
6400	2.38e-1	0.29	*		*		2.38e-1	0.29
12800	1.92e-1	0.31	*		*		1.92e-1	0.31

N	ϱ, v, T (2) + LLF		ϱ, V, T (rev) + LLF		LLF		Suliciu	
	$\ \text{err}_\varrho\ _M$	EOC	$\ \text{err}_\varrho\ _M$	EOC	$\ \text{err}_\varrho\ _M$	EOC	$\ \text{err}_\varrho\ _M$	EOC
100	7.34e-1		7.37e-1		7.42e-1		7.14e-1	
200	6.59e-1	0.16	6.60e-1	0.16	6.64e-1	0.16	6.34e-1	0.17
400	5.32e-1	0.31	5.33e-1	0.31	5.37e-1	0.31	4.95e-1	0.36
800	4.33e-1	0.30	4.33e-1	0.30	4.36e-1	0.30	3.95e-1	0.33
1600	3.51e-1	0.30	3.51e-1	0.30	3.53e-1	0.30	3.15e-1	0.33
3200	2.91e-1	0.27	2.91e-1	0.27	2.92e-1	0.27	2.59e-1	0.28
6400	2.38e-1	0.29	2.38e-1	0.29	2.39e-1	0.29	2.08e-1	0.31
12800	1.92e-1	0.31	1.92e-1	0.31	1.93e-1	0.31	1.64e-1	0.35

7.8 Slowly moving contact discontinuity

In this section, initial condition of the previous test case is used, but with a non-vanishing initial velocity, resulting in a slowly moving contact discontinuity as described by Toro (2009, Section

6.4, Test 5). The initial condition is given in primitive variables by

$$\varrho_0(x) = 1, \quad v_0(x) = -19.59745, \quad p_0(x) = \begin{cases} 1000, & x < \frac{4}{5}, \\ 0.01, & \text{else,} \end{cases} \quad (140)$$

and the conservative variables are again computed via $\varrho v_0 = \varrho_0 v_0$ and $\varrho e_0 = \frac{1}{2} \varrho_0 v_0^2 + \frac{p_0}{\gamma-1}$. The solution is computed on the domain $[0, 1]$ from $t = 0$ until $t = 0.012$ using the finite volume methods of section 7.4.

The results are shown in Table 14. As in the previous section 7.7, the fluxes using the pressure in the density flux are unstable. The scalar and LLF dissipation fluxes yield similar errors with some variances across the methods, but the Suliciu solver is superior. In most cases, it is also better than the scalar dissipation (SD).

Table 14: Errors and experimental order of convergence (EOC) for varying number of elements N for the slowly moving contact discontinuity (140) using several numerical fluxes.

N	Ch + SD DWGW $\ \text{err}_\varrho\ _M$	EOC	Ch + MD DWGW $\ \text{err}_\varrho\ _M$	EOC	Ch + HD DWGW $\ \text{err}_\varrho\ _M$	EOC	Ch + LLF $\ \text{err}_\varrho\ _M$	EOC
100	7.84e-1		4.82e-1		6.48e-1		7.85e-1	
200	6.64e-1	0.24	6.69e-1	-0.47	4.52e-1	0.52	6.65e-1	0.24
400	5.77e-1	0.20	2.38e-1	1.49	4.10e-1	0.14	5.77e-1	0.20
800	4.38e-1	0.40	3.41e-1	-0.52	2.47e-1	0.73	4.38e-1	0.40
1600	3.51e-1	0.32	2.32e-1	0.56	1.67e-1	0.57	3.51e-1	0.32
3200	2.97e-1	0.24	1.02e-1	1.18	1.40e-1	0.25	2.97e-1	0.24
6400	2.36e-1	0.33	1.14e-1	-0.16	8.15e-2	0.78	2.36e-1	0.33
12800	1.99e-1	0.25	8.59e-2	0.41	6.57e-2	0.31	1.99e-1	0.25

N	ϱ, v, β (2) + LLF $\ \text{err}_\varrho\ _M$	EOC	$\varrho, v, \frac{1}{p}$ + LLF $\ \text{err}_\varrho\ _M$	EOC	ϱ, v, p + LLF $\ \text{err}_\varrho\ _M$	EOC	ϱ, v, T (1) + LLF $\ \text{err}_\varrho\ _M$	EOC
100	7.86e-1		*		*		7.85e-1	
200	6.65e-1	0.24	*		*		6.65e-1	0.24
400	5.76e-1	0.21	*		*		5.77e-1	0.20
800	4.38e-1	0.40	*		*		4.38e-1	0.40
1600	3.51e-1	0.32	*		*		3.51e-1	0.32
3200	2.97e-1	0.24	*		*		2.97e-1	0.24
6400	2.36e-1	0.33	*		*		2.36e-1	0.33
12800	1.99e-1	0.25	*		*		1.99e-1	0.25

N	ϱ, v, T (2) + LLF $\ \text{err}_\varrho\ _M$	EOC	ϱ, V, T (rev) + LLF $\ \text{err}_\varrho\ _M$	EOC	LLF $\ \text{err}_\varrho\ _M$	EOC	Suliciu $\ \text{err}_\varrho\ _M$	EOC
100	7.86e-1		7.91e-1		7.96e-1		5.08e-1	
200	6.65e-1	0.24	6.66e-1	0.25	6.77e-1	0.23	2.80e-1	0.86
400	5.77e-1	0.21	5.77e-1	0.21	5.84e-1	0.21	2.85e-1	-0.03
800	4.38e-1	0.40	4.38e-1	0.40	4.45e-1	0.39	1.45e-1	0.97
1600	3.51e-1	0.32	3.51e-1	0.32	3.55e-1	0.33	9.77e-2	0.57
3200	2.97e-1	0.24	2.97e-1	0.24	2.99e-1	0.24	9.03e-2	0.11
6400	2.36e-1	0.33	2.36e-1	0.33	2.37e-1	0.33	4.81e-2	0.91
12800	1.99e-1	0.25	1.99e-1	0.25	1.99e-1	0.25	3.95e-2	0.29

7.9 Right half of the blast wave problem of Woodward and Colella

In this section, the right half of the blast wave problem of Woodward and Colella (1984, Section IV.a) as described by Toro (2009, Section 4.3.3, Test 4) is considered. In primitive variables, it is given by

$$\varrho_0(x) = 1, \quad v_0(x) = 0, \quad p_0(x) = \begin{cases} 0.01, & x < \frac{1}{2}, \\ 100, & \text{else,} \end{cases} \quad (141)$$

and the conservative variables are again computed via $\varrho v_0 = \varrho_0 v_0$ and $\varrho e_0 = \frac{1}{2} \varrho_0 v_0^2 + \frac{p_0}{\gamma-1}$. The solution is computed on the domain $[0, 1]$ from $t = 0$ until $t = 0.035$ using again the finite volume methods described in section 7.4.

The results are shown in Table 15. As before, the fluxes with variables ϱ, v and p or $\frac{1}{p}$ are unstable, and the other fluxes yield similar errors, while the matrix dissipation and Suliciu solver perform a bit better than the others.

Table 15: Errors and experimental order of convergence (EOC) for varying number of elements N for the right half (141) of the blast wave problem of Woodward and Colella (1984) using several numerical fluxes.

N	Ch + SD DWGW		Ch + MD DWGW		Ch + HD DWGW		Ch + LLF	
	$\ \text{err}_\varrho\ _M$	EOC	$\ \text{err}_\varrho\ _M$	EOC	$\ \text{err}_\varrho\ _M$	EOC	$\ \text{err}_\varrho\ _M$	EOC
100	7.25e-1		6.90e-1		6.89e-1		7.26e-1	
200	6.45e-1	0.17	6.11e-1	0.18	6.05e-1	0.19	6.45e-1	0.17
400	5.26e-1	0.29	4.91e-1	0.32	4.87e-1	0.31	5.26e-1	0.30
800	4.38e-1	0.26	4.02e-1	0.29	3.99e-1	0.29	4.38e-1	0.26
1600	3.58e-1	0.29	3.24e-1	0.31	3.22e-1	0.31	3.57e-1	0.29
3200	2.86e-1	0.32	2.53e-1	0.36	2.53e-1	0.35	2.86e-1	0.32
6400	2.33e-1	0.29	2.02e-1	0.33	2.03e-1	0.32	2.33e-1	0.29
12800	1.88e-1	0.31	1.64e-1	0.30	1.59e-1	0.35	1.88e-1	0.31

N	ϱ, v, β (2) + LLF		$\varrho, v, \frac{1}{p}$ + LLF		ϱ, v, p + LLF		ϱ, v, T (1) + LLF	
	$\ \text{err}_\varrho\ _M$	EOC	$\ \text{err}_\varrho\ _M$	EOC	$\ \text{err}_\varrho\ _M$	EOC	$\ \text{err}_\varrho\ _M$	EOC
100	7.24e-1		*		*		7.26e-1	
200	6.44e-1	0.17	*		*		6.45e-1	0.17
400	5.25e-1	0.29	*		*		5.26e-1	0.30
800	4.38e-1	0.26	*		*		4.38e-1	0.26
1600	3.57e-1	0.29	*		*		3.57e-1	0.29
3200	2.86e-1	0.32	*		*		2.86e-1	0.32
6400	2.33e-1	0.29	*		*		2.33e-1	0.29
12800	1.88e-1	0.31	*		*		1.88e-1	0.31

N	ϱ, v, T (2) + LLF		ϱ, V, T (rev) + LLF		LLF		Suliciu	
	$\ \text{err}_\varrho\ _M$	EOC	$\ \text{err}_\varrho\ _M$	EOC	$\ \text{err}_\varrho\ _M$	EOC	$\ \text{err}_\varrho\ _M$	EOC
100	7.25e-1		7.28e-1		7.35e-1		7.00e-1	
200	6.44e-1	0.17	6.46e-1	0.17	6.52e-1	0.17	6.16e-1	0.19
400	5.25e-1	0.29	5.26e-1	0.30	5.30e-1	0.30	4.92e-1	0.32
800	4.38e-1	0.26	4.38e-1	0.26	4.41e-1	0.27	4.03e-1	0.29
1600	3.57e-1	0.29	3.58e-1	0.29	3.59e-1	0.30	3.24e-1	0.31
3200	2.86e-1	0.32	2.86e-1	0.32	2.87e-1	0.32	2.54e-1	0.35
6400	2.33e-1	0.29	2.33e-1	0.29	2.34e-1	0.30	2.04e-1	0.32
12800	1.88e-1	0.31	1.88e-1	0.31	1.89e-1	0.31	1.60e-1	0.35

7.10 Left half of the blast wave problem of Derigs, Winters, Gassner and Walch

In this section, the left half of the blast wave problem of Derigs, Winters, Gassner, and Walch (2017, Section 6) is considered. In primitive variables, it is given by

$$\varrho_0(x) = 1, \quad v_0(x) = 10, \quad p_0(x) = \begin{cases} 1, & x < -\frac{1}{10}, \\ 10^{-6}, & \text{else.} \end{cases} \quad (142)$$

Here, $\gamma = \frac{5}{3}$ is used. The solution is computed on the domain $[-1, 1]$ from $t = 0$ until $t = 5.0 \times 10^{-2}$ using the finite volume methods of section 7.4.

The results are shown in Table 16. Designed as a test case to crash the flux of Roe (2006), the fluxes containing pressure influence in the density flux are unstable. However, there is nearly

no variance across the other fluxes that remain stable, since the problem needs a very high resolution to capture the solution.

Contrary to the results of Derigs, Winters, Gassner, and Walch (2017) for the MHD equations, the simple LLF dissipation is enough to stabilise the solution for the Euler equations in this case and their specially designed dissipation operator does not show any improvement over the LLF dissipation.

Table 16: Errors and experimental order of convergence (EOC) for varying number of elements N for the left half (142) of the blast wave problem of Derigs, Winters, Gassner, and Walch (2017) using several numerical fluxes.

N	Ch + SD DWGW		Ch + MD DWGW		Ch + HD DWGW		Ch + LLF	
	$\ \text{err}_\varrho\ _M$	EOC	$\ \text{err}_\varrho\ _M$	EOC	$\ \text{err}_\varrho\ _M$	EOC	$\ \text{err}_\varrho\ _M$	EOC
100	4.32e-1		4.33e-1		4.33e-1		4.33e-1	
200	3.13e-1	0.47	3.13e-1	0.47	3.13e-1	0.47	3.13e-1	0.47
400	3.08e-1	0.02	3.07e-1	0.02	3.08e-1	0.02	3.08e-1	0.02
800	2.64e-1	0.22	2.63e-1	0.23	2.63e-1	0.23	2.64e-1	0.22
1600	2.83e-1	-0.10	2.82e-1	-0.10	2.82e-1	-0.10	2.84e-1	-0.10
3200	2.60e-1	0.13	2.58e-1	0.13	2.58e-1	0.13	2.60e-1	0.13
6400	2.24e-1	0.21	2.23e-1	0.21	2.23e-1	0.21	2.24e-1	0.21
12800	1.78e-1	0.33	1.77e-1	0.33	1.77e-1	0.33	1.78e-1	0.33

N	ϱ, v, β (2) + LLF		$\varrho, v, \frac{1}{p}$ + LLF		ϱ, v, p + LLF		ϱ, v, T (1) + LLF	
	$\ \text{err}_\varrho\ _M$	EOC	$\ \text{err}_\varrho\ _M$	EOC	$\ \text{err}_\varrho\ _M$	EOC	$\ \text{err}_\varrho\ _M$	EOC
100	4.33e-1		*		*		4.33e-1	
200	3.13e-1	0.47	*		*		3.13e-1	0.47
400	3.08e-1	0.02	*		*		3.08e-1	0.02
800	2.64e-1	0.22	*		*		2.64e-1	0.22
1600	2.83e-1	-0.10	*		*		2.84e-1	-0.10
3200	2.60e-1	0.13	*		*		2.60e-1	0.13
6400	2.24e-1	0.21	*		*		2.24e-1	0.21
12800	1.78e-1	0.33	*		*		1.78e-1	0.33

N	ϱ, v, T (2) + LLF		ϱ, V, T (rev) + LLF		LLF		Suliciu	
	$\ \text{err}_\varrho\ _M$	EOC	$\ \text{err}_\varrho\ _M$	EOC	$\ \text{err}_\varrho\ _M$	EOC	$\ \text{err}_\varrho\ _M$	EOC
100	4.33e-1		4.33e-1		4.33e-1		4.33e-1	
200	3.13e-1	0.47	3.13e-1	0.47	3.13e-1	0.47	3.13e-1	0.47
400	3.08e-1	0.02	3.08e-1	0.02	3.09e-1	0.02	3.08e-1	0.02
800	2.64e-1	0.22	2.64e-1	0.22	2.64e-1	0.22	2.63e-1	0.23
1600	2.83e-1	-0.10	2.84e-1	-0.10	2.84e-1	-0.10	2.83e-1	-0.10
3200	2.60e-1	0.13	2.60e-1	0.13	2.60e-1	0.13	2.59e-1	0.13
6400	2.24e-1	0.21	2.24e-1	0.21	2.24e-1	0.21	2.23e-1	0.22
12800	1.78e-1	0.33	1.78e-1	0.33	1.78e-1	0.33	1.77e-1	0.33

7.11 Right half of the blast wave problem of Derigs, Winters, Gassner and Walch

In this section, the right half of the blast wave problem of Derigs, Winters, Gassner, and Walch (2017, Section 6) is considered. In primitive variables, it is given by

$$\varrho_0(x) = 1, \quad v_0(x) = 10, \quad p_0(x) = \begin{cases} 10^{-6}, & x < \frac{1}{10}, \\ 1, & \text{else.} \end{cases} \quad (143)$$

Here, $\gamma = \frac{5}{3}$ is used. The solution is computed on the domain $[-1, 1]$ from $t = 0$ until $t = 5.0 \times 10^{-2}$ using again the same finite volume methods as before.

The results are shown in Table 17. The results are similar to the left half of this problem in section 7.10: The pressure influence in the density flux results in unstable schemes while all other methods yield similar errors and are stable.

Table 17: Errors and experimental order of convergence (EOC) for varying number of elements N for the right half (143) of the blast wave problem of Derigs, Winters, Gassner, and Walch (2017) using several numerical fluxes.

N	Ch + SD DWGW		Ch + MD DWGW		Ch + HD DWGW		Ch + LLF	
	$\ \text{err}_\varrho\ _M$	EOC	$\ \text{err}_\varrho\ _M$	EOC	$\ \text{err}_\varrho\ _M$	EOC	$\ \text{err}_\varrho\ _M$	EOC
100	4.33e-1		4.32e-1		4.33e-1		4.33e-1	
200	3.13e-1	0.47	3.13e-1	0.47	3.13e-1	0.47	3.13e-1	0.47
400	3.09e-1	0.02	3.07e-1	0.03	3.08e-1	0.02	3.09e-1	0.02
800	2.64e-1	0.22	2.63e-1	0.23	2.63e-1	0.23	2.64e-1	0.22
1600	2.83e-1	-0.10	2.80e-1	-0.09	2.80e-1	-0.09	2.83e-1	-0.10
3200	2.58e-1	0.13	2.54e-1	0.14	2.55e-1	0.14	2.58e-1	0.13
6400	2.23e-1	0.21	2.18e-1	0.22	2.18e-1	0.22	2.23e-1	0.21
12800	1.79e-1	0.32	1.73e-1	0.33	1.74e-1	0.33	1.79e-1	0.32

N	ϱ, v, β (2) + LLF		$\varrho, v, \frac{1}{p}$ + LLF		ϱ, v, p + LLF		ϱ, v, T (1) + LLF	
	$\ \text{err}_\varrho\ _M$	EOC	$\ \text{err}_\varrho\ _M$	EOC	$\ \text{err}_\varrho\ _M$	EOC	$\ \text{err}_\varrho\ _M$	EOC
100	4.33e-1		*		*		4.33e-1	
200	3.14e-1	0.47	*		*		3.13e-1	0.47
400	3.09e-1	0.02	*		*		3.09e-1	0.02
800	2.64e-1	0.22	*		*		2.64e-1	0.22
1600	2.83e-1	-0.10	*		*		2.83e-1	-0.10
3200	2.59e-1	0.13	*		*		2.58e-1	0.13
6400	2.23e-1	0.21	*		*		2.23e-1	0.21
12800	1.79e-1	0.32	*		*		1.79e-1	0.32

N	ϱ, v, T (2) + LLF		ϱ, V, T (rev) + LLF		LLF		Suliciu	
	$\ \text{err}_\varrho\ _M$	EOC	$\ \text{err}_\varrho\ _M$	EOC	$\ \text{err}_\varrho\ _M$	EOC	$\ \text{err}_\varrho\ _M$	EOC
100	4.33e-1		4.33e-1		4.33e-1		4.32e-1	
200	3.14e-1	0.47	3.14e-1	0.47	3.13e-1	0.47	3.13e-1	0.47
400	3.09e-1	0.02	3.09e-1	0.02	3.08e-1	0.02	3.07e-1	0.03
800	2.64e-1	0.22	2.64e-1	0.22	2.64e-1	0.23	2.62e-1	0.23
1600	2.83e-1	-0.10	2.83e-1	-0.10	2.83e-1	-0.10	2.80e-1	-0.09
3200	2.59e-1	0.13	2.58e-1	0.13	2.58e-1	0.13	2.54e-1	0.14
6400	2.23e-1	0.21	2.23e-1	0.21	2.23e-1	0.21	2.18e-1	0.22
12800	1.79e-1	0.32	1.79e-1	0.32	1.79e-1	0.32	1.73e-1	0.33

7.12 Another blast wave problem

In this section, another blast wave problem is considered. In primitive variables, it is given by

$$\varrho_0(x) = \frac{1}{10}, \quad v_0(x) = 10, \quad p_0(x) = \begin{cases} 10^{-12}, & x < -\frac{1}{2}, \\ 10^{-3}, & \text{else.} \end{cases} \quad (144)$$

Here, $\gamma = \frac{5}{3}$ is used. The solution is computed on the domain $[-1, 1]$ from $t = 0$ until $t = 0.1$ using the same set of FV methods as in the previous test cases.

To the author's knowledge, this test problem has not been used before, and is designed to show the importance of positivity preserving for the pressure. As can be seen in the results shown in Table 18, the new scalar and matrix dissipation operators of Derigs, Winters, Gassner, and Walch (2017); Winters, Derigs, Gassner, and Walch (2016) are not stable for this problem. Indeed, they result in negative pressures. However, the simple LLF dissipation that has been reported to be less stable than these dissipation operators by Derigs, Winters, Gassner, and Walch (2017) for the MHD equations remains stable in this test case.

Of course, the fluxes containing an influence of the pressure in the density flux are unstable. The remaining fluxes (with LLF dissipation and Suliciu) are all stable and result in the same error (up to two digits of precision).

As another example demonstrating the positivity preserving issue for the pressure, explicit Euler FV steps (121) using the entropy conservative flux (61) of Chandrashekar (2013) with scalar and matrix dissipation operators by Derigs, Winters, Gassner, and Walch (2017); Winters, Derigs, Gassner, and Walch (2016) as well as LLF dissipation, respectively, have been performed with the states

$$\begin{pmatrix} \varrho \\ v \\ p \end{pmatrix}_{i-1} = \begin{pmatrix} \varrho \\ v \\ p \end{pmatrix}_i = \begin{pmatrix} 0.1 \\ 10 \\ 1.0 \times 10^{-12} \end{pmatrix}, \quad \begin{pmatrix} \varrho \\ v \\ p \end{pmatrix}_{i+1} = \begin{pmatrix} 10 \\ 10 \\ 1.0 \times 10^{-6} \end{pmatrix}. \quad (145)$$

As can be seen in Figure 2, the pressure becomes negative for both the scalar $[\frac{\Delta t}{\Delta x} \lesssim 0.3 \times 10^{-12}]$ and the matrix dissipation $[\frac{\Delta t}{\Delta x} \lesssim 0.1 \times 10^{-12}]$ operator, while the characteristic speeds on the left $(i-1, i)$ and right $(i+1)$ hand side are $v = 10$, $c_i = \sqrt{\gamma \frac{p_i}{\varrho_i}} = \sqrt{10^{-11} \gamma}$, and $c_{i+1} = \sqrt{10^{-13} \gamma}$. Thus, there does not seem to be a reasonable CFL condition for these two fluxes and for this initial condition. Contrary, the LLF dissipation operator results in a positive pressure.

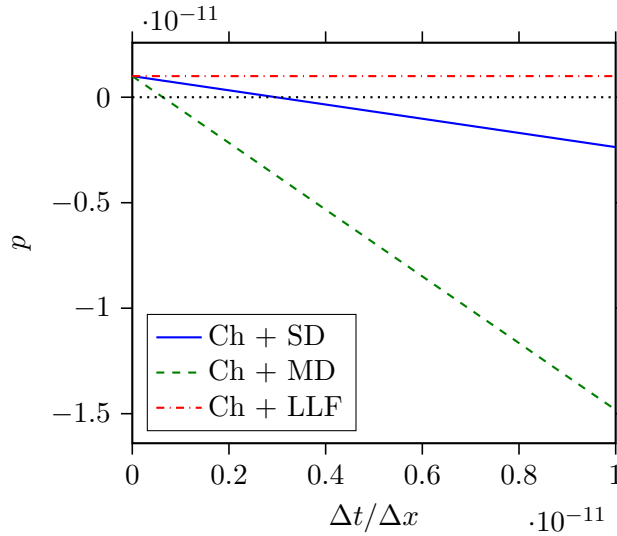


Figure 2: Pressure depending on the step size ratio $\frac{\Delta t}{\Delta x}$ for one FV step (121) using a scalar (solid), matrix (dashed), and LLF (dash-dotted) dissipation operator for the initial condition (145).

Table 18: Errors and experimental order of convergence (EOC) for varying number of elements N for the blast wave (144) using several numerical fluxes.

N	Ch + SD DWGW		Ch + MD DWGW		Ch + HD DWGW		Ch + LLF	
	$\ \text{err}_\varrho\ _M$	EOC	$\ \text{err}_\varrho\ _M$	EOC	$\ \text{err}_\varrho\ _M$	EOC	$\ \text{err}_\varrho\ _M$	EOC
100	*		*		*		1.73e-3	
200	*		*		*		5.82e-3	-1.75
400	*		*		*		4.66e-3	0.32
800	*		*		*		2.54e-2	-2.45
1600	*		*		*		1.83e-2	0.47
3200	*		*		*		1.83e-2	0.00
6400	*		*		*		1.82e-2	0.01
12800	*		*		*		1.78e-2	0.04

N	ϱ, v, β (2) + LLF		$\varrho, v, \frac{1}{p}$ + LLF		ϱ, v, p + LLF		ϱ, v, T (1) + LLF	
	$\ \text{err}_\varrho\ _M$	EOC	$\ \text{err}_\varrho\ _M$	EOC	$\ \text{err}_\varrho\ _M$	EOC	$\ \text{err}_\varrho\ _M$	EOC
100	1.73e-3		*		*		1.73e-3	
200	5.82e-3	-1.75	*		*		5.82e-3	-1.75
400	4.66e-3	0.32	*		*		4.66e-3	0.32
800	2.54e-2	-2.45	*		*		2.54e-2	-2.45
1600	1.83e-2	0.47	*		*		1.83e-2	0.47
3200	1.83e-2	0.00	*		*		1.83e-2	0.00
6400	1.82e-2	0.01	*		*		1.82e-2	0.01
12800	1.78e-2	0.04	*		*		1.78e-2	0.04

N	ϱ, v, T (2) + LLF		ϱ, V, T (rev) + LLF		LLF		Suliciu	
	$\ \text{err}_\varrho\ _M$	EOC	$\ \text{err}_\varrho\ _M$	EOC	$\ \text{err}_\varrho\ _M$	EOC	$\ \text{err}_\varrho\ _M$	EOC
100	1.73e-3		1.73e-3		1.73e-3		1.73e-3	
200	5.82e-3	-1.75	5.82e-3	-1.75	5.82e-3	-1.75	5.82e-3	-1.75
400	4.66e-3	0.32	4.66e-3	0.32	4.66e-3	0.32	4.66e-3	0.32
800	2.54e-2	-2.45	2.54e-2	-2.45	2.54e-2	-2.45	2.54e-2	-2.45
1600	1.83e-2	0.47	1.83e-2	0.47	1.83e-2	0.47	1.83e-2	0.47
3200	1.83e-2	0.00	1.83e-2	0.00	1.83e-2	0.00	1.83e-2	0.00
6400	1.82e-2	0.01	1.82e-2	0.01	1.82e-2	0.01	1.82e-2	0.01
12800	1.78e-2	0.04	1.78e-2	0.04	1.78e-2	0.04	1.78e-2	0.04

8 Summary and conclusions

Several new entropy conservative numerical fluxes for the Euler equations have been developed and compared with existing ones in two kinds of application.

Firstly, the entropy conservative fluxes can be used as building blocks of entropy stable high-order schemes using the flux differencing form of Fisher and Carpenter (2013a). Therefore, their theory has been extended in section 3 regarding the order of the resulting scheme and possible extension to SBP operators on simplices. This last extension may be possible, but to the author’s knowledge, there are no SBP operators on simplices in general fulfilling the conditions used there.

Moreover, numerical tests have been performed for one- and two-dimensional test problems using the flux differencing form and varying volume fluxes. There does not seem to be any clearly superior candidate outperforming the other ones in all cases. However, for smooth problems, the term consistent with zero in the flux $\varrho, v, T(\text{rev})$ (117) seems to introduce additional error, similar to the results for the shallow water equations (Ranocha 2016b). Whereas for smooth solutions some not entropy conservative volume fluxes performed better than their entropy conservative counterparts, this is different for discontinuous solutions. Here, the entropy conservative volume fluxes are more stable.

On the other hand, the entropy conservative fluxes can be enhanced by dissipation operators and be used in (first order) finite volume schemes. The dissipation operators of Derigs, Winters, Gassner, and Walch (2017); Winters, Derigs, Gassner, and Walch (2016) have been tested and compared with a simple local Lax-Friedrichs dissipation for the entropy conservative fluxes as well as with the LLF flux and the Suliciu relaxation solver of Bouchut (2004). In some problems, the hybrid and matrix dissipation operators yield similar results regarding stability and accuracy as the Suliciu solver, but they are less stable in general, as has been demonstrated in section 7.12. Therefore, the LLF dissipation seems to be advantageous regarding stability, contrary to the results of Derigs, Winters, Gassner, and Walch (2017) for the MHD equations.

However, the performance of the numerical fluxes has to consider also the costs. Here, the implementation has not been optimised for every flux in detail, but the Suliciu relaxation solver is the second cheapest one after the LLF flux. The fluxes relying on an entropy conservative baseline flux are significantly more expensive. Thus, the Suliciu relaxation solver of Bouchut (2004) seems to be the best one in this comparison.

There are still some open problems regarding the stability of the numerical fluxes based on entropy conservative ones. The positivity of the pressure using the LLF dissipation has been observed in all test cases but no analytical proof has been conducted yet. Another possibility is the addition of dissipation for the variables $\varrho, \varrho v, \varrho s$ followed by a conversion to the usual conserved variables as described by Bouchut (2004, Section 2.4.6).

Moreover, it has still to be investigated thoroughly in what regard the entropy conservative fluxes as ingredients in the flux differencing framework have advantages compared to the split forms tested by Gassner, Winters, and Kopriva (2016). Additionally, it is still unclear, whether there are some superior entropy conservative fluxes or cheaper ones.

References

- Barth, T. J. (1999). “Numerical methods for gasdynamic systems on unstructured meshes”. In: *An introduction to recent developments in theory and numerics for conservation laws*. Springer, pp. 195–285.
- Bouchut, F. (2004). *Nonlinear stability of finite volume methods for hyperbolic conservation laws and well-balanced schemes for sources*. Springer Science & Business Media.
- Chandrashekar, P. (2013). “Kinetic energy preserving and entropy stable finite volume schemes for compressible Euler and Navier-Stokes equations”. In: *Communications in Computational Physics* 14.5, pp. 1252–1286.
- Coquel, F., E. Godlewski, B. Perthame, A. In, and P. Rascle (2001). “Some new Godunov and relaxation methods for two-phase flow problems”. In: *Godunov methods*. Ed. by E. F. Toro. Springer, pp. 179–188.

- Derigs, D., A. R. Winters, G. J. Gassner, and S. Walch (2016). “A novel high-order, entropy stable, 3D AMR MHD solver with guaranteed positive pressure”. In: *Journal of Computational Physics* 317, pp. 223–256.
- Derigs, D., A. R. Winters, G. J. Gassner, and S. Walch (2017). “A novel averaging technique for discrete entropy-stable dissipation operators for ideal MHD”. In: *Journal of Computational Physics* 330, pp. 624–632.
- Ducros, F., F. Laporte, T. Souleres, V. Guinot, P. Moinat, and B. Caruelle (2000). “High-order fluxes for conservative skew-symmetric-like schemes in structured meshes: application to compressible flows”. In: *Journal of Computational Physics* 161.1, pp. 114–139.
- Fisher, T. C. and M. H. Carpenter (Feb. 2013a). *High-Order Entropy Stable Finite Difference Schemes for Nonlinear Conservation Laws: Finite Domains*. Technical Report NASA/TM-2013-217971. NASA Langley Research Center, Hampton VA 23681-2199, United States: NASA.
- Fisher, T. C. and M. H. Carpenter (2013b). “High-order entropy stable finite difference schemes for nonlinear conservation laws: Finite domains”. In: *Journal of Computational Physics* 252, pp. 518–557.
- Gassner, G. J., A. R. Winters, and D. A. Kopriva (2016). “Split Form Nodal Discontinuous Galerkin Schemes with Summation-By-Parts Property for the Compressible Euler Equations”. In: *Journal of Computational Physics* 327, pp. 39–66.
- Gottlieb, S. and C.-W. Shu (1998). “Total variation diminishing Runge-Kutta schemes”. In: *Mathematics of Computation* 67.221, pp. 73–85.
- Hicken, J. E., D. C. D. R. Fernández, and D. W. Zingg (2016). “Multidimensional Summation-By-Parts Operators: General Theory and Application to Simplex Elements”. In: *SIAM Journal on Scientific Computing* 38.4, A1935–A1958.
- Hicken, J. E. and D. W. Zingg (2013). “Summation-by-parts operators and high-order quadrature”. In: *Journal of Computational and Applied Mathematics* 237.1, pp. 111–125.
- Ismail, F. and P. L. Roe (2009). “Affordable, entropy-consistent Euler flux functions II: Entropy production at shocks”. In: *Journal of Computational Physics* 228.15, pp. 5410–5436.
- Jameson, A. (2008). “Formulation of kinetic energy preserving conservative schemes for gas dynamics and direct numerical simulation of one-dimensional viscous compressible flow in a shock tube using entropy and kinetic energy preserving schemes”. In: *Journal of Scientific Computing* 34.2, pp. 188–208.
- Kennedy, C. A. and A. Gruber (2008). “Reduced aliasing formulations of the convective terms within the Navier–Stokes equations for a compressible fluid”. In: *Journal of Computational Physics* 227.3, pp. 1676–1700.
- Morinishi, Y. (2010). “Skew-symmetric form of convective terms and fully conservative finite difference schemes for variable density low-Mach number flows”. In: *Journal of Computational Physics* 229.2, pp. 276–300.
- Pirozzoli, S. (2011). “Numerical methods for high-speed flows”. In: *Annual review of fluid mechanics* 43, pp. 163–194.
- Ranocha, H. (2016a). “SBP operators for CPR methods”. MA thesis. TU Braunschweig.
- Ranocha, H. (2016b). “Shallow water equations: Split-form, entropy stable, well-balanced, and positivity preserving numerical methods”. In: *GEM – International Journal on Geomathematics*. DOI: 10.1007/s13137-016-0089-9. arXiv:1609.08029 [math.NA].
- Roe, P. L. (2006). *Affordable, entropy-consistent Euler flux functions*. Talk presented at the Eleventh International Conference on Hyperbolic Problems: Theory, Numerics, Applications. Lyon. URL: http://www2.cscamm.umd.edu/people/faculty/tadmor/references/files/Roe_Affordable_entropy_Hyp2006.pdf.
- Shu, C.-W. (Nov. 1997). *Essentially Non-Oscillatory and Weighted Essentially Non-Oscillatory Schemes for Hyperbolic Conservation Laws*. Final Report NASA/CR-97-206253. Institute for Computer Applications in Science and Engineering, NASA Langley Research Center, Hampton VA United States: NASA.
- Sod, G. A. (1978). “A survey of several finite difference methods for systems of nonlinear hyperbolic conservation laws”. In: *Journal of Computational Physics* 27.1, pp. 1–31.

- Tadmor, E. (1987). “The numerical viscosity of entropy stable schemes for systems of conservation laws. I”. In: *Mathematics of Computation* 49.179, pp. 91–103.
- Tadmor, E. (2003). “Entropy stability theory for difference approximations of nonlinear conservation laws and related time-dependent problems”. In: *Acta Numerica* 12, pp. 451–512.
- Toro, E. F. (2009). *Riemann solvers and numerical methods for fluid dynamics: A practical introduction*. Springer Science & Business Media.
- Winters, A. R., D. Derigs, G. J. Gassner, and S. Walch (2016). “A Uniquely Defined Entropy Stable Matrix Dissipation Operator for High Mach Number Ideal MHD and Compressible Euler Simulations”. In: *Journal of Computational Physics*.
- Woodward, P. and P. Colella (1984). “The numerical simulation of two-dimensional fluid flow with strong shocks”. In: *Journal of Computational Physics* 54.1, pp. 115–173.
- Zhang, X. and C.-W. Shu (2010). “On positivity-preserving high order discontinuous Galerkin schemes for compressible Euler equations on rectangular meshes”. In: *Journal of Computational Physics* 229.23, pp. 8918–8934.
- Zhang, X. and C.-W. Shu (2011). “Maximum-principle-satisfying and positivity-preserving high-order schemes for conservation laws: survey and new developments”. In: *Proceedings of the Royal Society of London A: Mathematical, Physical and Engineering Sciences*. Vol. 467. 2134. The Royal Society, pp. 2752–2776.